Lawrence Berkeley National Laboratory
Recent Work

Title
THE CIRCULAR DICHROISM STUDY OF NINE SPECIES OF TRANSFER RIBONUCLEIC ACID

Permalink
https://escholarship.org/uc/item/2v66k8fm

Author
Blum, Arlene Diane.

Publication Date
1971-11-01

LBL-538

c.1

THE CIRCULAR DICHROISM STUDY OF NINE SPECIES OF TRANSFER RIBONUCLEIC ACID

Arlene Diane Blum
(Ph. D. thesis)

November 1971

LBL-538

c.1

DISCLAIMER

This thesis is
dedicated to John.

ACKNOWLEDGEMENTS

Laboratory of Chemical Biodynamics of the Lawrence Radiation Laboratory is gratefully acknowledged.

And, finally, I would like to thank Ester, Denali, Andy, and Howard for making the last years more fun.

LIST OF ABBREVIATIONS

A,U,C,G	The ribonucleosides adenosine, uridine, cytidine, and guanosine, respectively. (Abbreviations used for modified nucleosides are given in Fig. 3-4.)
X,Y	A general nucleoside.
XY	3'-5' nucleoside diphosphate.
poly rX	Homopolymer of ribonucleoside X.
poly rXY	Homopolymer of alternating X and Y residues.
poly X:poly X'	1:1 complex of poly X and poly X'.
poly XY:poly X'Y'	1:1 complex of poly XY and poly X'Y'.
RNA	Ribonucleic acid.
DNA	Deoxyribonucleic acid.
$tRNA^{F \cdot Met}$(E. coli)	Formyl methionine transfer RNA from E. coli. Similar abbreviations are used for the other species of tRNA discussed here.
mRNA	Messenger RNA.
rRNA	Ribosomal RNA.
ORD	Optical rotatory dispersion.
CD	Circular dichroism.
UV	Ultraviolet.
O.D.	Optical density.
O.D. unit or A_{260} unit	An amount which when dissolved in 1 ml, has an optical density at 260 mμ of 1 in a 1 cm path length cell.

λ	Wavelength.
$[\theta]$	Mean molar ellipticity.
ε_λ	Extinction coefficient (liters/ mole cm) at wavelength λ (mμ); expressed per mole of monomer for polymers.
EDTA	Ethylenediamine tetraacetic acid.
NMR	Nuclear Magnetic Resonance.
BD cellulose	Benzoylated DEAE cellulose.
tris HCl	tris (hydroxymethyl) aminomethane. adjusted to pH indicated with HCl.
F. Met	Formyl methionine.
Leu	Leucine.
Phe	Phenylalanine.
Tryp	Tryptophan.
Tyr	Tyrosine.
Val	Valine.
monomer	Mononucleotide.
dimer	Dinucleoside monophosphate.
trimer	Trinucleoside diphosphate.

The Circular Dichroism Study of Nine Species of

Transfer Ribonucleic Acid

Arlene Diane Blum

Abstract

A detailed CD study of nine species of tRNA was
undertaken to see how much information about the struc-
ture of these molecules could be obtained from their
CD spectra. The purification of three of these tRNAs
is described. Accurate extinction coefficients are
measured for all nine tRNAs.

Methods for calculating the CD of single and double
stranded regions of tRNA are discussed. The change in
the characteristics of calculated CD spectra of RNA
with changes in base composition, sequence, and per
cent double strand are shown. CD spectra are calculated
from sums of mononucleotides, dinucleoside monophos-
phates, and double strand polynucleotide spectra and
compared with experimental tRNA spectra.

Single stranded tRNA is prepared by dialysing
tRNA solutions until the concentration of magnesium is
less than 10^{-5} M, and heating to 40°C. Temperature-
absorbance profiles show that at 40°C the dialysed tRNA
is single stranded while tRNA in the presence of 1 mM
magnesium is native. Comparison of the CD of this
single stranded tRNA with appropriate sums of dinucleo-
side monophosphate spectra shows that the CD of the

dinucleoside monophosphates is not a good model for
the CD of single stranded tRNA.

The CD of native tRNA at 40°C may be calculated
with reasonable accuracy using the experimental single
strand spectrum to represent the CD of the single
stranded regions of the tRNA, and double stranded
pairing interaction spectra based upon polymer spectra
to represent the double strand regions. No CD contri-
butions for tertiary structure were used. The approx-
imations necessary for this calculation are discussed
in some detail. Quantitative comparisons between
calculated and experimental spectra for native tRNA
were made assuming various models for the structure.
For most tRNAs about three base pairing interactions
in addition to those due to the cloverleaf secondary
structure of the molecule are suggested.

The difference between the CD of native and de-
natured tRNA^{Leu} and tRNA^{Tryp} are compared with sums of
pairing interactions corresponding to the opening of
the various double strand regions of these tRNAs. This
comparison suggests the native to denatured transition
for tRNA^{Leu} involves the loss of about four base pairing
interactions and for tRNA^{Tryp} some sort of major re-
arrangement. A and B forms of 5S RNA exhibit similar
CD behavior to that of native and denatured forms of
tRNA^{Tryp}.

A new model for the tertiary structure of tRNA is

proposed based on the extensive published work in addition to the present CD work. This model consists of a continuous stack from the ACC end to the TψC loop with the dihydrouridine loop interacting with the TψC loop, and the anticodon helix parallel to the TψC helix. It is similar to other recent models.

TABLE OF CONTENTS

CHAPTER I

INTRODUCTION

> "The time has come," the Walrus said,
> "To talk of many things:
> Of shoes--and ships--and sealing wax--
> Of cabbages and kings--
> And why the sea is boiling hot--
> And whether pigs have wings." (1)

For a better understanding of cabbages, kings, and whether pigs have wings, we study DNA, RNA, and proteins. What is their structure, their function, and most important, how do the molecular structure and biological function of these macromolecules influence each other?

The structure of DNA is regular and may be simply and elegantly related to many of the biological functions of this macromolecule. The secondary and tertiary structure of protein molecules is much more complex, and has not in most cases yet been clearly correlated with protein function, although it is known that function is very senstive to secondary and tertiary protein structure. The RNAs share characteristics of both the regularity of DNA and the complexity of proteins.

The many roles of the various types of RNA in protein syntheses are well-known, but the physical details of the way in which these processes occur will probably remain unknown until the three-dimensional structure of these molecules is understood. The

relatively small tRNA molecules are a good place to begin the study of the relation between the biological function and molecular structure of RNA. The ultimate goal of such a study is to propose a reasonable model for the secondary and tertiary structure of tRNA and use it to explain how tRNA functions in protein synthesis.

1. Transfer RNA Has a Complex Life History

Transfer RNA molecules are of central importance in the transfer of information from the nucleic acids to the proteins. In order for successful protein synthesis to occur, tRNA must interact with great specificity with the other components of the protein synthesizing system.

Transfer RNA has a complex and intriguing life history. The precursor tRNA (2) is synthesized in a chain of about 120 nucleotides with a lengthy 5' segment that might be responsible for regulating the amount of tRNA in the cell. This precursor tRNA contains no modified bases but does contain the sequence ACC at the 3' end. It has been suggested that the precursor has a similar structure to the functional tRNA. Endonucleases remove the extra nucleotides resulting in a chain about 76 nucleosides long. Then about 10% of the bases are modified by methylases and other enzymes. For example, there are enzymes that

convert uracil to pseudouracil.

Detailed explanations of the processes that are summarized very briefly here may be found in Reference (3). The tRNA interacts with the aminoacyl synthetase which adds the correct amino acid to the 3' OH terminal adenosine. The tRNA is then "charged." The specificity of this step is extremely high, with errors thought to occur less than one time in 10^3 (4). The question of how the synthetase recognizes the correct tRNA and discriminates against all others is an important unsolved problem central to molecular biology (3).

The tRNA then interacts with various transfer factors. In E. coli, charged tRNA, the transfer factor T_u, and GTP form a complex in all cases except that of tRNA$^{F.Met}$.

The complex migrates to the aminoacyl site (A) of the ribosome, and the 3 nucleotides of the anticodon bind to the messenger RNA. The first two anticodon nucleotides bind to their complementary bases, but the third nucleotide may "wobble" allowing one tRNA to bind to more than one type of triplet (5). This step provides for the specificity of information transfer from the messenger RNA to the polypeptide.

Then the growing polypeptide chain is transferred from the peptidyl site (P) to the (A) site where it is joined to the amino acid on the tRNA, and then the tRNA moves from the (A) site to the (P) site. The polypeptide is removed and the deacylated tRNA is released.

This tRNA may be charged again and take part in protein synthesis many times before it is degraded.

A knowledge of the correct three dimensional structure of tRNA should help explain the physical details of all these processes. It is quite possible that tRNA exhibits different structures at different times in its life history.

2. A Model Building Study Suggests Possible Conformations of tRNA

A. Different Species of tRNA Have Similar Unique Secondary Structure.

Presently the primary structure, or sequence of the nucleotides, in at least 25 species of tRNA are known. Several review articles discuss the striking similarity between these sequences (6-8). There are 16 positions that contain same base in all the species of tRNA that have been sequenced. These homologous nucleotides are mostly located in single strand regions of the molecule.

The secondary structure of tRNA is defined by the base paired double helical regions of the molecule. The cloverleaf secondary structure was proposed by Holley when he determined the first known tRNA primary sequence (9). This structure was designed to maximize base pairing according to the Watson and Crick rule that guanine pairs with cytosine and that adenine pairs

with uracil. All known tRNA sequences can be fitted
into the Holley cloverleaf structure.

Figures 1-1 to 1-3 show the primary and likely
secondary structure of the nine species of tRNA being
studied in this work. There are obvious similarities
between these nine tRNA structures. At the 3' end
of each molecule is the ACC which provides the attach-
ment site for the amino acid through the hydroxyl
group on the terminal adenosine residue. Then there
is a helix consisting of 12 base pairs and a loop
which contains the sequence TψC. This loop is often
called the TψC loop as this sequence has been found
in this position in all known tRNA primary structures.
It has been suggested that this sequence is necessary
for ribosomal binding (10). Next to the TψC loop there
is a variable length region consisting of from 5 to 12
nucleotides. Across from the TψC loop in the figures
is the anticodon loop, so called since its middle
three bases pair with the codon of the messenger RNA
on the ribosome. This loop is always closed with five
base pairs. Then there is a single base and then
another double strand region of three of four base
pairs. These pairs close a loop which consists of
nine to 12 nucleotides and usually contains one or
more dihydrouridine residues. It is commonly referred
to as the D loop. Thus each tRNA molecule consists of
three large loops, three double stranded helical regions,

Figures 1-1 to 1-3. Nucleotide sequences of the nine
species of tRNA studied in this work. The sources and
sequences of these tRNAs are listed in Table 2-1.
Structures of modified nucleotides are shown in
Figure 3-4.
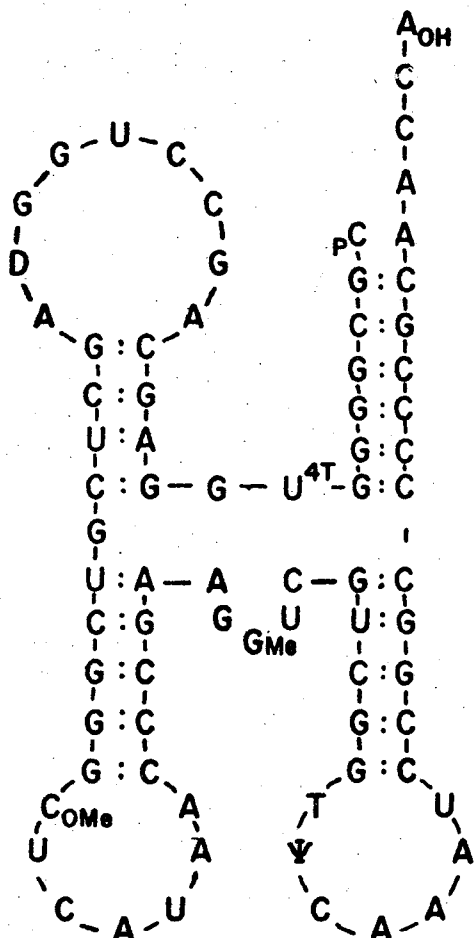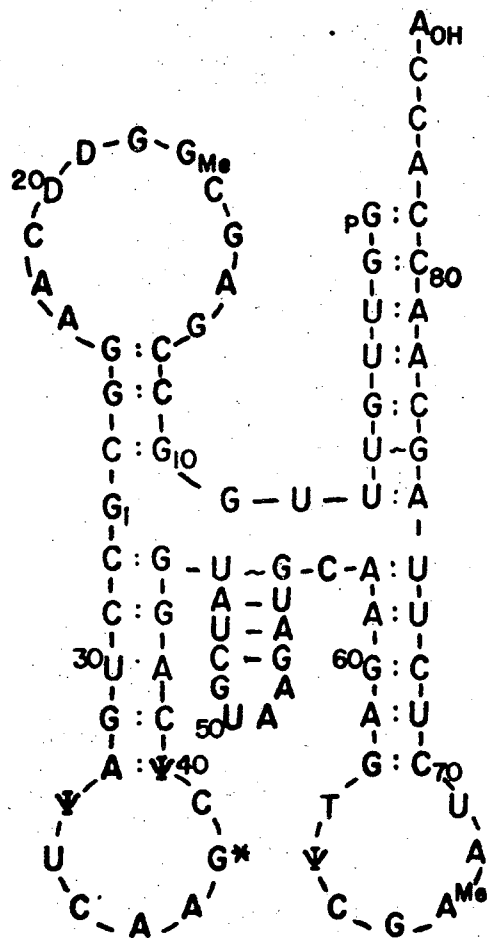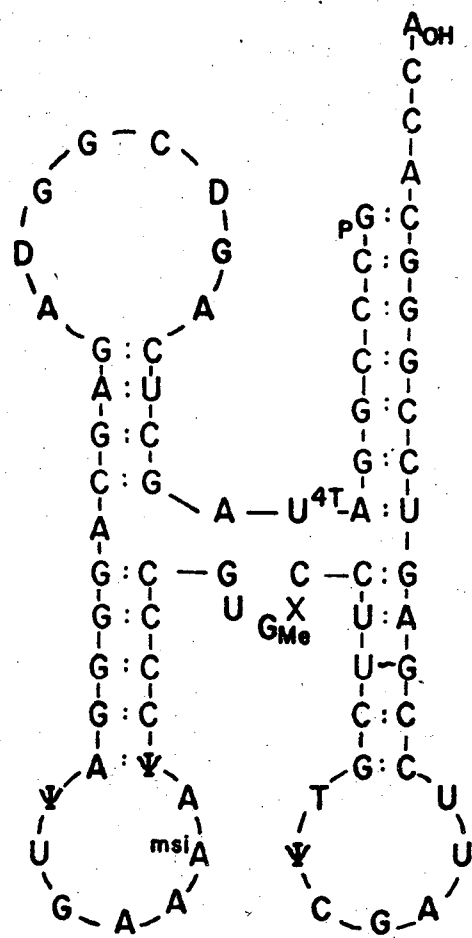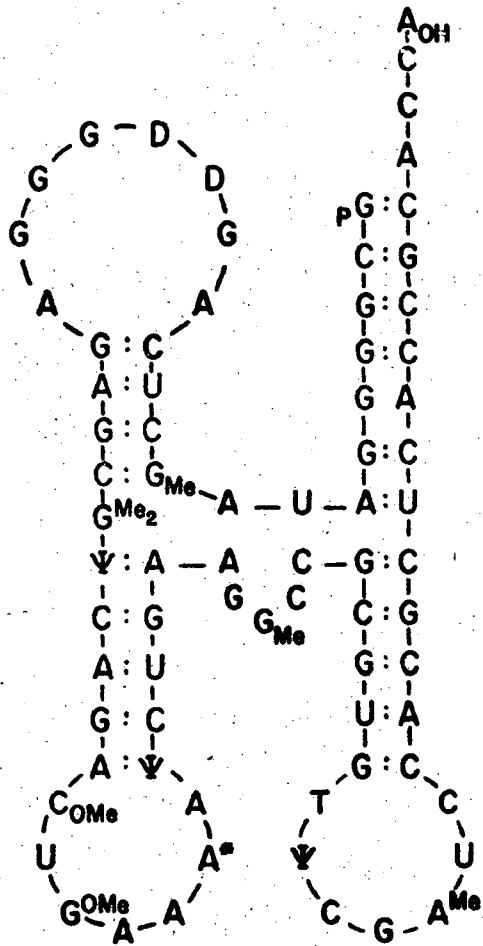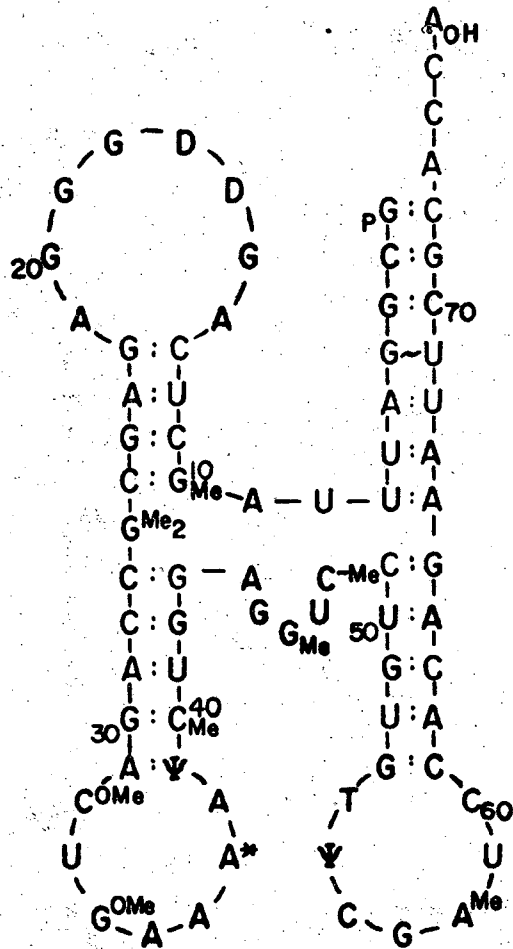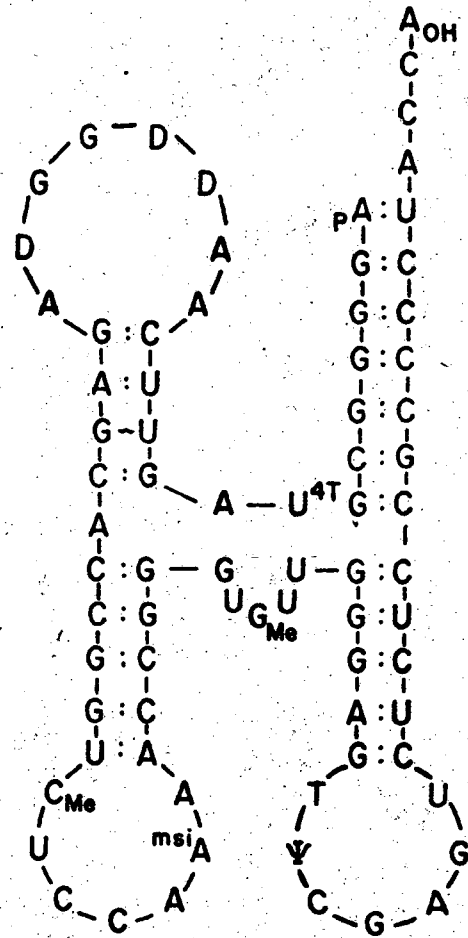
Figure 1-1

Figure 1-2
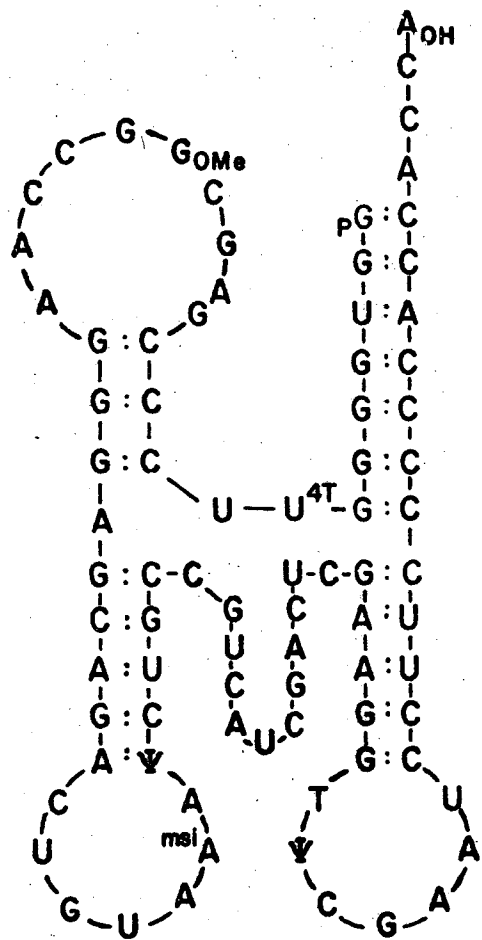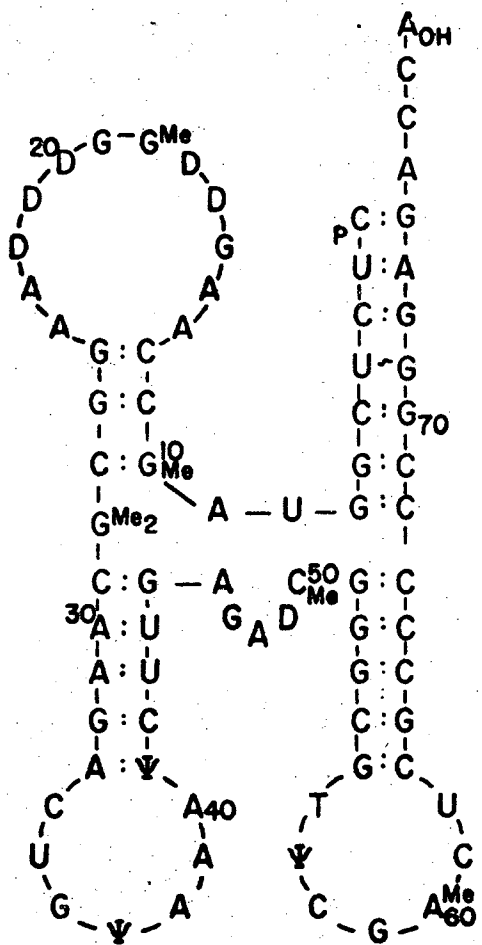
tRNA$_{Su-}^{Tyr}$ (E. Coli)   tRNA^{Tyr} (Yeast)   tRNA^{Val} (E. Coli)
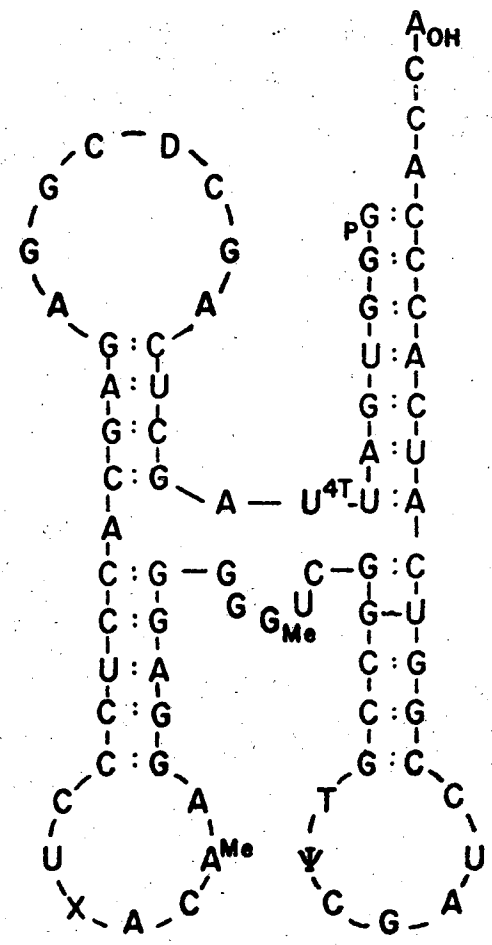
Figure 1-3

and a variable length region.

In addition to this secondary structure, it has
been shown that tRNA has a three-dimensional structure
that is more compact and stable than would result from
merely an unordered combination of these helical regions
(11). This is called the tertiary structure of tRNA.
Evidence for tertiary structure is provided by a large
change in the sedimentation coefficient of the molecule
below the temperature where secondary structure is lost
(12). Also the small radius of gyration (13-15) of
tRNA and its stability to phosphorolysis (16) suggest
a compact defined strucutre. The integrity of this
tertiary structure is requisite for the proper function
of tRNA (17).

B. A Plausible Structure for tRNA Resembles
an H

A molecular model building study was used to
gain insights into the nature of reasonable tertiary
structures for tRNA. Corey, Pauling, and Koltun
spacefilling models were used to construct a molecular
model of tRNA^{Phe} (Yeast) as shown in Fig. 1-2. The
primary structure of this molecule was put together
by students in Biochemistry 206 at Berkeley during
the winter of 1968.

The tRNA was oriented in a manner that would maxi-
mize the length of the helical double strand regions

and the amount of stacking in the single strand regions.
Assuming the secondary structure proposed by Holley,
we looked for a tertiary structure that would apply
equally well to all the tRNAs whose primary sequence
was known. We tried to make the molecule as compact
as possible with a constant distance between the anti-
codon and the amino acid.

Furthermore, we used results of X-ray studies on
reovirus RNA which suggest that double strand regions
are composed of an 12-fold double helix consisting of
Watson Crick base pairs (18). The plane of the base
pairs was tilted from the helix axis.

This model building study suggested that tRNA
might be stable in a conformation resembling an H.
This model consists of two long parallel helical regions
as is shown in Figs. 1-4 and 1-5. The anticodon loop
is across from the TψC loop and the D loop is across
from the ACC terminus. This is a preliminary model
of the tertiary structure which may be altered to agree
with experimental observations on the structure of
tRNA.

C. Many Models for tRNA Structure Have Been
Suggested

Since our model building study, numerous other
models for the three dimensional structure of tRNA
have been proposed. Six of these models were recently

-12-

CBB 685-3186

Fig. 1-4

-13-
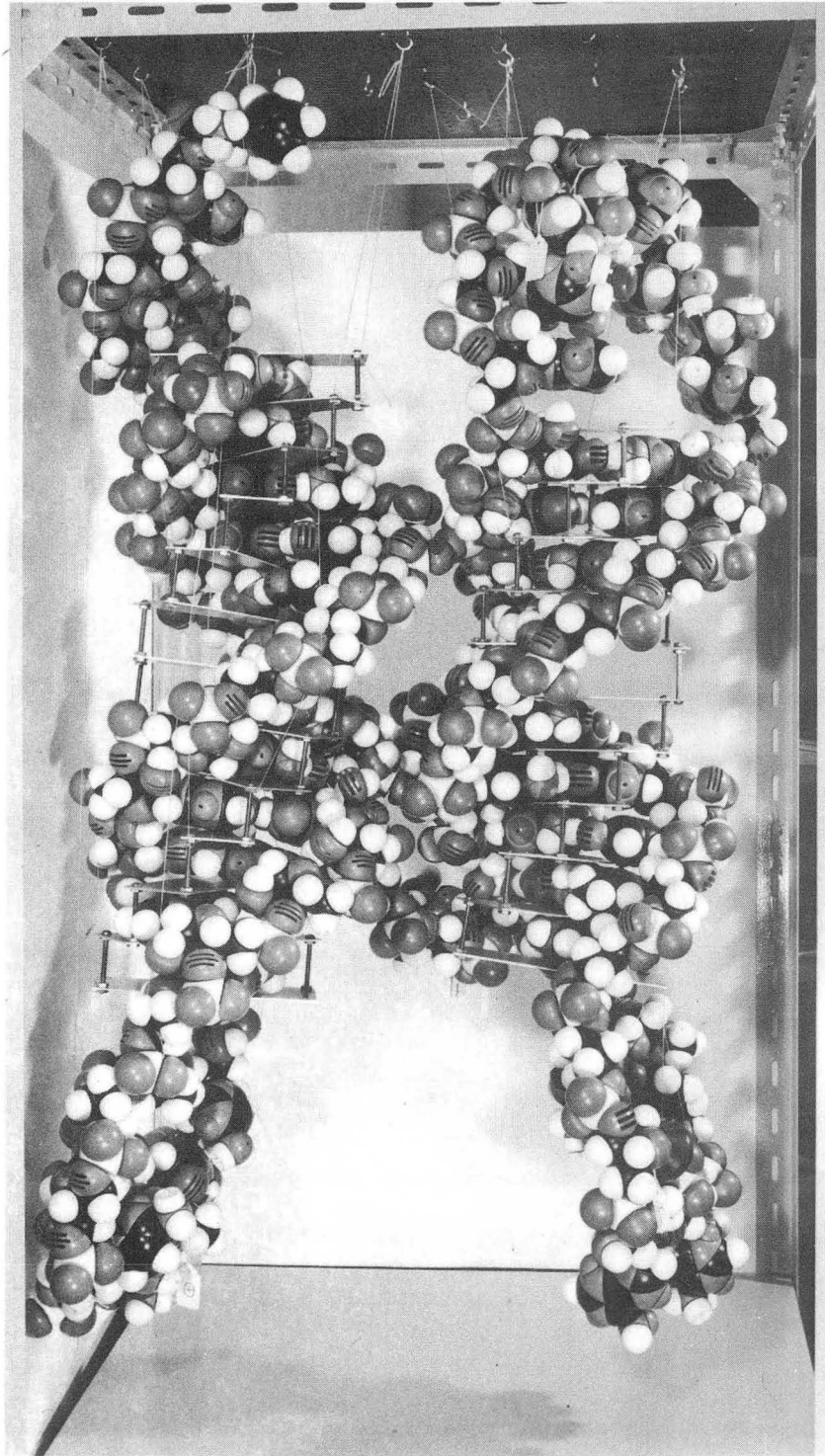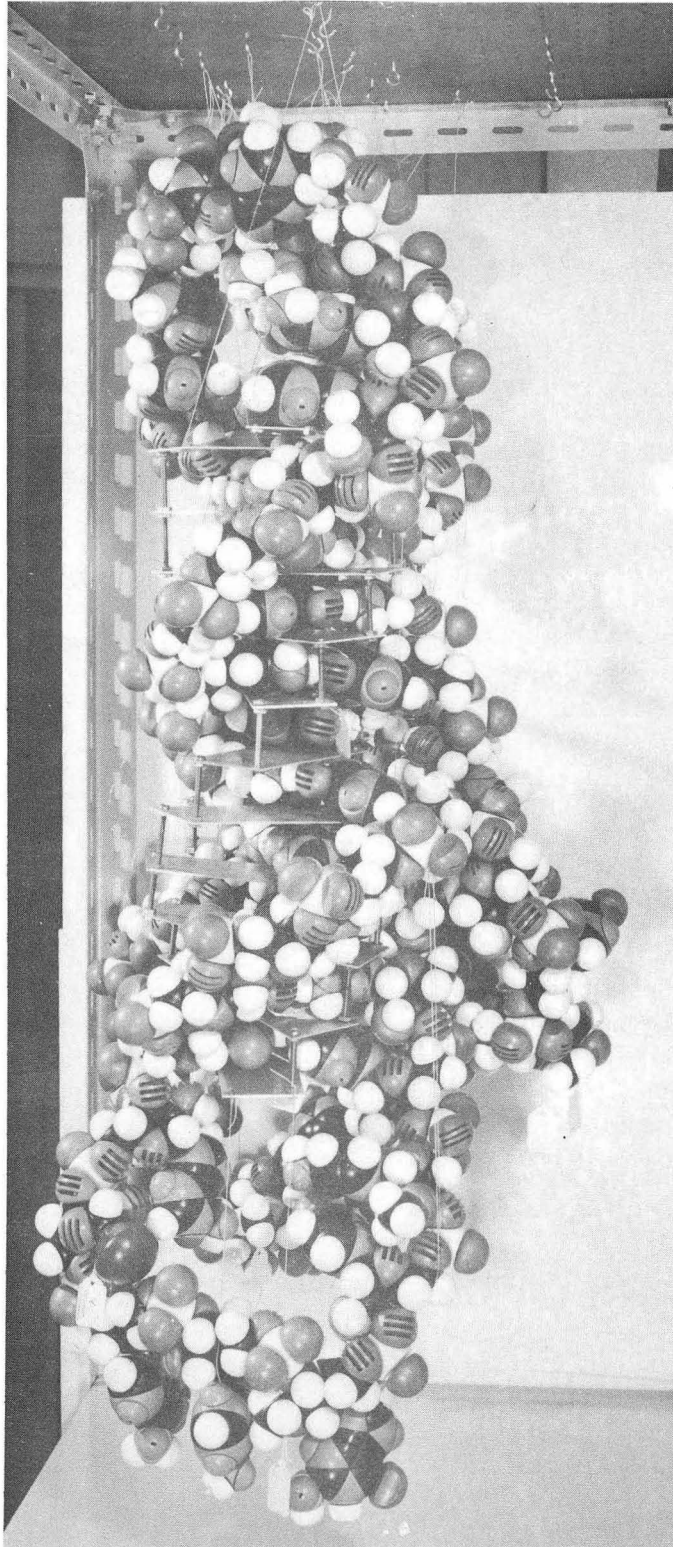
CBB 685-3184

Fig. 1-5

reviewed by Arnott (8). He compares the models proposed by Cramer (19), Levitt (20), Connors (21), Fuller (22), Ninio (23), and Melher (24) with a number of experimental results and structural requirements. Arnott concludes that the model that best fits these requirements is the model of Arnott which consists of a long helix from the ACC to the TψC loop. Coaxial with this is the anticodon helix. Only the D and anticodon loops are excluded from the stack.

In a similar review by Cramer, the same models and evidence of the same sort are examined (11). The conclusion is quite different. Cramer concludes that the best model is that of Cramer which consists of a continuous double strand helix from the anticodon through to the CCA end with the TψC and D loops bent toward the CCA and forming additional base pairs with each other and with the CCA.

Danchin recently suggested an imaginative dynamic model for the structure of tRNA (25). He suggests that charged and uncharged forms of tRNA have different structures and proposed that the D loop forms a sort of "slip-knot" around the main helix during movement between the two structures.

In summary, it should be noted that model building studies may provide an unlimited number of possible structures for tRNA, but experiments are necessary to show whether these structures are correct.

3. <u>Transfer RNA Structure Has Been Studied by Diverse</u>
   <u>Techniques</u>

There have been an incredible number of studies
of tRNA structure in the past few years. For example,
Reference 26 contains a bibliography of 712 items
giving "recent results of tRNA research." To thoroughly
review all the literature on the structure of tRNA
is neither plausible nor interesting. In this work,
only a few appropriate experiments will be discussed.
For further information, there are a large number of
review articles that may be consulted (6-8, 12, 27-29).

A. Crystallography

Eventually, crystallographic studies should pro-
vide reasonably exact information about tRNA structure
in a crystalline lattice. Many investigators have
succeeded in crystallizing tRNA (30-33). Resolution of
the X ray patterns varies from no better than 20 Å in
most cases to as low as 3 Å in some cases (8).

Some qualitative results have emerged from these
studies. Doctor <u>et</u> <u>al</u>. find evidence that the helices
within each tRNA molecule are more nearly parallel to
each other than perpendicular. They "favor an H-type
model for tRNA^{Tyr} (<u>E</u>. <u>coli</u>) in which the stem to which
the amino acid is attached is stacked to the TψC arm
and the anticodon arm is stacked on the arm which in
tRNAs usually contains D residues" (34). The

crystallization of mixed yeast tRNA by Fresco (35)
suggest that all species of tRNA do have a similar
tertiary structure. Of course, it is not known
whether the crystalline structure of tRNA is the same
as its structure in the cell or in solution. This is
the major objection to results obtained on crystalline
tRNA. To learn more directly about the structure of
tRNA in solution other physical and chemical techniques
are employed.

B. Chemical Studies of tRNA Structure

A number of structural investigations have involved
reacting tRNA with reagents that are specific for cer-
tain bases. Information is obtained concerning what
parts of the tRNA are accessible to these reagents.
The inaccessible regions are assumed to be involved in
or shielded by the tertiary structure of the tRNA.
Furthermore, the ability of this modified tRNA to
carry out its normal functions should provide clues
concerning what parts of the molecule are involved in
these functions.

Kethoxal was found to interact with G in tRNA^{Phe}
(yeast) at positions 20 and 34, thereby destroying
acceptor activity (36). Radioactive carbodiimides
react with most single strand bases that are outside
the TψC loop (37). It is found to destroy acceptor
activity but not ribosome binding (38). The conversion

of C to U by bisulphite treatment is found not to
destroy the ability of tRNA to accept an amino acid
(39). Other studies involving N-bromosuccinimide
(40) and nitrous acid (40,41) indicate that the TψC
loop is least accessible to modification.

A covalent bond may be formed between the 4tU
in position 8 and the C in position 13 by UV irradiation
at 335 mμ of several species of tRNA (42,43). This
modified tRNA is capable of participating in all
phases of protein synthesis although its affinity for
the aminoacyl synthetase is decreased somewhat (44,45).

The objection that may be raised to some of
studies is that the addition of bulky reagents or the
formation of covalent bonds within the molecule may
greatly alter the structure of the tRNA. The modified
tRNA may have an entirely different structure from
that of the native tRNA.

For this reason, physical measurements which
perturb the system less should prove more satisfactory.

C. Physical Studies

Examples of some physical techniques that have been
used to study the structure of tRNA and the sort of
information that may be derived from them will be given.

Equilibrium dialysis has been used to deter-
mine the availability of the various regions of several
species of tRNA for binding complementary oligonucleo-

tides (47). Only the four 3' terminal bases, the 5 bases on the 5' side of the anticodon loop, several bases on the 3' or 5' side of the D loop, and part of the variable length region would bind complementary radio-active oligomers. Oligomers would not bind to the double strand regions or to the TψC loop. Binding of oligomers to one part of the tRNA is shown not to affect binding to other parts, suggesting that the tertiary structure of the molecule is not greatly altered by the binding of oligomers. Thus a good model for the tertiary structure of tRNA should have the TψC loop protected and allow for the accessibility of those regions that will bind complementary oligomers.

Most <u>ultraviolet spectral studies</u> have involved analysis of the change in the UV spectrum upon thermal denaturation of the tRNA. A detailed investigation of the melting behavior of tRNA^{Phe} (Yeast) in solutions containing various amounts of Mg^{++} and K^{+} indicates the Mg^{++} ions are essential for the native structure of tRNA (48). Using differential melting and tempera-ture jump techniques three conformation transition of tRNA^{Ala} (Yeast), and five transitions of tRNA^{Phe} (Yeast) have been characterizied (49,50). The differ-ence in the UV spectra of the native and denatured forms of tRNA^{Leu} (Yeast) have been compared with spectra for the formation of A:U and G:C base pairs. This compari-son suggests that denatured tRNA contains 3 or 4 less

base pairs than does native tRNA (51).

Infrared spectroscopy has been used to deter-
mine the fractions of A:U and G:C base pairs in partly
double helical RNAs in solution (52). The relative
intensities of the IR bands of tRNA$^{F \cdot Met}$ (E. coli)
in solution agree with those predicted by the Holley
coverleaf model (53).

Fluorescence measurements utilizing the fluores-
cent base adjacent to the anticodon in tRNA^{Phe} (Yeast)
indicate that the anticodon is more than 40 $\overset{o}{A}$ away from
the CCA end of this molecule (54). Fluorescence may
also be used to monitor the interaction between the
amino acyl synthetase and the tRNA (55).

Nuclear magnetic resonance is most useful in
studying the modified bases as the four major nucleo-
sides in tRNA all exhibit similar chemical shifts.
Recently, high resolution PMR studies at 220 MHZ have
shown that the protons of most of the minor bases may
be distinguished (56). The resistance of areas con-
taining these nucleosides to solvent denaturation in
dimethylsulfoxide has been investigated. Segments
containing T and C_{Me} were found to be most resistant
(57).

Other physical techniques that provide some infor-
mation include electron paramagnetic resonance of
spin labelled tRNA (58), and electron microscopy (59).

The varied physical techniques just discussed
provide different ways of probing the structure of

tRNA and complement one another to some extent. However, there is one physical technique that is very sensitive to molecular conformation that has not yet been mentioned.

4. What can Circular Dichroism Spectroscopy Tell Us About the Structure of tRNA?

CD spectroscopy is a tool with great potential for the study of the structure of nucleic acids. It is a solution measurement so that pH, temperature, and salt concentration may be varied continuously to observe conformation changes dependent on small changes in the environment. Only very small amounts of sample are necessary to obtain a CD spectrum.

The CD spectrum of a nucleic acid is much more sensitive to small conformational changes than is the UV spectrum. Most of the intensity of UV absorption bands is a result of transitions within one base. Interactions with transitions on neighboring bases will perturb the UV absorption, but are not responsible for most of its intensity. The intensity of a CD spectrum is directly dependent upon the asymmetry of its environment. For example, nucleotides have a very small CD due to the asymmetric sugar, but quite considerable UV absorption. Thus, CD spectra are much more sensitive to changes in the geometry of adjacent bases than are UV spectra.

A. Past CD and ORD Studies of tRNA Structure

ORD spectra have been reported for tRNA^{Ala} and tRNA^{Tyr} from yeast (61), and tRNA^{Asp}, tRNA^{Gly}, and tRNA^{Lys} from yeast (62), as have the CD spectra of tRNA^{Val} and tRNA$^{F.Met}$ from E. coli (63), two species of tRNA^{Ala} (Yeast), mixed yeast tRNA (64), and tRNA^{Phe}, (65), tRNA^{Arg}, and tRNA^{Gly} from E. coli (66). ORD spectra may be converted to CD using the Kronig Kramers transform (60), which should allow qualitative comparison of these spectra. In general, though, careful comparison of these spectra is difficult as these spectra were measured in various buffers. Moreover, some of the values used for molar extinction coefficients (ε) are questionable. Some authors (63) incorrectly state that all species of tRNA have the same value of $\varepsilon = 7.5 \times 10^{-3}$ in a given buffer. In other papers (64), values of ε as low as 5.56×10^{-3} have been used under similar conditions. Thus a reliable set of CD or ORD spectra of tRNAs is not available.

CD has been used for a number of specialized studies of tRNA structure. CD studies of charged and uncharged purified tRNAs have shown that there is no large structural change when tRNA is charged (63,67). Also, it has been shown that tRNA structure is very sensitive to magnesium concentration as there is a large change in the CD spectrum when Mg^{++} is removed (48,64,66).

The base 4-thiouridine (4tU) found in several

species of tRNA results in a CD band at about 335 mμ.
CD studies (66,68) of the base 4tU in purified tRNA
have been carried out using quite concentrated tRNA
solutions ($A_{260} \approx 40$). The variability of these
spectra suggests that 4tU is in fairly different
environments in the different species of tRNA. A
study of the CD of 4tU in charged and uncharged
tRNA$^{F \cdot Met}$ (E. coli) indicates conformation changes
upon charging of this tRNA (69). Since the CD of
this molecule as a whole is not greatly altered, the
site of change is localized to the vicinity of the
4tU residue. It is in studies of small structural
changes of nucleic acids such as this that CD has the
greatest potential.

    B.   Approach to be Used in this Study

    The goal of this study is to determine how much
structural information may be obtained from a thorough
analysis of the CD spectra of different species of
tRNA between 210 and 310 mμ. We will study nine tRNAs
from three organisms that are specific for six differ-
ent amino acids. It will be possible to compare the
spectra of the same tRNA from different organisms as
well as different tRNAs from the same organism.

    First, methods for calculating the CD of single
and double strand regions of tRNA from the CD of
simpler nucleic acids will be discussed. Examples
showing the change in the characteristics of RNA CD

spectra with base composition, sequence, and percent double strand will be given.

It is assumed that the CD of native tRNA may be represented by a sum of contributions from the single strand regions, the double strand regions, and the tertiary structure of the molecule. Although tertiary structure probably does contribute to the CD spectrum, we presently have no knowledge of the details and will assume that the contribution of tertiary structure is negligible. Then, experimental spectra of the native tRNAs will be qualitatively discussed and compared with spectra constructed from simpler nucleic acids. A similar discussion and comparison will be carried out for single stranded tRNA and sums of dimer spectra. This should provide a good test for the "nearest neighbor" approximation.

A number of previous studies of the CD of tRNA involved analysis of the difference between the conformation of the tRNA in the presence and absence of magnesium at room temperature. We will show that room temperature corresponds to an arbitrary point in the helix-coil transition of the tRNA and therefore does not correspond to a well defined conformation of the tRNA molecule in the absence of magnesium. A temperature where the tRNA molecule is totally single stranded can be determined from the temperature-absorbance profile. We will study the difference between the spectra of tRNA in the presence and absence of magnesium at

this temperature, which should correspond to the formation of the secondary and perhaps tertiary structure of the molecule. This difference will be shown to agree fairly well with a sum of the CD spectra corresponding to the formation of the base pairing interactions of the structures in Figs. 1-1 to 1-3.

Thus the usefulness of CD as an analytic tool for providing information on the secondary and tertiary structure of tRNAs will be investigated. A judicious summing of experimental and calculated spectra will allow quite accurate calculation of the CD of native tRNA.

Examples of the application of these techniques to an analysis of the difference between native and denatured tRNAs and also 5S RNA will be given. It will be shown that the sensitivity of CD to details of RNA structure may be exploited to provide fairly accurate information concerning conformational change in nucleic acids.

REFERENCES TO CHAPTER I

1. Lewis Carroll, Alice's Adventures in Wonderland, Whitney Co., 1954, p. 154.

2. S. Altman and J. Smith, Nature, New Biology, 233, 35 (1971).

3. Cold Spring Harbor Symposia, 34 (1969).

4. J. D. Watson, Molecular Biology of the Gene, W. A. Benjamin, New York, 1965.

5. F. H. C. Crick, J. Mol. Biol., 19, 548 (1966).

6. J. T. Madison, Ann. Rev. Biochem., 37, 131 (1968).

7. H. G. Zachau, Angew. Chem. Int. Ed. Engl., 8, 711 (1969).

8. S. Arnott, Progress in Biophysics and Molecular Biology, 22, 181 (1971).

9. R. W. Holley, J. Apgar, G. A. Everett, J. T. Madison, M. Marquisee, S. H. Merrill, J. R. Penswick, and Z. Zamir, Science, 147, 1462 (1965).

10. R. W. Holley, Sci. American, 214(2), 30 (1966).

11. F. Cramer, Progress in Nucleic Acid Research and Molecular Biology, 11, 391 (1971).

12. D. Henley, T. Lindahl, and J. Fresco, Proc. Natl. Acad. Sci. U.S., 55, 191 (1966).

13. W. R. Krigbaum and R. W. Goodwin, Science, 154, 423 (1966).

14. J. A. Lake and W. W. Beeman, J. Mol. Biol., 31, 115 (1968).

15. W. Krigbaum and R. W. Godwin, _Macromolecules_, 1, 375 (1968).

16. M. N. Thang, B. Beltchev, and M. Grunberg-Manago, _Eur. J. Biochem._, 19, 184 (1971).

17. J. Fresco, A. Adams, R. Ascione, D. Henley, and T. Lindahl, _Cold Spring Harbor Symposia_, 31, 527 (1966).

18. W. Fuller, F. Hutchison, M. Spencer, and M. H. F. Wilkins, _J. Mol. Biol._, 27, 507 (1967).

19. F. Cramer, H. Dupner, F. Von der Haar, E. Schlimme, and H. Seidel, _Proc. Natl. Acad. Sci. U.S._, 61, 1384 (1968).

20. M. Levitt, _Nature_, 224, 759 (1969).

21. P. G. Connors, M. Labanauskas, and W. W. Beeman, _Science_, 166, 1528 (1969).

22. W. Fuller, S. Arnott, and J. Creek, _Biochem. J._, 114, 269 (1969).

23. J. Ninio, A. Faure, and M. Yaniv, _Nature_, 223, 1333 (1969).

24. G. Melcher, _FEBS Lett._, 3, 185 (1969).

25. A. Danchin, _FEBS Lett._, 13, 152 (1971).

26. D. H. Gauss, F. Von der Haar, A. Maelicke, and F. Cramer, _Ann. Rev. Biochem._, 40, 1045 (1971).

27. K. Miura, _Progress in Nucleic Acid Research and Molecular Biology_, 6, 39 (1967).

28. R. W. Chambers, _Progress in Nucleic Acid Research and Molecular Biology_, 11, 489 (1971).

29. T. H. Jukes, Curr. Top. Microbiol. Immunol., 49, 178 (1970).

30. B. Vold, Biochem. Biophys. Res. Commun., 35, 222 (1969).

31. A. Hampel, M. Labanauskas, P. G. Connors, L. Kirkegard, U. L. RajBhandary, P. B. Sigler, and R. M. Bock, Science, 162, 1381 (1968).

32. H. Kim and A. Rich, Science, 162, 1381 (1968).

33. M. Labanauskas, P. G. Connors, J. D. Young, R. M. Bock, J. W. Anderegg, and W. W. Beeman, Science, 166, 1527 (1969).

34. B. P. Doctor, W. Fuller, and N. L. Webb, Nature, 221, 58 (1969).

35. J. R. Fresco, R. D. Blake, and R. Langridge, Nature, 220, 1285 (1968).

36. M. Litt, Biochemistry, 10, 2223 (1971).

37. S. W. Brostoff and V. M. Ingram, Science, 158, 668 (1967).

38. D. H. Metz and G. L. Brown, Biochemistry, 8, 2329 (1969).

39. Z. Kucan, K. Freude, I. Kucan, Nature, 232, 178 (1971).

40. J. Nelson, S. Ristow, and R. Holley, Biochim. Biophys. Acta, 149, 590 (1967).

41. M. S. May and R. W. Holley, J. Mol. Biol., 52, 19 (1970).

42. A. Favre, M. Yaniv, and A. M. Michelson, Biochem.
    Biophys. Res. Commun., 37, 266 (1969).

43. M. Yaniv, A. Chestier, and F. Gros, J. Mol. Biol.,
    58, 381 (1971).

44. A. Favre, A. Michelson, and M. Yaniv, J. Mol.
    Biol., 58, 367 (1971).

45. L. Chaffin, D. Omilianowski, and R. M. Bock,
    Science, 172, 854 (1971).

46. O. C. Uhlenbeck, J. Baller, and P. Doty, Nature,
    225, 508 (1970).

47. O. C. Uhlenbeck, J. Mol. Biol., submitted.

48. F. A. Fried, Thesis, University of Oregon (1970).

49. R. Römer, D. Riesner, and G. Mass, FEBS Lett.,
    10, 352 (1970).

50. D. Riesner, R. Römer, and G. Maas, Eur. J. Biochem.,
    15, 85 (1970).

51. A. Adams, T. Lindahl, and J. Fresco, Proc. Natl.
    Acad. Sci. U.S., 57, 1685 (1967).

52. G. Thomas, Biopolymers, 7, 325 (1969).

53. M. Tsuboi, S. Higuchi, Y. Kyogoku, and S.
    Nishimura, Biochim. Biophys. Acta, 195, 23 (1969).

54. K. Beardsley and C. R. Cantor, Proc. Natl. Acad.
    Sci. U.S., 65, 39 (1970).

55. C. Hélène, F. Brun, and M. Yaniv, J. Mol. Biol.,
    58, 349 (1971).

56. I. Smith, T. Yamane, and R. Schulman, Science,
    159, 1360 (1968).

57. J. Carwford, S. Chan, and M. Schweizer, Biochem. Biophys. Res. Commun., 44, 1 (1971).

58. B. Hoffman, B. Schofield, and A. Rich, Proc. Natl. Acad. Sci. U.S., 62, 1195 (1969).

59. L. O. Froholm and B. R. Olsen, FEBS Lett., 3, 182 (1969).

60. J. R. MacDonald and M. K. Brackmen, Rev. Mod. Phys., 28, 393 (1956).

61. J. N. Vournakis and H. A. Scheraga, Biochemistry, 5, 2997 (1966).

62. P. S. Sarin, P. C. Zamecnik, P. Z. Bergquist, and J. F. Scott, Biochemistry, 55, 579 (1966).

63. A. J. Adler and G. D. Fasman, Biochim. Biophys. Acta, 204, 183 (1970).

64. R. H. Reeves, C. R. Cantor, and R. W. Chambers, Biochemistry, 9, 3993 (1970).

65. B. Robison and T. P. Zimmerman, J. Biol. Chem., 246, 110 (1971).

66. G. E. Willick and C. M. Kay, Biochemistry, 10, 2216 (1971).

67. E. Wickstrom, Biochem. Biophys. Res. Commun., 43, 976 (1971).

68. J. F. Scott and P. Schofield, Biochemistry, 64, 931 (1969).

69. K. Watanabe and K. Imahore, Biochem. Biophys. Res. Commun., 45, 488 (1971).

CHAPTER II

MATERIALS AND METHODS

1. Preparation of Crude Aminoacyl-tRNA Synthetases

  A. E. Coli Synthetase

  In a typical E. Coli synthetase preparation (1),
one part frozen E. Coli B cells (Grain Processing)
were ground with one and a half parts aluminum oxide
(Baker) and a pinch of Macaloid (Barroid) in a mortar
and pestle at $4°C$ until lysis (about 10 minutes). Two
parts grinding buffer (.01 M Tris buffer, pH 7.4,
.01 M $MgCl_2$, .05 M NH_4Cl, and 5 mm β-mercaptol ethanol)
and one-half mg electrophoretically pure pancreatic
DNase (Worthington) were added to the paste. The
mixture was allowed to react for 15 min at $4°C$, and
then the debris was spun out in a Sorvall RC2-B centri-
fuge at 30,000 g. Ribosomes were pelleted at 100,000 g
for 3 hrs in a Beckman Model L ultracentrifuge. The
top three quarters of the supernatant was carefully
removed and gradually brought to 67% saturation with
solid ammonium sulfate (4.36 g/10 cc) while stirring
at $4°C$. The precipitated protein was spun at 15,000 g
for 20 minutes. The pellet was dissolved in a small
volume of grinding buffer and dialysed overnight versus
grinding buffer in .3 M ammonium chloride. The synthe-
tase mixture was then assayed for its ability to charge
tRNAs. Usually 1 µl of enzyme would fully charge an

A_{260} unit of mixed E. coli tRNA under assay conditions
described below. The synthetase was frozen in small
aliquots at -20°C.

B. Yeast Synthetase

Yeast synthetase was purified in a manner similar
to that described by Morris and Herbert (2).

One-half lb. crumbled cake yeast from Virginia
Bakery, Berkeley, was added to 750 ml toluene cooled
to -40°C in a dry ice-acetone bath. The yeast was
allowed to freeze for three hrs with occasional stirr-
ing. Toluene was poured off through cheesecloth and
the frozen cells thawed for 8 hrs. One hundred ml of
1 M Tris HCl, .5 M HCl, (pH about 8), was added and
the cells were allowed to autolyze until enzyme activ-
ity was maximized. For charging of tRNA^{Phe} (yeast),
11 hrs autolysis time was found to be optimal. After
this time, solution was spun at 15,000 g for 20
minutes two times to remove debris. The pellet and
lipids floating on the top surface were discarded.
The solution was then spun in the Beckman Model L
ultracentrifuge at 100,000 g for two hrs to remove
ribosomes.

Ammonium sulfate was added to precipitate the
protein as before. The solution was spun at 15,000 g
for 20 min, the pellet dissolved in 10 mM KH_2PO_4
(pH 7.5), 10^{-4} M EDTA, and dialysed overnight against

this solvent. The yield was about 40 ml of enzyme with an $A_{280} = 88$, and an $A_{260}/A_{280} = 1.3$. The synthetase mixture was stored in 40% glycerol at $-20°C$.

2. Assay for Amino Acid Acceptor Activity of tRNA

A typical assay mixture consisted of about 2 mμMoles of mixed tRNA or .04 mμMoles of purified tRNA, .05 μCuries of L-[^{14}C] amino acid (specific activity = 50 C/M), several μl of synthetase mixture and enough distilled water to bring the total volume of the assay mixture to 50 μl in a solution of .1 M Tris HCl (pH 7.4), 10 mM $MgCl_2$, .5 mM β-mercaptoethanol, and 2 mM ATP (sodium salt).(1).

The reaction mixture was incubated for ten min at 37°C, stopped with 3 ml of ice-cold 5% trichloroacetic acid (TCA), and the precipitated tRNA collected on a millipore filter (HA .45 μ) which had been soaked in cold TCA. The filters were rinsed with 3 ml more TCA, and dried under an infrared lamp. The amount of L-[^{14}C] amino acid incorporated was determined by counting in 5 ml of toluene based PPO-POPOP scintillation fluid (Amershan Searle), in a Beckman LS-250 liquid scintillation counter. Counting efficiency was found to be 93% by counting a known amount of [^{14}C] amino acid. The increase in specific activity (cpm/OD μl) upon purification was compared with published estimates of the relative amounts of different

tRNAs in mixed tRNA (3,4). Most tRNAs were assayed
for biological activity before and after optical
measurements to verify that degradation had not
occurred.

The amount of charged tRNA in column fractions
was simply determined by precipitating a volume of
the column fraction corresponding to about .05 A_{260}
units of tRNA in cold TCA, filtering on a Millipore
filter, and counting.

3. Purification of tRNAs

A. E. coli Tryptophan tRNA

E. coli tryptophan tRNA was purified in a manner
similar to that developed by Maxwell et al. (5) for
the purification of yeast tryptophan tRNA. First the
fraction of the mixed tRNA that elutes from benzoy-
lated DEAE (BD) cellulose only in ethanol was separa-
ted on a 200 ml column. Most of the other species of
tRNA had already been eluted with 1 M NaCl. This
resulted in a six-fold enrichment for tryptophan tRNA.

A 50 ml column was packed with BD cellulose, washed
with 2 M NaCl, and equilibrated with 1 M NaCl, .01 M
$MgCl_2$, and .01 M NaAcetate, (pH 4.5).

The enriched fraction was loaded with L-[^{14}C]
tryptophan (Schwartz) using a scaled up version of the
assay conditions described in Section 2. The charged
tRNA was precipitated with ice-cold ethanol, dissolved

Figure 2-1. Purification of tRNA^{Tryp} (E. coli).
Absorbance (——) and specific activity (X) of
fractions eluted from a BD cellulose column with
a gradient of ethanol (0-20% v/v). Peak I is
tRNA^{Tryp} (E. coli) and peak II is other tRNAs.
Three successive columns were run as shown in (a),
(b), and (c) resulting in highly purified tRNA^{Tryp}.
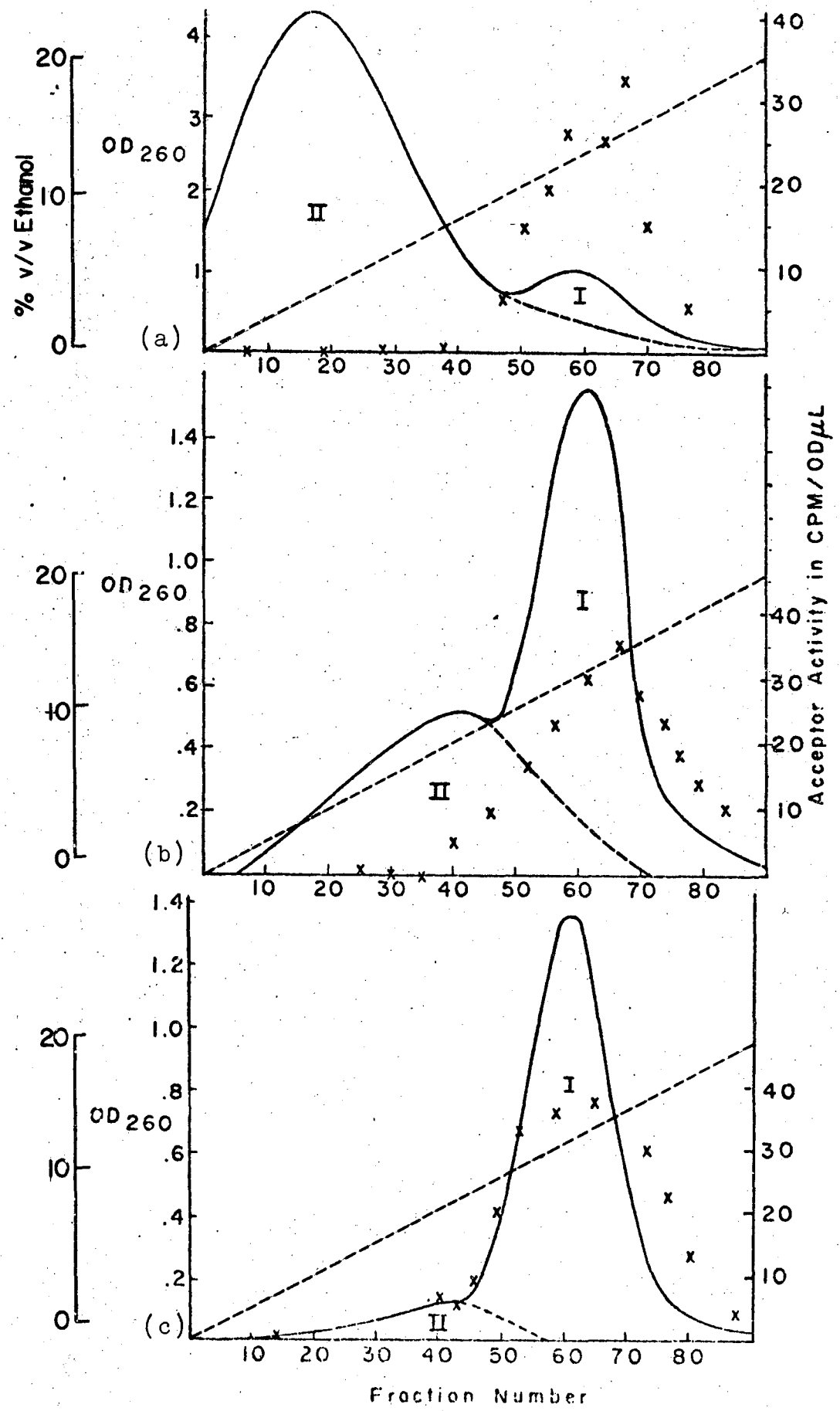
Figure 2-1

in .3 M NaCl, and applied to the column. The column
was washed with 1 M NaCl until the material being
eluted had a very low OD. Then the sample was eluted
with a linear gradient of ethanol varying from 0% to
20% EtOH (v/v) in 1 M NaCl (800 ml total volume). The
flow rate was 30 ml an hour and 5 ml aliquots were
collected.

The absorbance and acceptor activity of the column
fractions is shown in Fig. 2-1a. The fractions of
highest specific activity (tubes 52 to 80) were pooled,
diluted with 1 M NaCl to reduce ethanol concentration
by a factor of 3 or 4, and reapplied to the column.
This time separation was better as shown in Figure
2-1b. The fractions of highest specific activity
were pooled, diluted, and chromatographed under the
same conditions a third time as shown in Figure 2-1c.
The tRNA was deacylated by incubation at pH 9.0 in
Tris-Cl buffer for 20 min at 37°C. The tRNA was then
assayed and found to be at least 90-fold purified
relative to the mixed E. coli tRNA. Since Tryp is
about 1% of mixed tRNA, this corresponds to a purity
of about 90% (4).

B. Yeast Phenylalanine and Tyrosine tRNAs.

Two grams of mixed Baker's yeast tRNA (Plenum
Laboratories) were dissolved in 60 ml of water. A
300 ml column (3.5 cm by 32 cm) was packed with BD

cellulose in 2 M NaCl and then equilibrated with .4 M NaCl. The sample was applied and the column washed with .4 M NaCl. The eluted material was enriched for methionine tRNA. Elution was continued with .7 M NaCl resulting in a fraction enriched for tryptophan tRNA. Next a tyrosine enriched fraction was obtained by eluting with 1 M NaCl. Finally the column was eluted with 10% ethanol resulting in a fraction containing mostly tRNA^{Phe}.

The fractions were each concentrated by ultrafiltration in a Diaflo apparatus (Amicon Corporation, Cambridge, Massachusetts) using a UM-3 membrane. They were then assayed for Phe and Tyr acceptor activity. The ethanol fraction was found to be 12 fold enriched for tRNA^{Phe}, and the 1 M NaCl fraction was 2 fold enriched for tRNA^{Tyr}.

Yeast tRNA^{Phe} was further purified in a manner similar to that described by Litt (6). The fraction that eluted in ethanol was charged with L-[^{14}C] phenylalanine (Schwartz Stanistar) using standard assay conditions. This tRNA was applied to a 50 ml BD cellulose column equilibrated with .9 M NaCl. Then the column was eluted with 150 ml of a gradient from .8 M to 1 M NaCl in 15% ethanol, followed by 350 ml of 1 M NaCl in 15% ethanol. The fractions were counted and those of highest specific activity were pooled and rechromatographed with a similar gradient. The fractions of highest specific activity were concentrated

by ultrafiltration, deacylated, and assayed for amino-
acyl acceptor activity. The tRNA^{Phe} was found to be
17-fold purified which corresponds to a purity of
about 95% (7).

Then the fraction of the tRNA which had been
enriched for tyrosine was charged with L-[^{14}C] tyro-
sine (Schwartz), and loaded on a BD cellulose column
following the method of Maxwell et al. (5). It was
eluted with a one liter linear gradient from 0% to
10% (v/v) ethanol in 1 M NaCl. Most of the tyrosine
activity was found to elute between 5 and 8% ethanol.
These fractions were pooled and deacylated by incuba-
tion at pH 8.1 for 20 minutes at 37°C. The deacylated
tRNA was ethanol precipitated and rechromatographed
on BD cellulose in a gradient from .4 M to 1.1 M NaCl
(600 ml total volume). The tubes of highest activity
were pooled, concentrated, and assayed. The tRNA^{Tyr}
was 25-fold enriched, corresponding to a purity of about
90% (5).

4. Sources of Other tRNAs Used in This Work/

As can be seen from Table 2-1, three of the tRNAs
being studied were purified as part of this work, and
the other six were gifts from Oak Ridge National
Laboratory, Dr. Olke Uhlenbeck, Dr. J. Fresco, and
Dr. B. S. Dudock. The 5S RNA was a gift from Dr. Jim
Lewis. The source of the sequences shown in Figures

Table 2-1

tRNA	Source of tRNA	Sequence
F. Met (E. coli)	Gift, Oak Ridge National Laboratory	S. K. Dube, et al. (8)
Leu (Yeast)	Gift, J. Fresco, Princeton University	J. Fresco (9)
Phe (E. coli)	Gift, O. Uhlenbeck, University of Illinois	B. G. Barrell and F. Sanger (10)
Phe (Wheat)	Gift, B. S. Dudock, State University of New York, Stonybrook, New York	B. S. Dudock, et al. (11)
Phe (Yeast)	This work	U. L. RajBhandary et al. (12)
Tryp (E. coli)	This work	D. Hirsh (13)
Tyr (E. coli)	Gift, O. Uhlenbeck, University of Illinois	H. M. Goodman et al. (14)
Tyr (Yeast)	This work	J. T. Madison et al. (15)
Val (E. coli)	Gift, Oak Ridge National Laboratory	M. Yaniv and B. G. Barrell (16)

1-1 to 1-3 are also listed.

5. Sources of Dimers

The CD of 16 dimers and 4 monomers were measured at 40°C in 10 mM Tris-HCl (pH 7.8), 1 mM $MgCl_2$. The GG was purchased from Nutritional Biochemicals, and the other 15 dimers from Calbiochem and Amersham Searle. Purity was checked by spotting 2 μl of each dimer on paper and chromatographing overnight in 70% EtOH, 30% NH_4Ac.

6. Extinction Coefficients and Concentration Determinations

In collaboration with Dr. Marc Maestre, extinction coefficients for all nine species of purified tRNA were determined by degrading the tRNAs to nucleotides and using the known nucleotide extinction coefficients (17). The UV spectra of stock solutions of tRNA (1 OD unit/ml) in 10 mM Tris-HCl (pH 7.8), 1 mM $MgCl_2$ were recorded. 30 μl of 5 M NaOH was added to duplicate blanks and samples of the 9 species of tRNA each of volume .5 ml. Tubes were weighed after the addition of each solution, incubated for 24 hrs at 37°C, heated to 60°C for 2 min to insure degradation, incubated 12 more hours at 37°C and reweighed. The samples and blanks were neutralized with 30 μl of 5 mM HCl and 20 μl of 1 M Tris-HCl, pH 7.8. Volumes of each solution added were calculated from their density

(g/cc). The OD at 258 mμ of the degraded tRNA was obtained and corrected for dilution.

The initial extinction coefficient could then be calculated from:

$$\varepsilon_{tRNA} = \frac{V_{tRNA}}{V_{nucleosides}} \times \frac{A_{258\ tRNA}}{A_{258\ nucleosides}} \times \varepsilon_{nucleotides}$$

$$(2\text{-}1)$$

where ε is the extinction coefficient at 258 mμ in 10 mM Tris-HCl and 1 mM $MgCl_2$, V is the volume of the solution, and A_{258} is the absorbance at 258 mμ. Agreement between duplicate samples was within 1%. The extinction coefficients so determined are listed in Table 2-2.

Table 2-2

Extinction Coefficients of Nine tRNAs in

.01 M Tris-HCl (pH 7.8)

tRNA	$\varepsilon_{258} \times 10^{-3}$
F. Met (E. coli)	7.06
Leu (Yeast)	7.37
Phe (E. coli)	7.15
Phe (Wheat)	7.42
Phe (Yeast)	6.63
Tryp (E. coli)	6.71
Tyr (E. coli)	7.40
Tyr (Yeast)	7.11
Val (E. coli)	7.52

7. Atomic Absorption Measurements

Magnesium concentrations were measured with a
Perkin Elmer Model 303 Atomic Absorption Spectro-
photometer equipped with a Westinghouse hollow cathode
lamp. An air acetylene flame was used and the absorpt-
ion was monitored at 285 mμ. Standard solutions con-
taining between .1 and 1 ppm of $MgCl_2$ were measured
and a linear plot of absorbance versus concentration
was made before each run. About 1 cc of solution
was used for each measurement. The per cent absorption
of the standards and samples was measured at least
three times unless there was an insufficient amount
of sample to allow this. Error was less than 10%
except in very dilute solution.

8. Desalting Procedures

Extensive dialysis was used to remove as much Mg^{++}
and other salts from tRNA solutions. The following
buffers were prepared using twice distilled water:
(a) 0.5 M NaCl, 10 mM EDTA pH 7.5; (b) 0.2 M NaCl,
1 mM EDTA pH 7.5; (c) 1 mM EDTA pH 7.5; (d) .01 mM
EDTA pH 8.5. Solutions were dialysed for about 6 hours
at 4°C against four changes each of buffers (a), (b),
and (c), and against 8 changes of buffer (d). After
desalting, the concentration of Mg^{++} was measured by
atomic absorption, and found to be about 1 Mg^{++} per
tRNA molecule. Spectral measurements of low salt tRNA

were made in 10^{-5} M EDTA which is about 1 EDTA per Mg^{++}, and should ensure there is no more than 1 Mg^{++} bound to each tRNA molecule.

9. Optical Measurements

A. Cells and Solutions

All CD measurements were made using a standard strain-free cylindrical fused quartz cell (Opticel) of 1.0 cm pathlength and about .6 ml volume. Cells were frequently washed in chromic-sulfuric acid cleaning solution and rinsed at least 20 times with glass distilled water. Cells to be used for measurements in very low salt were soaked in dilute EDTA and then thoroughly rinsed with glass distilled water. The concentration of Mg^{++} in the distilled water was periodically checked using atomic absorption and found to be less than 10^{-5} M.

For all measurements above room temperature, cells were closed with ground glass stoppers wrapped in Teflon tape to assure a tight seal. Cells were weighed before and after high temperature measurements to verify that no evaporation had occurred.

UV measurements were either made in the CD cell or in rectangular quartz stoppered cells of 1 cm pathlength and 1 ml volume (Pyrocel).

"Native" RNA spectra were measured in solutions of 10^{-2} M Tris-HCl (pH 7.5), 10^{-3} M MgCl$_2$. There was

found to be no change in the magnitude of absorption
or CD in this buffer between pH 7.0 and pH 9.0.
Spectra of "single stranded" RNA in low salt were
obtained in 10^{-5} M EDTA adjusted to pH 8.5. The EDTA
was used to insure the absence of Mg^{++} bound to the
tRNA as atomic absorption measurements had indicated
a Mg^{++} concentration of about 10^{-5}. No additional
buffer was added to avoid adding divalent cation
impurities. The pH of these solutions was checked
after optical measurements with a Beckman Expandomatic
pH meter equipped with a microelectrode to verify
that it had not dropped below 7.0.

Samples used in optical studies had A_{260}'s at
260 mμ between .5 and 1.0.

B. Absorption and CD Measurements

All UV absorption spectra were measured at room
temperature (25°C) on a Cary 15 spectrophotometer.
Absorption spectra were recorded for all solutions
prior to CD studies.

The change in absorbance with temperature at
260 mμ was recorded between 10°C and 95°C using a
modified Beckman DU spectrophotometer on a Gilford
Model 2000 multiple sample absorbance recorder. Tempera-
ture was increased at a rate of about 20°C/hr by
means of a temperature programmer connected to a Haake
Model I circulating bath. Absorbance and temperature

were recorded very two minutes. Three samples and
one blank were run simultaneously.

CD measurements were made using a Cary Model 60
spectropolarimeter equipped with a circular dichroism
attachment (Model 6001). Temperature was controlled
using a circulating water bath and electronic cell
block designed by Dr. Donald Gray (18). Control could
be maintained to $\pm$ 0.1°C with an accuracy of $\pm$ 0.5°C.
The Cary 60 was operated at a scan rate of about
3 mμ per minute, a pen time constant of 0.3 seconds
and a full range scale of 0.04. Spectra were measured
between 350 and 205 mμ. Base line spectra of the
solvent in the same cell were obtained before and
after each set of CD spectra.

REFERENCES TO CHAPTER II

1. O. C. Uhlenbeck, personal communication.

2. R. W. Morris and E. Herbert, Biochemistry, 9, 4819 (1970).

3. I. Gillam, S. Millward, D. Blew, M. von Tigerstrom, E. Wimmer, and G. M. Tener, Biochemistry, 6, 3043 (1967).

4. K. H. Muench and P. A. Safille, Biochemistry, 7, 2799 (1968).

5. E. Wimmer, I. H. Maxwell, and G. M. Tener, Biochemistry, 7, 2623 (1968).

6. M. Litt, Biochem. Biophys. Res. Commun., 32, 507 (1968).

7. I. H. Maxwell, E. Wimmer, and G. M. Tener, Biochemistry, 7, 2629 (1968).

8. S. K. Dube, K. A. Marcker, B. F. C. Clark, and S. Cory, Nature, 218, 232 (1968).

9. J. Fresco, personal communication.

10. B. G. Barrell and F. Sanger, FEBS Lett., 3, 275 (1969).

11. B. S. Dudock, G. Katz, E. Taylor, and R. Holley, Proc. Natl. Acad. Sci. U.S., 62, 941 (1969).

12. U. L. RajBhandary, S. H. Chano, A. Stuart, R. D. Faulkner, R. M. Hoskinson, and H. G. Khorana, Biochemistry, 57, 751 (1967).

13. D. Hirsh, Nature, 228, 57 (1970).

14. H. M. Goodman, J. Abelson, A. Landy, S. Brenner, and J. D. Smith, _Nature_, 217, 1019 (1968).

15. J. T. Madison, G. A. Everett, and H. King, _Science_, 153, 531 (1966).

16. M. Yaniv and B. G. Barrell, _Nature_, 222, 278 (1969).

17. P-L Biochemicals, Inc., Circular OR-10. Values used for ε_{258} were 15.4 for AMP, 9.7 for UMP, 7.0 for CMP, and 12.7 for GMP.

18. F. S. Allen, D. M. Gray, G. P. Roberts, and I. Tinoco, Jr., _Biopolymers_, submitted.

CHAPTER III

CALCULATION OF CD SPECTRA AND DATA ANALYSIS

1. CD Spectra May be Used to Characterize RNAs

    The positions, magnitudes, and shapes of the bands
in a CD spectrum of an RNA provide information about
the structure of this molecule. It is informative to
consider the general characteristics of some CD spectra
of RNA that have been calculated by summing appropri-
ate spectra of simpler RNAs. The nature of this calcu-
lation will be discussed in detail later in this chapter.

    Figure 3-1 shows some typical CD spectra of an
RNA that is equimolar in A,U,C, and G calculated as
a function of the percent of the nucleosides that are
in hydrogen-bonded double strand regions. There are
several characteristics of these spectra that are of
special interest.

    Scanning from high wavelength, the first feature
of note is a small negative CD band centered around
295 mμ. This band was first observed by Sarkar et al.
(1) who noted that it is more sensitive to melting of
secondary structure of RNAs than is the large positive
band around 270 mμ. Upon heating the tRNA, this band
disappears at lower temperature than those necessary
to melt the secondary structure of the polymers. This
implies that the 295 mμ band corresponds to some sort
of structure other than secondary, perhaps to tertiary

Figure 3-1
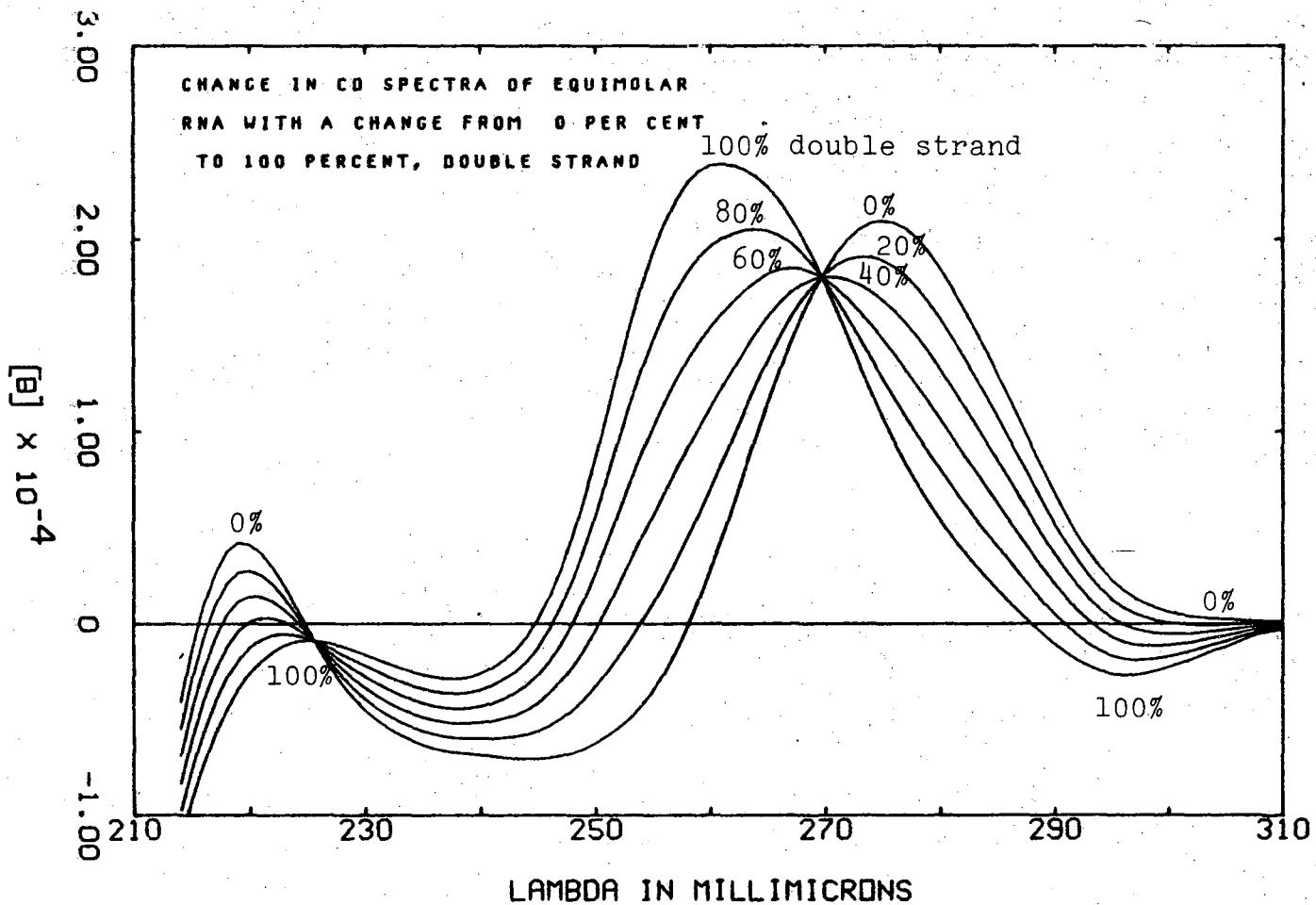
Spectra were calculated from sums of monomer, dimer, and polymer spectra using Equation 3-11.

structure.

Calculated spectra in Fig. 3-1 show that the band
at 295 mμ decreases in magnitude with an increase
in the single strand character of the RNA. Figure 3-6
shows that for double stranded RNA, the band decreases
with an increase in the percent of G:C pairing inter-
actions.

The next feature of the spectrum is a large posi-
tive peak between 260 and 280 mμ which is caused by
several $\pi-\pi^*$ transitions. This large CD is the result
of interactions between the 260 mμ transitions of one
base with the electronic transitions of its neighbor
bases (2,3). The magnitude of this peak is quite
sensitive to the pairing and stacking interactions
of the bases in the RNA. As shown in Fig. 3-1, its
position will shift to the red with a decrease in the
number of hydrogen-bonded bases in the molecule. A
change in the type of bases that are paired also
produces a change in this spectrum, as shown in Fig.
3-6.

The position of the crossover wavelength in the
vicinity of 240 mμ will also vary with the type and
amount of hydrogen-bonding in the molecule. There
may be a small negative band centered around 235 mμ.
Finally, there is a small positive band around 220 mμ;
this band is particularly sensitive to the base composi-
tion of the single strand RNA as shown in Fig. 3-5.

Most past CD studies of tRNA structure have involved tabulation of the positions and magnitudes of extrema and of crossovers. In this work, computer data analysis makes it possible to study the entire spectral curve of each RNA. This allows a maximal amount of structural information to be extracted from the CD spectra.

In order to calculate the spectra of native tRNA, it is necessary to calculate the single strand and double strand contributions to the CD. Each of these will be considered separately and in some detail.

2. The Optical Properties of Trinucleoside Diphosphates and Homopolynucleotides May be Calculated from Those of Dinucleoside Monophosphates.

The optical properties of some RNAs have been derived from those of oligomers with qualitative success (4,5). These calculations are based upon the spectra of dinucleoside monophosphates (dimers) and mononucleosides (monomers) and two assumptions. First, it is assumed that base stacking and geometry are similar in dimers and in longer RNA molecules. Second, it is assumed that all of the optical properties observed are caused by interactions among nearest neighbors. This latter assumption is called the nearest neighbor approximation.

For example, consider some optical property of the trinucleoside diphosphates (trimer) XYZ, such as $[\theta]$,

the mean molar ellipticity per residue. [θ] can be
approximated at each wavelength by:

$$(XYZ) = \frac{1}{3}\Big(2(XY) + 2(YZ) - (Y)\Big) \qquad (3\text{-}1)$$

where the mean molar ellipticity of the trimer XYZ,
the dimers XY and YZ, and the monomer Y are given by
(XYZ), (XY), (YZ), and (Y) respectively at each wave-
length. In this work, parentheses () will denote
experimental CD spectra.

Equation 3-1 has been used to calculate the ORD
of several trimers (4). CD and ORD are related by
the Kronig-Kramers transform and may be used almost
interchangeably (6). In most cases good agreement is
found between measured trimer spectra and those based
on nearest neighbor calculations. Figure 3-2 shows
this agreement for the ORD of the trimers A_3, AAC,
AAU, GAU, and AGU as measured by Cantor and Tinoco (4).
It should be noted that in the first three of these
trimers, the calculated spectra are shifted to slightly
higher wavelengths than the experimental spectra.

Similarly, optical properties of homopolyribonucleo-
tides (homopolymers) may be calculated from the nearest
neighbor approximation:

$$(\text{poly } X) = 2(XX) - (X) \qquad (3\text{-}2)$$

The ellipticity of poly X is thus simply two times the
ellipticity of the dimer XX minus the ellipticity of
the monomer X.

Figure 3-2. A comparison of the measured ORD of
some trimers (———) and the ORD calculated
from the nearest neighbor approximation (-----).
These spectra were obtained by C. R. Cantor and
I. Tinoco, Jr. (4).
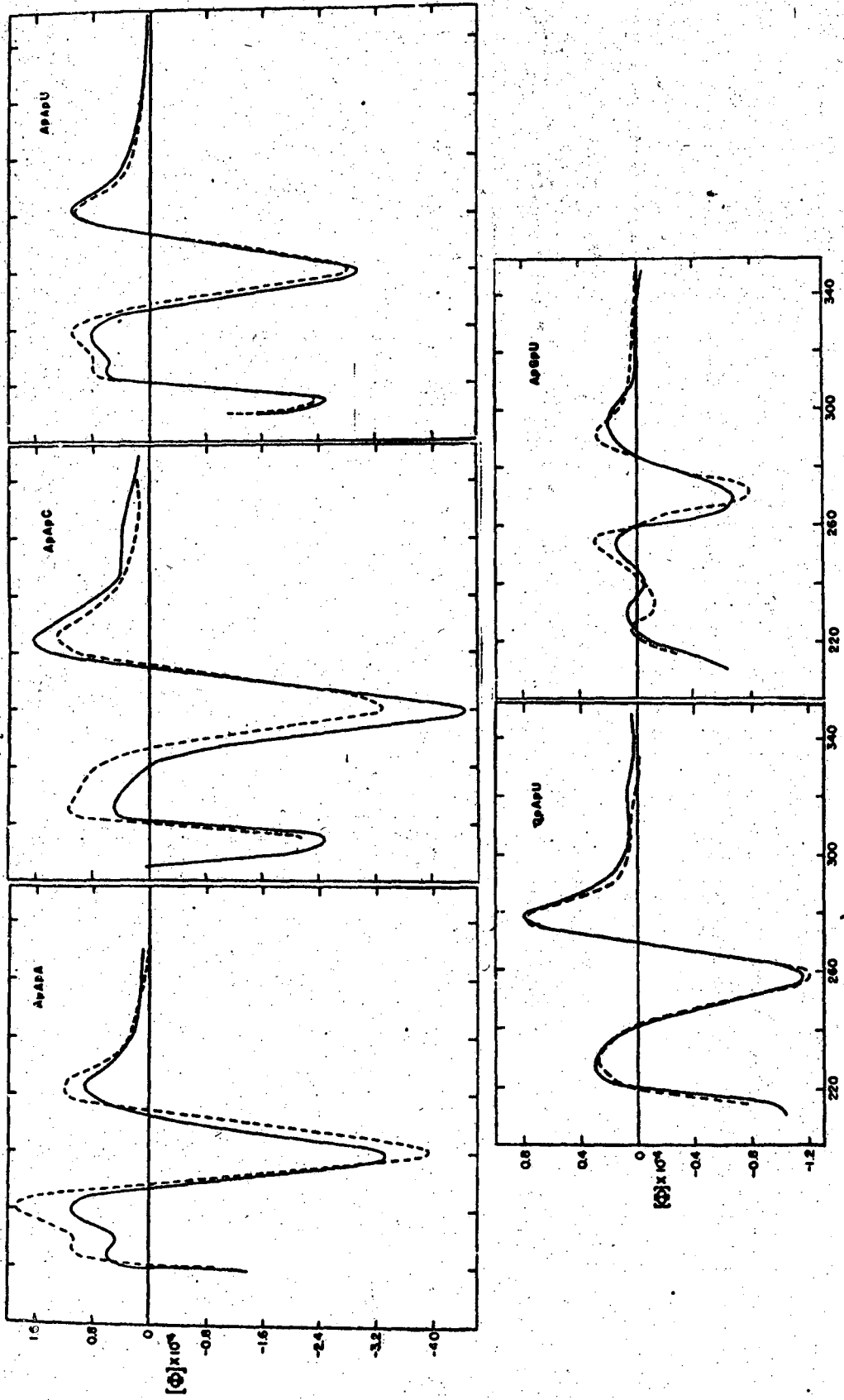
Figure 3-2

The ORD of the homopolymers of the four common RNA bases (5) and the CD of poly I (7) have been compared with the nearest neighbor calculation using Equation 3-2. The calculated and experimental spectra of poly rA, poly rU, poly rC, and poly rG are shown in Fig. 3-3.

Qualitative agreement is fairly good, though less so than in the case of trimer calculations. The agreement is best in the case of poly rU and worst for poly rG, which is probably aggregated (5). Again the calculated spectra are shifted to higher wavelengths relative to the experimental spectra. This shift is much larger for polymers than for trimers.

This discrepancy suggests that dimers and polymers have different spectral properties. This could be caused either by a difference in polymer geometry or by long range interactions in the polymer. The fact that poly rU, which is the least stacked polymer, agrees best with the nearest neighbor approximation suggests that long range symmetry of similarly stacked bases might alter the optical properties of the homopolymers. Another possibility is that intrastrand phosphate repulsion could change the orientation of the bases in the polymer.

It should be noted that dimers are a better model for trimers than for homopolymers.

Figure 3-3. The experimental ORD of four homopolymers
at neutral pH (———) is compared with the nearest
neighbor calculation (-----). (a) poly A, (b) poly C,
(c) poly U, and (d) poly G. These curves were taken
from S. R. Jaskunas (5).
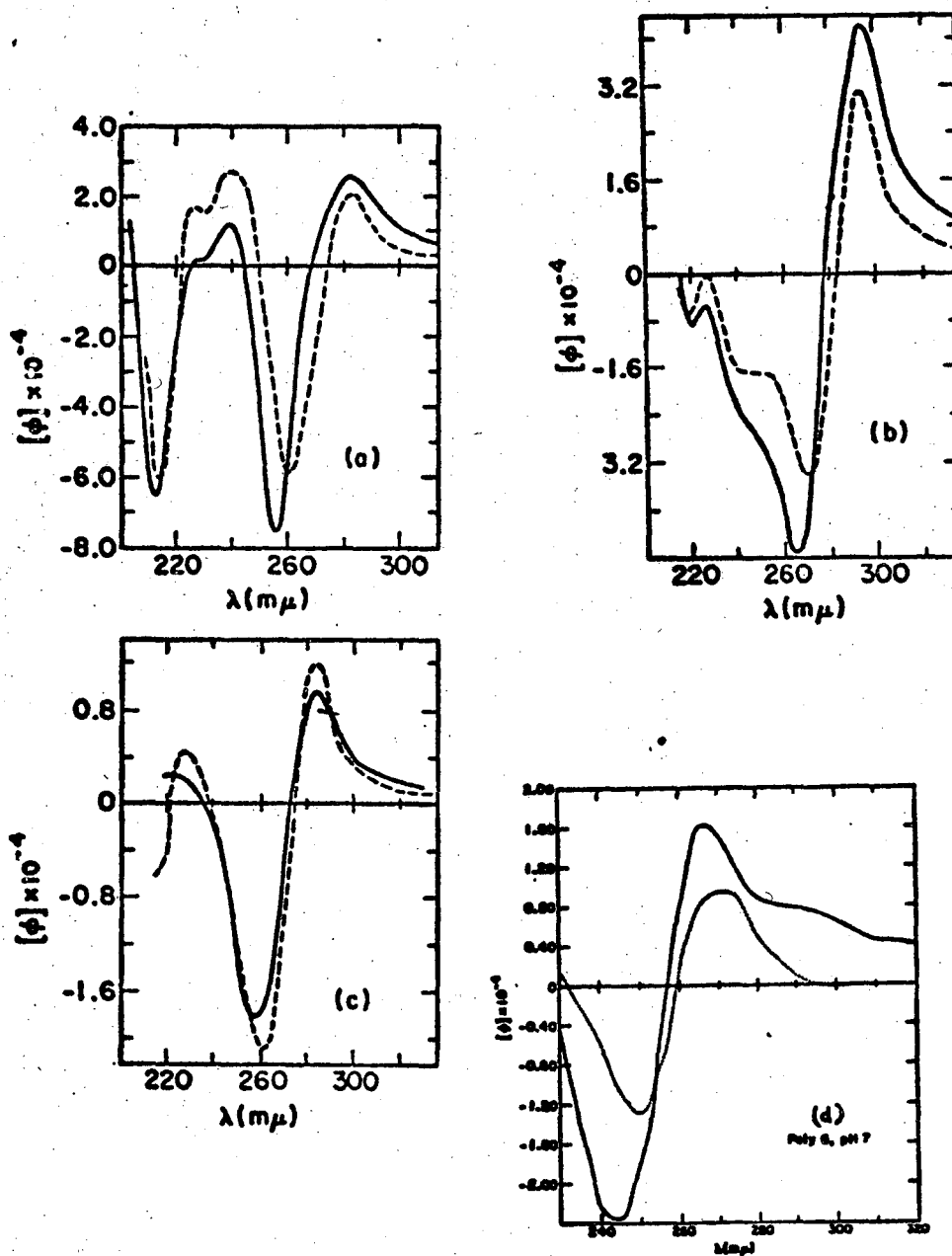
Figure 3-3

3. <u>The CD of Single Strand tRNA May be Approximated</u>
<u>by a Sum of Dinucleoside Monophosphate Basis</u>
<u>Spectra</u>.

Ignoring end effects, the CD of any single strand RNA
of known nearest neighbor frequency may be calculated in a
manner similar to that described for trimers and homo-
polymers using the nearest neighbor approximation:

$$(RNA) = \sum_{x=1}^{N} \sum_{y=1}^{N} 2F_{xy} (XY) - \sum_{x=1}^{N} F_x(X) \qquad (3-3)$$

where the RNA consists of N different types of bases.
F_{xy} and F_x are the number of times that the dimer
XY and the monomer X occur divided by the total
number of bases in the RNA, and (XY) and (X) are their
respective CD spectra. The mole fractions are obtained
by counting the number of times an interaction occurs
in the polymer and dividing by the total number
of interactions present in the RNA.

A. Single Strand Basis Spectra

For ease in calculating the CD of large RNAs it is
convenient to define a basis spectrum corresponding
to the contribution of the CD of the dimer XY to the
CD of an RNA:

$$[XY] = 2(XY) - \frac{1}{2} (X) - \frac{1}{2} (Y) \qquad (3-4)$$

where the quantities are as previously defined and [XY]

is a single strand basis spectrum.

Then, to calculate a spectrum it is necessary to merely count the number of each type of nearest neighbor interactions present and add a term for the two monomers at the end of the chain. For example, consider the oligomer ABCDE:

$$\frac{1}{5}\left((ABCDE) = [AB] + [BC] + [CD] + [DE] + \frac{1}{2}(A) + \frac{1}{2}(E)\right)$$

$$(3-5)$$

The single strand basis spectra of the four common bases at 25°C were obtained from 16 dimer and 4 monomer spectra of Cantor, et al. (10). Single strand basis spectra at 40°C were also needed for this study. The CD spectra of the 16 dimers and 4 monomers were measured at 40°C and are listed in Appendix 1 along with four spectra of dimers containing dihydrouridine measured by Dr. Carl Formoso (11).

The dimer spectra at 40°C have the same shapes and positions of extrema as at 25°C. However, the magnitudes of many of the peaks and troughs are decreased at 40°C. Different buffers were used for the 25°C and 40°C dimer measurements. Since the CD of the dimers is not very sensitive to salt concentration (8), the difference between these two sets of spectra is attributable to unstacking due to temperature, rather than to solvent effects.

B.   Modified Nucleoside Approximations

In addition to the four usual nucleosides A,U,C, and G, nearly all species of tRNA contain an average of 10% of modified bases, commonly referred to as minor or "odd" bases. Figure 3-4 shows the structures of most of these unusual nucleosides along with the abbreviations that will be used to represent them in this work.   The frequency with which they occur in the single and double strand regions of the nine species of tRNA being studied here is listed in Table 3-1. A* and X are bases whose structures are presently unknown.

The function of these minor bases in the activities of tRNA is one of the intriguing mysteries surrounding this molecule. It is reasonable to assume that they influence the structure or have some definite role in the function of tRNA.   If the unusual bases have no function it seems likely that they would disappear, thereby saving the cell the unnecessary work of synthesizing the enzymes to modify the precursor tRNA (7).

It should be noted that 91% of the modified bases in these tRNAs are found in single strand regions of the molecule (Table 3-1). The N_2-dimethyl, 1-methyl or greatly modified purines, D, 4tU and 3-methyl C will not form proper Watson-Crick base pairs. This suggests that at least some of the odd bases function to pre-
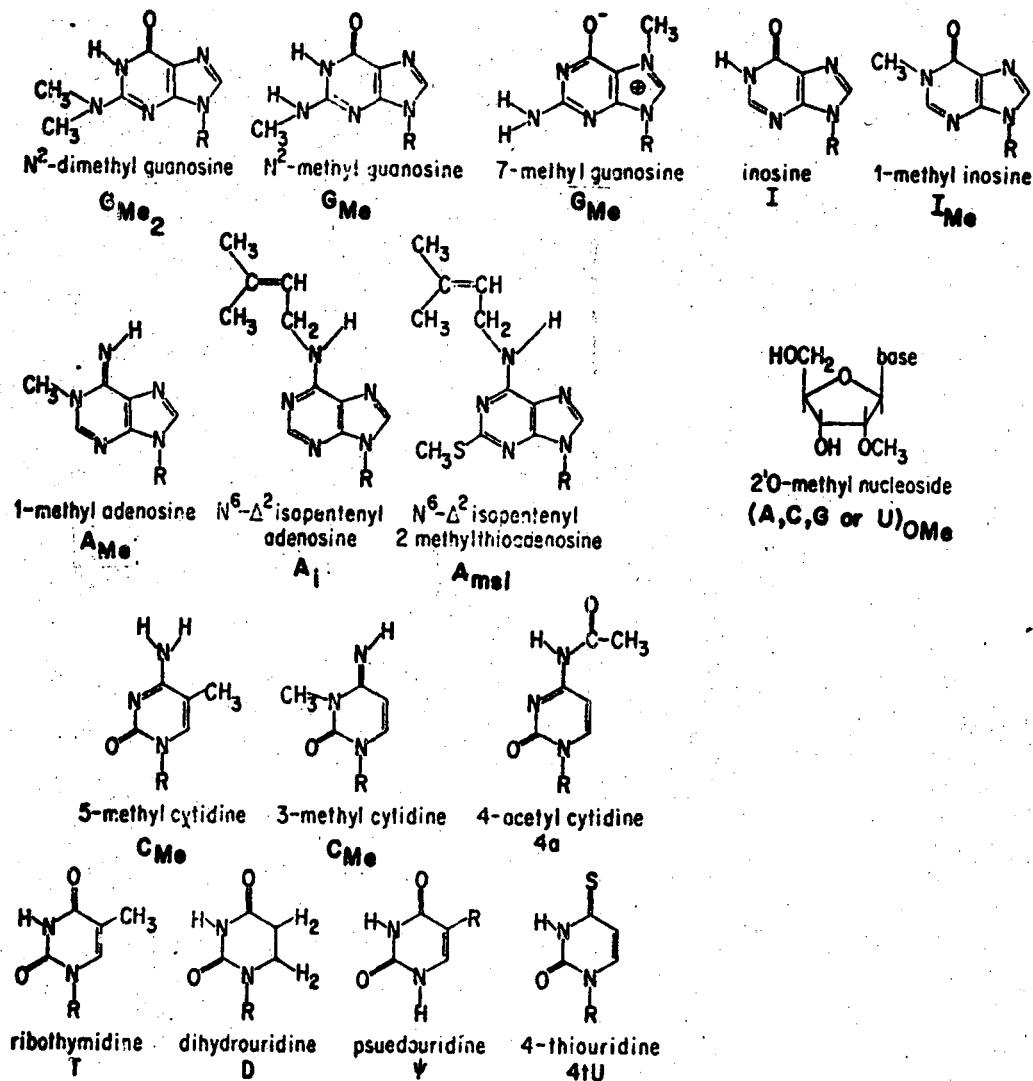
Figure 3-4

Some of the modified nucleosides found in tRNA and
abbreviations used to represent them. (R = ribose).
Taken from C. J. Formoso (7).

Table 3-1

Frequency of Modified Nucleosides in Nine tRNAs

	Single Strand Regions	Double Strand Regions
Adenine		
A_{Me}	4	
A_{msi}	2	
A_i	1	
A^*	3	
Uracil		
D	19	
T	9	
ψ	13	6
4tU	5	
Cytosine		
C_{Me}	2	2
C_{OMe}	3	
Guanine		
G_{Me}	9	
G_{Me_2}	3	
G_{OMe}	3	
G_i	1	
G^*	1	
X	2	
	80	8

vent the tRNA from assuming an incorrect secondary structure.

Dr. Carl Formoso carried out a study of the optical properties of two of the minor nucleosides, I and C (7). His CD spectra of AD, DA, GD, DD, and D at 40°C and 25°C are used in this work. The extrema of the dimers containing D are smaller and different in shape from those of their U-containing counterparts. Of the 28 nearest neighbor interactions involving D in these nine tRNAs, 20 are either DA, AD, GD, or DD. The remaining interactions involving D are assumed to have the same CD spectrum as DD, which consists of only a small peak and trough below 240 mμ. This is better than assuming these dimers have the same spectral properties as the analogus dimers containing U since D is not aromatic and doesn't absorb at 260 mμ . The CD of the 4 dimers containing D at 40°C are also tabulated in Appendix 1.

It would be very useful to have data on the optical properties of ψ which accounts for 22% of the modifications in these tRNAs and 16% of the total number of U's present. Only the CD of the dimers Aψ and ψA have been studied (12). They exhibit a CD spectrum of opposite sign but similar shape to those of AU and UA. To see if this was also the case for the ψ in the sequence TψCG, the CD of this sequence was calculated using the nearest neighbor approximation and assuming that $[T\psi] = - [UU]$ and that $[\psi C] = - [UC]$.

Agreement with the experimental TψCG CD spectrum
measured by Dr. Carl Formoso (7) was very poor (Fig. 3-5).
Thus it was not valid to assume that dimers containing
ψ exhibit the negative CD behavior of analogous dimers
containing U. ψ does behave like U in that it forms
stable base pairs with A. Until more information is
available, it is assumed that U and ψ have the same
optical properties.

One-third of the modifications in these tRNAs
involve only the addition of one or two methyl groups
to a base. This should not cause a great change in
the CD of the nucleotide, and it is valid to assume
that the spectral properties of methylated bases
approximate those of their unmethylated counterparts.

In this study, it is assumed that the CD spectral
properties of the other odd bases in tRNA are also
the same as those of the unmodified bases. The more
exotic bases, especially the heavily modified purines
usually found on the 3' end of the anticodon, will
probably have different CD spectra (12). However, until
the optical properties of these bases have been studied,
it must be assumed that they too resemble their
unmodified counterparts. Since about 2% of the bases
in the tRNAs are of this sort, only a small amount of
error is introduced into the nearest neighbor calcula-
tions by this assumption.

CD SPECTRA OF TψCG

····· Calculated assuming [Tψ] = -[UU] and [ψC] = -[UC]
----- Calculated assuming [Tψ] = [UU] and [ψC] = UC
───── Experimental spectrum (7).

LAMBDA IN MILLIMICRONS

[θ] × 10⁻⁴
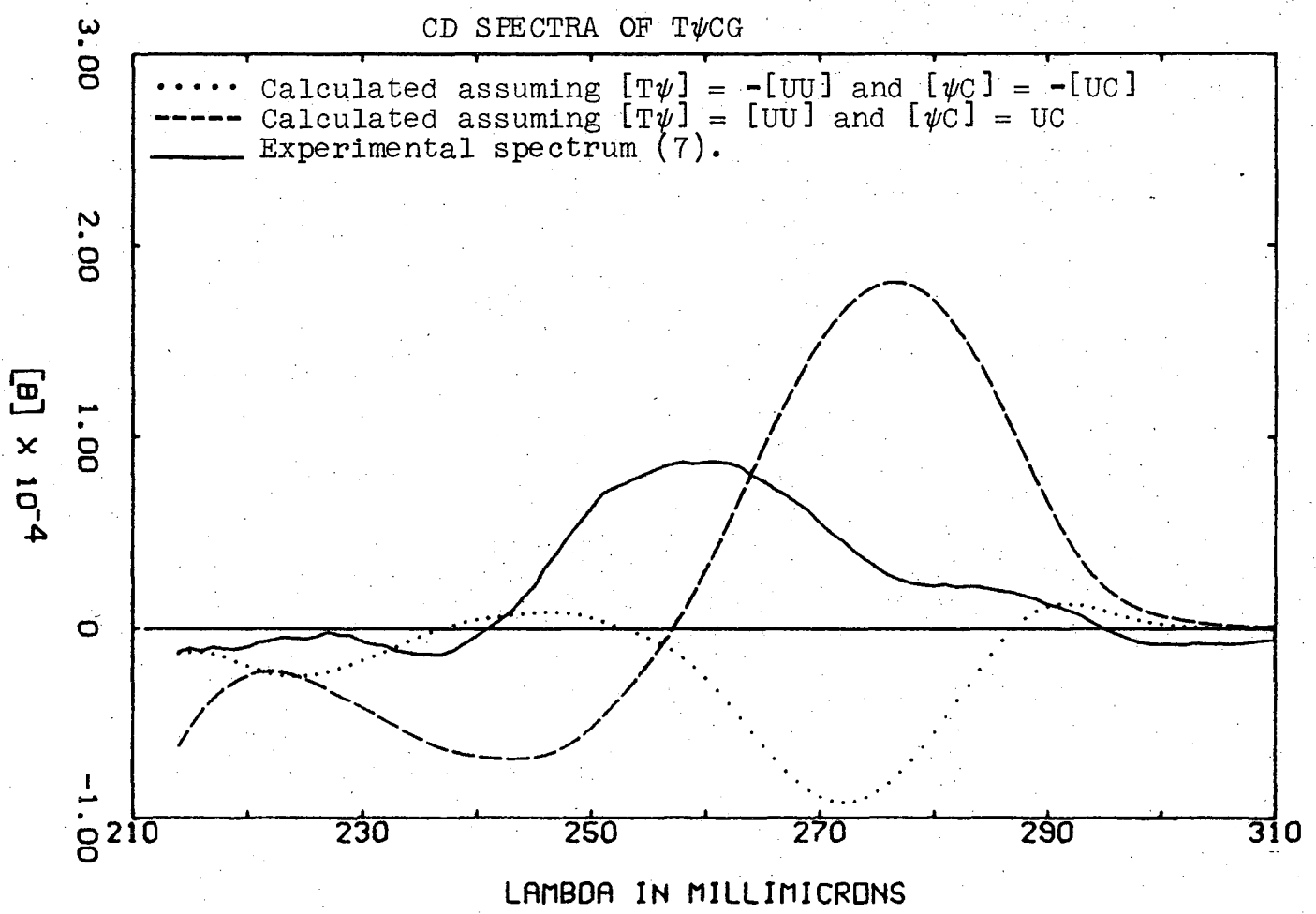
Figure 3-5

65

C. Single Strand RNA Spectra are Sensitive to
Base Composition and Sequence

To obtain some feeling for the meaning of changes
in the CD spectra of single strand RNAs it is useful
to calculate the spectra as a function of base composi-
tion. It is assumed that G and C are present in equal
amounts as are A and U, and that otherwise nearest
neighbor interactions are random. The CD of single
strand RNA between 0% and 100% GC may be calculated
using Equation 3-3 and the single strand basis spectra
as defined in Equation 3-4:

$$(RNA) = \sum_{x=1}^{4} \sum_{y=1}^{4} F_{xy}[XY] + \frac{1}{2} \sum_{x=1}^{2} F_x(X) \qquad (3-6)$$

where all terms are as previously defined and the
second sum is taken over the two end nucleosides.
The result is shown in Fig. 3-6 for polymers where
end effects are ignored.

It should be noted that the peak at 221 mμ is
particularly sensitive to the base composition and
shows an almost linear decrease in magnitude with an
increase in the percent of G and C present. A similar
effect has been observed in DNA (13).

The magnitude of the large peak also decreases
with increasing G and C until 80% GC, when it begins
to increase again. The position of this peak shifts to
higher wavelengths while the crossover shifts to lower
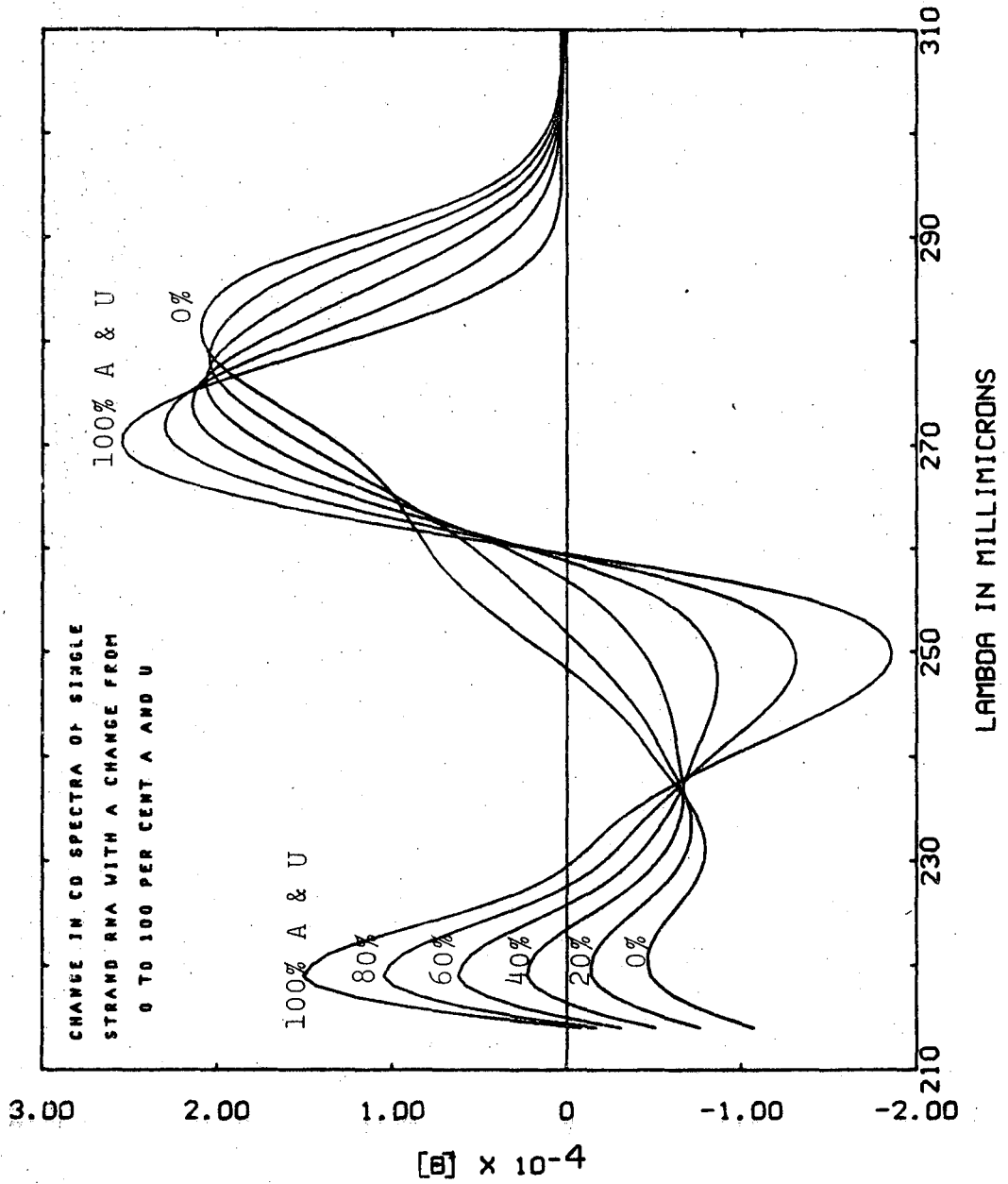
Figure 3-6

Spectra were calculated from sums of dimer basis
spectra using Equation 3-6.

wavelengths with increasing G and C.

There is a large negative trough at about 250 mμ in RNA that is composed of all A's and U's. This band decreases with an increase in the percent G and C and completely disappears in the sample that is all G's and C's. There is no band observed around 295 mμ in any of the single strand RNAs.

The CD of an RNA is also quite sensitive to sequence effects. To better understand this, we consider a somewhat extreme example of sequence variation. The calculated CD of four equimolar RNAs of different sequence are shown in Fig. 3-7. These RNAs each contain only four of the 16 possible nearest neighbor interactions. Although this example is somewhat artificial, it shows that CD spectra will vary with sequence.

Thus it is seen that CD spectra are quite sensitive to base composition and to sequence. The CD spectrum could plausibly be used as an analytic tool to obtain some measure of the composition of an unknown single strand RNA.

Figure 3-7. CD of equimolar single strand RNAs of varying sequence calculated using Equation 3-6 and assuming only certain nearest neighbor interactions are present.

CD OF EQUIMOLAR SINGLE STRAND RNA

—·— AG,GA,CU, and UC
······ AC,CA,GU, and UG
——— AU,UA,CG, and GC
— — AA,UU,CC, and GG

LAMBDA IN MILLIMICRONS

$[\theta] \times 10^{-4}$
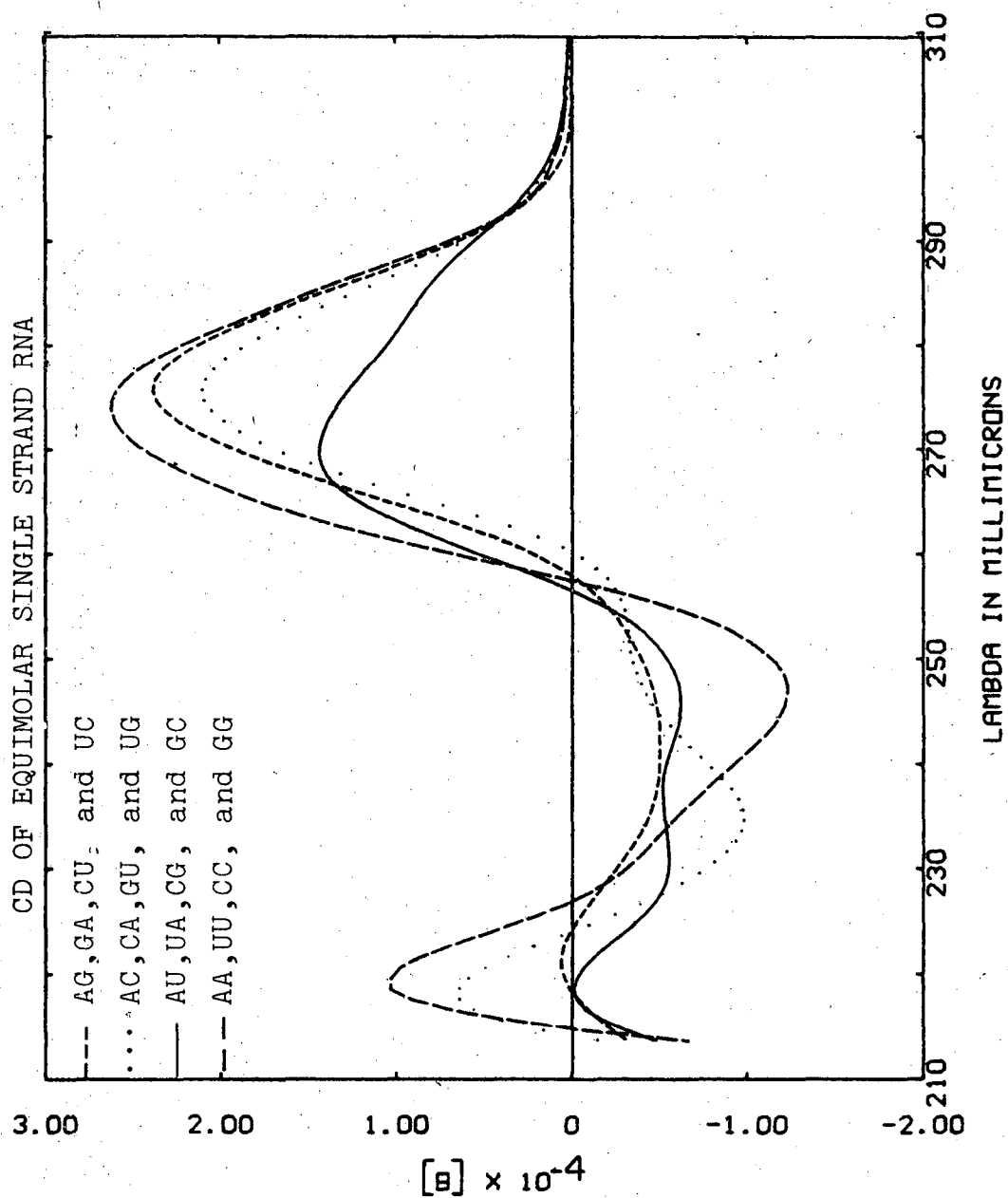
D. Variation in Nearest Neighbor Frequencies
of Nine tRNAs

From the sequences of the nine tRNAs the frequency
of each of 20 nearest neighbor interactions is tabu-
lated in Table 3-2. As previously discussed, it
was assumed that the minor nucleosides other than
D had the same CD as their unmodified counterparts.

Then the calculated CD of these tRNAs was found
by summing the basis spectra corresponding to these
nearest neighbor frequencies using Equation 3-6. The
results of these calculations are tabulated and com-
pared with the experimental CD of these single strand
tRNAs in the next chapter.

4. The CD of Double Strand Regions of RNA May be
Approximated by a Sum of Double Strand Polymer
Spectra.

The CD of the double strand regions of tRNA
may be calculated similarly to the method used for
single strand RNA. To do this, it is necessary to
know the spectra corresponding to the ten possible
double strand polymer interactions:

Table 3-2

Variation in Nearest Neighbor Frequencies of Nine tRNAs

	AA	AU	AC	AG	UA	UU	UC	UG	CA	CU	CC	CG	GA	GU	GC	GG	DD	AD	DA	GD
F. Met (E. coli)	5	2	2	4	1	1	7	2	5	3	9	9	2	5	7	10	0	0	1	1
Leu (Yeast)	6	4	2	8	3	6	6	4	7	4	4	5	5	5	7	5	2	0	0	1
Phe (E. coli)	3	4	1	6	1	4	6	3	4	2	9	6	5	4	4	8	1	0	1	2
Phe (Wheat)	4	3	4	6	1	1	6	3	6	4	3	7	7	3	6	6	3	0	0	2
Phe (Yeast)	4	4	3	7	1	4	5	5	6	4	3	4	8	3	6	5	2	0	0	1
Tryp (E. coli)	4	0	3	6	2	3	7	2	3	4	8	5	3	7	3	9	2	1	1	1
Tyr (E. coli)	6	3	4	5	1	4	8	3	6	4	11	6	6	5	4	8	0	0	0	0
Tyr (Yeast)	5	1	3	6	2	2	5	2	3	5	6	7	6	3	5	7	5	1	1	2
Val (E. coli)	1	3	4	6	2	3	7	1	7	3	8	4	5	4	4	11	2	0	0	0

$$(1)\ \overleftarrow{\underset{\text{UU}}{\text{AA}}}\ ,\ (2)\ \overleftarrow{\underset{\text{CC}}{\text{GG}}}\ ,\ (3)\ \overleftarrow{\underset{\text{UA}}{\text{AU}}}\ ,\ (4)\ \overleftarrow{\underset{\text{AU}}{\text{UA}}}\ ,\ (5)\ \overleftarrow{\underset{\text{CG}}{\text{GC}}}\ ,\ (6)\ \overleftarrow{\underset{\text{GC}}{\text{CG}}}\ ,$$

$$(7)\ \overleftarrow{\underset{\text{UG}}{\text{AC}}}\ ,\ (8)\ \overleftarrow{\underset{\text{GU}}{\text{CA}}}\ ,\ (9)\ \overleftarrow{\underset{\text{AG}}{\text{UC}}}\ ,\ (10)\ \overleftarrow{\underset{\text{GA}}{\text{CU}}}\ .$$
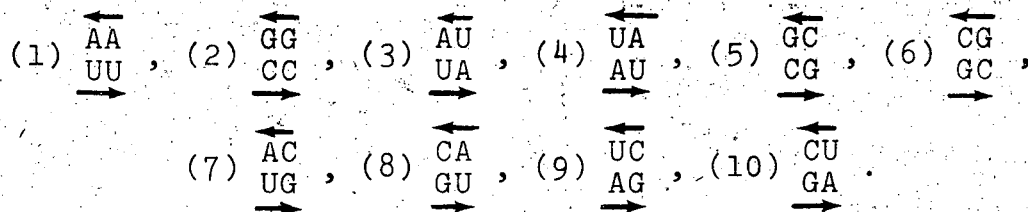
Then, at each wavelength, the CD of a double strand RNA is given by:

$$(\text{RNA})\ =\ \sum_{P=1}^{10}\ F_P\ (P) \tag{3-7}$$

where F_P is the frequency of the interaction P and the sum is taken over 10 interactions listed above.

Work is in progress in this laboratory to obtain the optical properties of all 10 of these interactions from a set of double strand RNA oligomers (14). However, this information is not yet available, and the calculations in this work are based on the spectra of five RNA double strand polymers and several approximations.

A. Double Strand Polymer Approximations

The polymer spectra which have been measured in this laboratory by Dr. Donald Gray and Dr. Dana Carroll are listed in Appendix 2. These polymers are poly A:poly U, poly G:poly C, poly AU:poly AU, poly GC:poly GC, and poly CA:poly GU. In order to approximate the double strand regions of tRNA using only these polymer spectra, a number of approximations are necessary:

(i) It was assumed that the following inter-actions were the same:

$$\frac{\overleftarrow{AU}}{\underrightarrow{UA}} = \frac{\overleftarrow{UA}}{\underrightarrow{AU}} \; ; \; \frac{\overleftarrow{GC}}{\underrightarrow{CG}} = \frac{\overleftarrow{CG}}{\underrightarrow{GC}} \; ; \; \frac{\overleftarrow{AC}}{\underrightarrow{UG}} = \frac{\overleftarrow{CA}}{\underrightarrow{GU}} \; ; \; \frac{\overleftarrow{UC}}{\underrightarrow{AG}} = \frac{\overleftarrow{CU}}{\underrightarrow{GA}} \; . \qquad (3-8)$$

This assumption will be valid if either the spectra of the two interactions are similar or there are nearly the same number of each of a pair of interactions. We have no information about the former assumption but the validity of the latter for the nine species of tRNA being studied can be determined from Table 3-3 which lists the frequency of each of the 10 inter-actions for the nine tRNAs being studied.

(ii) The CD spectrum of the double strand ribo-polymer poly GA:poly CU has not been measured. It is approximated using the observation that this polymer consists of one strand of purines and another of pyrimidines. Switching every second base from one chain to the other would result in the poly GU:poly CA whose optical properties are known. Since a similar alternation would change $\frac{\overleftarrow{AA}}{\underrightarrow{UU}}$ to $\frac{\overleftarrow{AU}}{\underrightarrow{UA}}$ and $\frac{\overleftarrow{GG}}{\underrightarrow{CC}}$ to $\frac{\overleftarrow{GC}}{\underrightarrow{CG}}$ it was assumed that

$$\frac{\overleftarrow{GA}}{\underrightarrow{CU}} - \frac{\overleftarrow{GU}}{\underrightarrow{CA}} = \frac{1}{2}\left(\frac{\overleftarrow{AA}}{\underrightarrow{UU}} - \frac{\overleftarrow{AU}}{\underrightarrow{UA}} + \frac{\overleftarrow{GG}}{\underrightarrow{CC}} - \frac{\overleftarrow{GC}}{\underrightarrow{CG}} \right). \qquad (3-9)$$

Spectra corresponding to several other methods of approximating this interaction were tried. How-ever, this method was chosen as it gave the best agree-ment with experimental results.

(iii) Since there are no polymer spectra avail-
able to represent interactions involving the G:U base
pairs which are occasionally found in tRNA, these
interactions are approximated by the average of the
corresponding interactions involving G:C and A:U base
pairs. For example, it is assumed that

$$\left(\overrightarrow{\frac{AGU}{UUA}}\right) = \frac{1}{2}\left(\overleftrightarrow{\frac{AG}{UC}}\right) + \frac{1}{2}\left(\overleftrightarrow{\frac{AA}{UU}}\right) + \frac{1}{2}\left(\overleftrightarrow{\frac{GU}{CA}}\right) + \frac{1}{2}\left(\overleftrightarrow{\frac{AU}{UA}}\right) . \qquad (3\text{-}10)$$

(iv) Odd base approximations are not nearly so
important in the calculation of double strand regions
of tRNA as in single strand regions. Since only 1%
of the nucleosides in double strand regions of tRNA
are modified, the assumption that their spectra are
the same as of the unmodified nucleosides should not
greatly affect the validity of the calculation of the
CD of double strand regions of tRNA.

B. Double Strand RNA Spectra Vary with Type of
     Base Pairs Present

Figure 3-8 shows the change in the CD spectra of
random double strand RNA as the relative percent of
A:U and G:C base pairs present varies. These curves
were calculated using Equation 3-7, five experimental
double strand RNA polymer spectra and approximation
(ii) discussed above for the unknown polymer spectrum.

Again there is a linear variation in the magnitude
of the band at 220 mμ with percent of G:C pairs. There
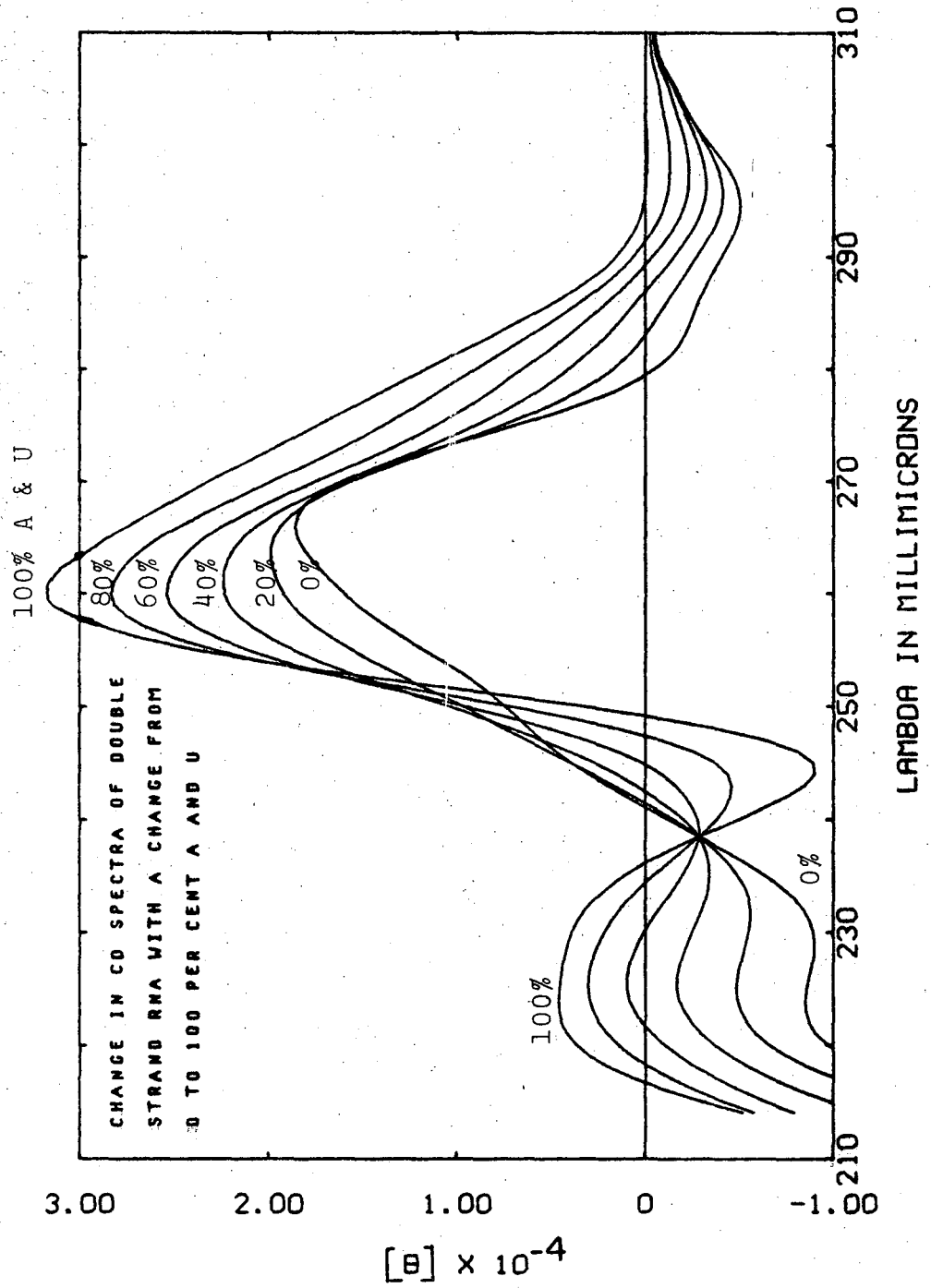
Figure 3-8

Double strand RNA spectra were calculated from
sums of polymer spectra using Equation 3-7.

is a similar change in the 260 mμ band, which also

shifts to slightly higher wavelengths with an increase

in G:C. At the same time, the crossover around

240 mμ shifts to lower wavelengths. The trough at

295 mμ increases with increasing percent G:C inter-

actions.

C. Variation of Double Strand Interaction
    Frequencies in Nine tRNAs

The double strand regions of tRNA may be thought

of as three helical regions. The first helix, which

contains 11 double strand interactions, extends from

the AGCX to the TψC loop. The second helix of four

interactions closes the anticodon loop. The third

helix contains two or three double strand interactions

and is adjacent to the D loop.

The number of each of the 10 possible double

strand interactions in each of these three helical

regions were counted for each tRNA and are listed in

Table 3-3. It can be seen that there is considerable

variation in interaction frequencies among the tRNAs

being studied though in general these regions are

much more rich in GC interactions than in AU inter-

actions.

Table 3-3

Variation in Polymer Interaction Frequencies of Nine tRNAs

	← AA / UU →	← GG / CC →	← AU / UA →	← UA / AU →	← GC / CG →	← GG / GC →	← GU / CA →	← UG / AC →	← GA / CU →	← AG / UC →
F. met (E. coli)	0	15	0	0	5	6	1	0	5	2
Leu (Yeast)	5	6	2	3	3	1	5	2	6	7
Phe (E. coli)	2	14	0	0	4	3	2	1	7	4
Phe (Wheat)	0	4	0	0	6	4	3	5	8	6
Phe (Yeast)	6	6	2	0	4	2	2	6	8	6
Tryp (E. coli)	1	14	0	0	3	4	3	0	5	6
Tyr (E. coli)	2	16	0	0	2	0	4	4	5	4
Tyr (Yeast)	2	12	0	0	4	4	0	3	5	4
Val (E. coli)	0	2	2	0	3	2	3	4	7	4

5. The CD Spectra of Native tRNA May be Approximated by a Sum of CD Spectra of Simpler RNAs.

    A. Calculation of tRNA at 25°C from Dimer and Polymer Sum

The CD spectrum of a native tRNA at 25°C can be considered as the sum of contributions from the single strand parts of the molecule, the double strand parts, and the tertiary structure:

$$(tRNA) = \sum_{x=1}^{5} \sum_{y=1}^{5} F_{xy}[XY] + \sum_{P=1}^{6} F_P(P) + \sum_{M=1}^{2} F_M(M) + (T)$$

(3-11)

[XY] is a dimer basis spectrum and the sum is taken over the bases A,U,C,G, and D, (P) is a polymer spectrum and the sum is taken over the six double strand polymers, (M) is the CD of the monomers at the ends of the RNA chain, and (T) is the contribution of the tertiary structure to the CD of tRNA.

Ways of approximating all of these quantities except the tertiary structure have been discussed. For the present the tertiary structure contribution to the CD spectrum of the tRNA will be ignored, and (T) will be set equal to zero.

End effects between single and double strand regions are accounted for by including these nucleosides in both the single and double strand regions.

This method can be better understood by considering in detail the interactions present in one loop of a tRNA molecule.

For example, let us consider the TψC loop of tRNA^{Phe} (Yeast) which contains 17 nucleosides:
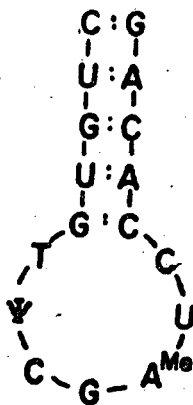
```
        C : G
        U : A
        G : C
        U : A
       G ' C
      T       C
     Ψ          U
      C         A^Me
        G —
```

$$(loop) = \frac{1}{17}\left\{ 2\left(\overset{\longleftarrow}{\underset{\longrightarrow}{\begin{matrix}CU\\GA\end{matrix}}}\right) + 2\times 2\left(\overset{\longleftarrow}{\underset{\longrightarrow}{\begin{matrix}UG\\AC\end{matrix}}}\right) + 2\left(\overset{\longleftarrow}{\underset{\longrightarrow}{\begin{matrix}GU\\CA\end{matrix}}}\right) + [GU] + [UU] \right.$$

$$+ [UC] + [CG] + [GA] + [AU] + [UC]$$

$$\left. + [CC] + \frac{1}{2}(C) + \frac{1}{2}(G) \right\} \qquad\qquad (3\text{-}12)$$

Square brackets denote single strand basis spectra, terms such as $\left(\overset{\longleftarrow}{\underset{\longrightarrow}{\begin{matrix}CU\\GA\end{matrix}}}\right)$ are double strand polymer CD spectra and (C) and (G) are monomer CD spectra.

It should be noted that the CD of the interactions involving T, ψ, and U_{Me} are assumed to be the same as those involving U. Tertiary structure is not considered in this calculation. It is assumed that the spectra of the bases in a loop is the same as that of the bases in single stranded RNA.

B. Calculation of tRNA CD Spectra at 40°C

from a Sum of Single Strand tRNA and

Base Pairing Interaction Basis Spectra

An alternate method for approximating the CD of the loop above is as the sum of the CD of the single stranded loop and the CD from the formation of the appropriate base pair interactions.

$$(RNA,N)_T = (RNA,SS)_T + \sum_{P=1}^{6} F_P \{P\} \qquad (3\text{-}13)$$

where $(RNA,N)_T$ is the CD of the native RNA at some temperature T, $(RNA,SS)_T$ is the CD of the RNA in a single stranded form at T, F_P is the frequency of the base pairing interaction $\{P\}$ at T, and the sum is taken over the six polymer pairing interactions.

As will be shown in Chapter IV, temperatures of about 40°C and very low salt are needed for the formation of single stranded tRNA. Therefore, it is necessary to construct a set of double strand basis spectra corresponding to the formation of base pairs at 40°C; that is, the difference between the single stranded and double stranded polymers. The approximations previously discussed were used along with the five experimental spectra for the double strand polymers. The single strand polymers were approximated using the nearest neighbor approximation and the dimer and monomer spectra at 40°C listed in

Appendix 1. Since the spectra of both the dimers and the polymers approach those of the monomers at high temperatures, it is likely that the dimers at 40°C provide a better model for the single strand polymers at this temperature than do the dimers at 25°C for the polymers at 25°C.

A base pairing interaction basis spectrum is defined as:

$$\left\{\overleftrightarrow{\begin{matrix}X\ Y\\X'Y'\end{matrix}}\right\} = \left(\overleftarrow{\begin{matrix}X\ Y\\X'Y'\end{matrix}}\right) - \tfrac{1}{4}[XY] - \tfrac{1}{4}[YX] - \tfrac{1}{4}[X'Y'] - \tfrac{1}{4}[Y'X']$$

$$(3-14)$$

where square brackets, [ ], denote dimer basis spectra which according to the nearest neighbor approximation represent the single strand polymer spectra, and curly brackets, { }, represent the double strand pairing basis spectrum of the poly rXY:poly rX'Y', and, as usual, curved brackets, ( ), represent an experimental CD spectrum.

Using these basis spectra, we may approximate the CD of the above TψC loop in a second manner:

$$(loop,N)_{40°} = \tfrac{1}{17}\left(9(loop,SS)_{40°} + 2\left\{\overleftrightarrow{\begin{matrix}CU\\GA\end{matrix}}\right\} + 2\times2\left\{\overleftrightarrow{\begin{matrix}UG\\AC\end{matrix}}\right\} + 2\left\{\overleftrightarrow{\begin{matrix}GU\\CA\end{matrix}}\right\}\right)$$

$$(3-15)$$

where the terms are as previously defined.

C.   Change in Calculated tRNA Spectrum with Base
Composition

According to the Holley model, about one-half
of the nucleotides in a tRNA molecule are in double
stranded regions. Therefore, it is of interest to
consider the effect of base composition upon an RNA
that is 50% double strand and 50% single strand.
Assuming that the amounts of G and C are equal and
the amounts of A and U are also equal, curves may
be calculated corresponding to the CD spectra as a
function of percent G and C. A set of such curves
are shown in Fig. 3-9. With an increase in percent
GC, both peaks decrease, the crossover shifts to lower
wavelengths, and the peak at 295 mμ increases in
magnitude. The shifts in the position of the large
maximum observed in the cases of single strand and
double strand RNA considered separately seem to cancel
each other, so this peak does not move much.

The position and magnitude of the maxima of
the calculated curves as a function of percent GC for
100%, 50% and 0% double strand RNA are tabulated in
Table 3-4.

6.   Computers are Used to Record and Analyze Data

A.   Data is Recorded by an On-Line Computer

CD data were recorded by a Digital Equipment

CHANGE IN CD SPECTRA OF HALF SINGLE
AND HALF DOUBLE STRAND RNA WITH CHANGE
FROM 0 TO 100 PERCENT A AND U
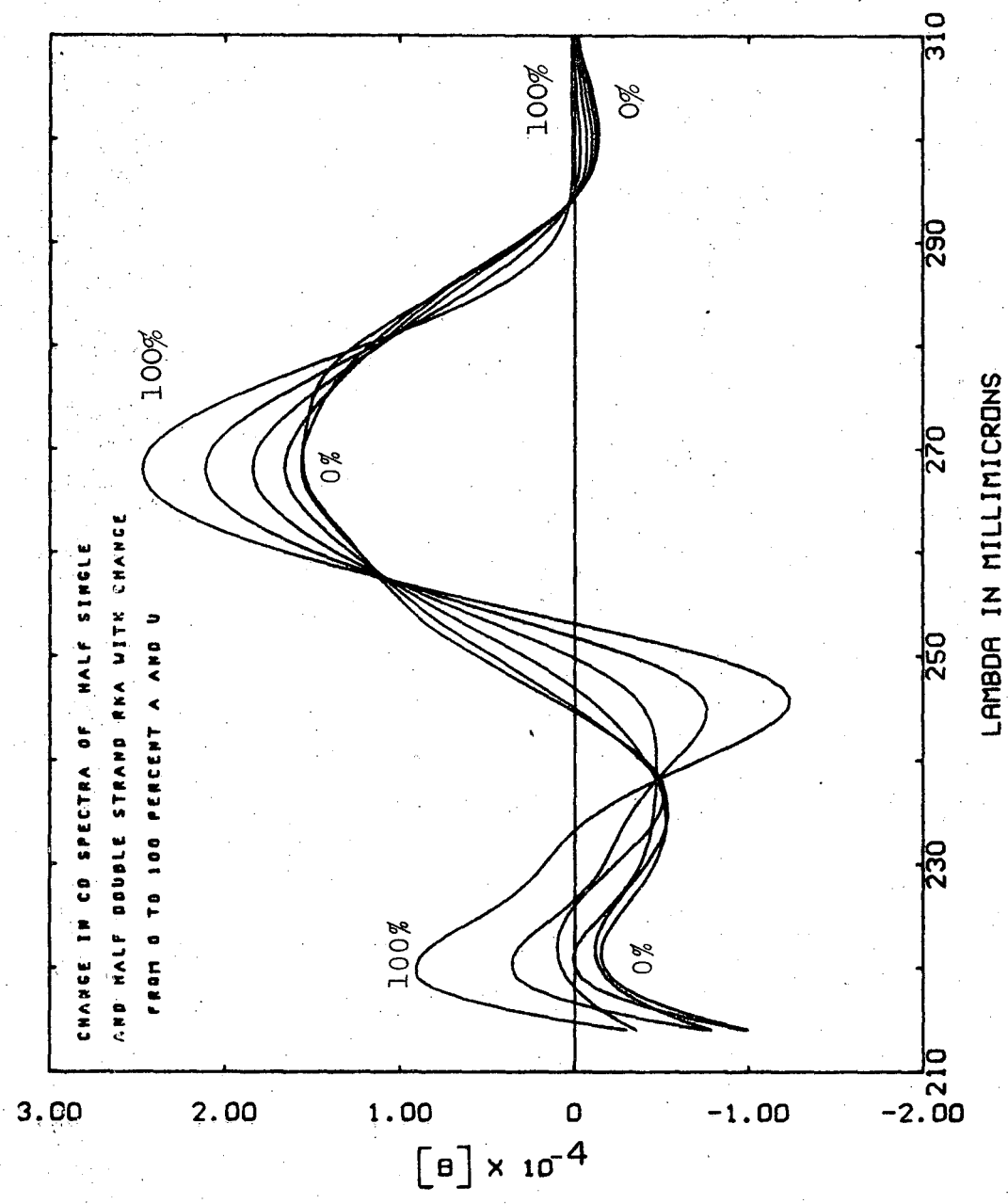
Figure 3-9

Spectra were calculated using Equation 3-11

Table 3-4

Position and Magnitude of CD Maximum in Calculated RNA Spectra

% G & C	100% Single Strand RNA				50% Single Strand and 50% Double Strand				100% Double Strand			
	λ_{max}	$[\theta] \times 10^{-4}$	λ_{max}	$[\theta] \times 10^{-4}$	λ_{max}	$[\theta] \times 10^{-4}$	λ_{max}	$[\theta] \times 10^{-4}$	λ_{max}	$[\theta] \times 10^{-4}$	λ_{max}	$[\theta] \times 10^{-4}$
0	270	2.54	219	1.51	268	2.47	220	.91	260	3.12	224	.46
20	272	2.30	219	1.05	268	2.12	220	.36	260	2.84	225	.31
40	274	2.14	219	.62	268	1.85	221	.01	260	2.54	225	.10
60	276	2.06	219	.22	268	1.67	221	-.14	261	2.24	225	-.16
80	279	2.05	220	-.13	268	1.57	222	-.12	264	1.99	225	-.48
100	281	2.09	221	-.45	268	1.47	222	-.67	266	1.86	224	-.85

Corporation PDP 8/S computer. SUPERSPECTRUM, a program written by Dr. B. L. Tomlinson, was used to calculate data points from the average of about 300 points taken over 1 mμ (15). The CD data, expressed as molar ellipticity per residue was calculated from:

$$\text{data} = (\text{spectrum} - \text{baseline}) \times \varepsilon/OD \qquad (3\text{-}16)$$

where ε is the extinction coefficient at 258 mμ as previously discussed. The CD data was punched onto a paper tape following the recording of each spectrum. Data points were recorded every 1 mμ. For the analytic procedures, 100 data points between 310 and 210 mμ were used.

B. Further Analysis is Carried out by a CDC 6600

The paper tapes are converted to cards using BAKER, a program written by Dr. Martin Itzkowitz.

The spectra are then plotted by a program entitled GLACER,* which also corrects for baseline shifts and provides the opportunity to change the values of ε and OD that were originally used to calculate the data points. This program and those that will be subsequently discussed are listed in Appendix 3.

The data plots are examined by eye for obviously bad points due to mispunched tapes or errors in recording the spectra. These points are replaced with values

---

*Titles of the 6600 computer are limited to six letters and names of mountains are therefore abbreviated.

interpolated from the points adjacent to the bad point.

The data is then read into the program TAHOMA
which fits 13 data points with a cubic which reduces
the noise level of the data (16). The smoothed data
for each of two or three similar scans is then
averaged at each wavelength by RANIER. The experi-
mental tRNA spectra being studied are thus the average
of several smoothed spectra taken at different times.

STHLNS was used to obtain difference spectra
between sets of experimental or between calculated
and experimental spectra at 100 wavelengths.

C. Calculation of Spectra from Basis Spectra

CD spectra for tRNA were calculated from dimer
and polymer basis spectra using SHASTA which is based
upon Equation 3-11. Double strand pairing inter-
actions were calculated using MTADMS which is
based on Equation 3-12. Both of these programs were
adopted from NNPOLY which was written by Mr. Phil
Borer (17). Single strand basis spectra were calcu-
lated using LASSEN, and double strand pairing
interactions were calculated from a slightly modified
version of SHASTA. Another version of SHASTA called
TINA was used to generate sets of CD curves as a
function of base composition and percent single
strand such as Figures 3-6 to 3-8.

Calculated and experimental spectra were compared
by MTHOOD, which calculated the root mean square

deviation between the two spectra and normalizes by
dividing by the square of the experimental values:

$$\text{Fit} = \left(\frac{\sum_{i=1}^{N} (E_i - C_i)^2}{\sum_{i=1}^{N} (E_i)^2} \right)^{1/2} \qquad (3\text{-}17)$$

where E_i is the value of the experimental curve at
the i-th wavelength, C_i is the value of the calculated
CD curve at this same wavelength, and the sum is taken
over N wavelengths. Thus "Fit" is a measure of how
well two curves agree. Values of "Fit" will be later
tabulated comparing experimental and calculated CD
spectra.

The relationship of the programs just described
is shown in Fig. 3-10. Listings of these programs and
a discussion of their use is to be found in Appendix 3.

Figure 3-10

The relationship of computer programs used to
analyse, calculate, and compare CD spectra of tRNAs.

REFERENCES TO CHAPTER III

1. P. K. Sarkar, B. Wells, and J. T. Yang, J. Mol. Biol., 25, 563 (1967).

2. M. M. Warshaw and I. Tinoco, Jr., J. Mol. Biol., 19, 29 (1966).

3. M. M. Warshaw and I. Tinoco, Jr., J. Mol. Biol., 13, 54 (1965).

4. C. R. Cantor and I. Tinoco, Jr., Biopolymers, 5, 821 (1967).

5. S. R. Jaskunas, Jr., Thesis, University of California, Berkeley (1968).

6. J. R. MacDonald and M. K. Brackmen, Rev. Mod. Phys., 28, 393 (1956).

7. C. J. Formoso, Thesis, University of California, Berkeley (1970).

8. R. Davis, Thesis, University of California, Berkeley (1967).

9. C. Cantor, S. Jaskunas, and I. Tinoco, Jr., J. Mol. Biol., 20, 39 (1966).

10. M. Warshaw and C. Cantor, Biopolymers, 9, 1079 (1970).

11. C. Formoso and I. Tinoco, Jr., Biopolymers, 10, 1533 (1971).

12. M. P. Schweizer, R. Thedford, and J. Stama, Biochim. Biophys. Acta, 232, 217 (1971).

13. F. S. Allen, D. M. Grey, G. P. Roberts, and I. Tinoco, Jr., Biopolymers, submitted.

14. P. Borer, personal communication.

15. B. L. Tomlinson, Thesis, University of California, Berkeley (1968).

16. A. Savitzy and J. J. E. Golay, <u>Anal. Chem</u>., 36, 1627 (1964).

17. P. Borer, personal communication.

CHAPTER IV.

RESULTS

1. The UV Absorption of tRNA in the Presence and Absence of Magnesium is Quite Different

The temperature dependence of the 260 mμ absorbance of nine species of tRNA in 10^{-5} M EDTA and 1 mM $MgCl_2$ (pH 7.8) is shown in Figs. 4-1 to 4-9. The two curves shown in each figure were obtained from one sample of tRNA that was first heated in the absence of Mg^{++}, cooled, and then reheated in the presence of Mg^{++}.

There is qualitative similarity between the temperature versus absorption curves for these nine tRNAs. In the absence of Mg^{++}, there is a gradual increase in absorption with temperature which is nearly complete at 40°C. The addition of 10^{-3} M Mg^{++}, which is about 10 Mg^{++} ions per tRNA nucleotide, causes the curve to become much steeper and to shift to higher temperatures. The peculiar looking decrease in absorption around 50°C in the curves for tRNA^{Leu} (Fig. 4-2) and tRNA^{Tryp} (Fig. 4-6) in the presence of Mg^{++} is due to the existence of two stable forms of these tRNAs which are called native and denatured. This phenomenon will be discussed in detail later in this chapter.

Figures 4-1 to 4-9. The change in absorption of the
nine species of tRNA with temperature. The curve on
the left was measured in 10^{-5} M EDTA at pH 8.5 after
sample had been dialysed to remove as much salt as
possible. The curve on the right was measured in
1 mM $MgCl_2$, 10 mM tris HCl, pH 7.8. These conditions
were also used for the measurement of single strand
and native CD spectra shown in Figures 4-10 to 4-27.
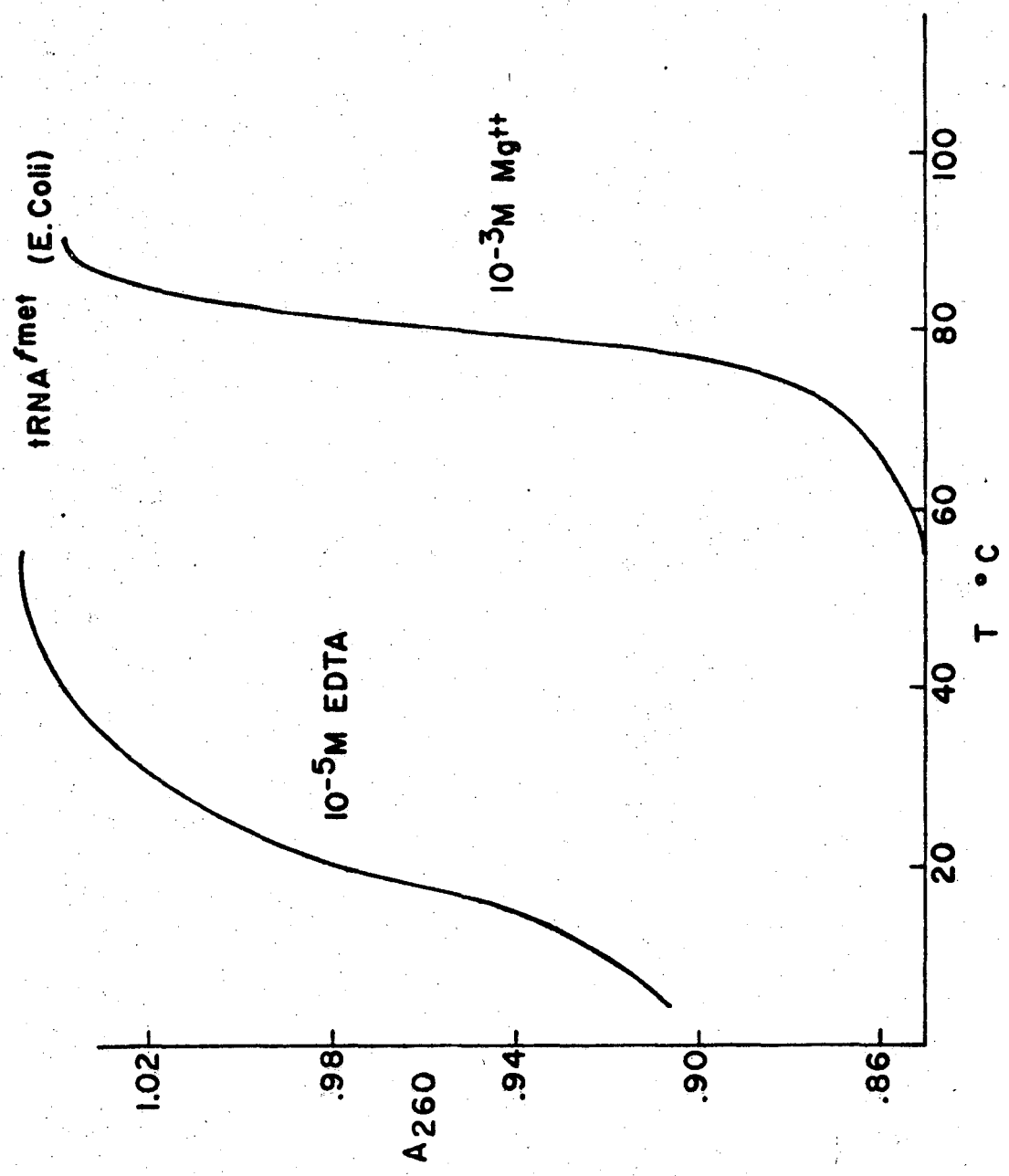
Figure 4-1

Figure 4-2

Figure 4-3

tRNA Phe (Wheat Germ)

10^{-3}M Mg^{++}

10^{-5}M EDTA

T °C

A$_{260}$

.96 .92 .88 .84 .80

20 40 60 80 100
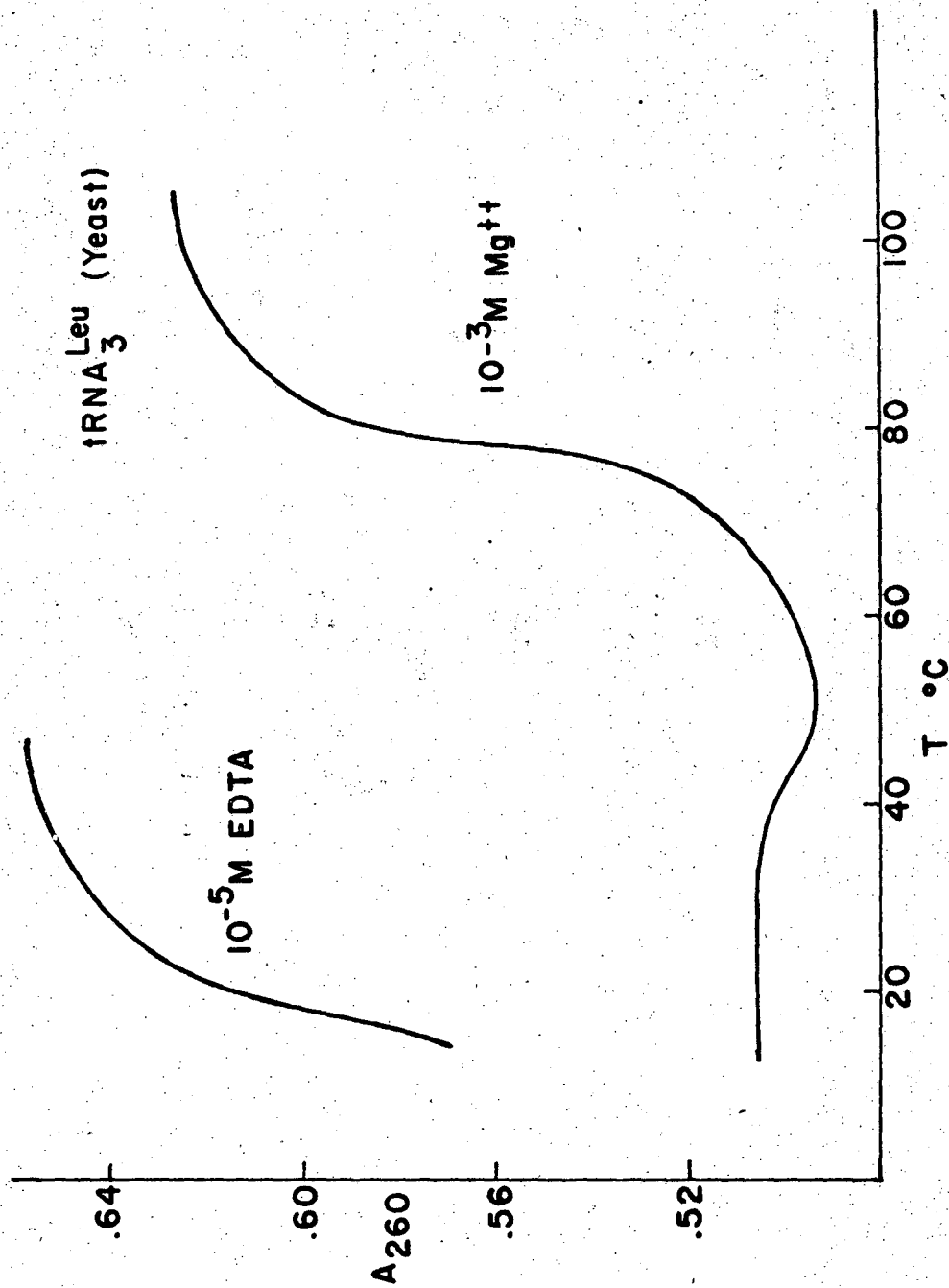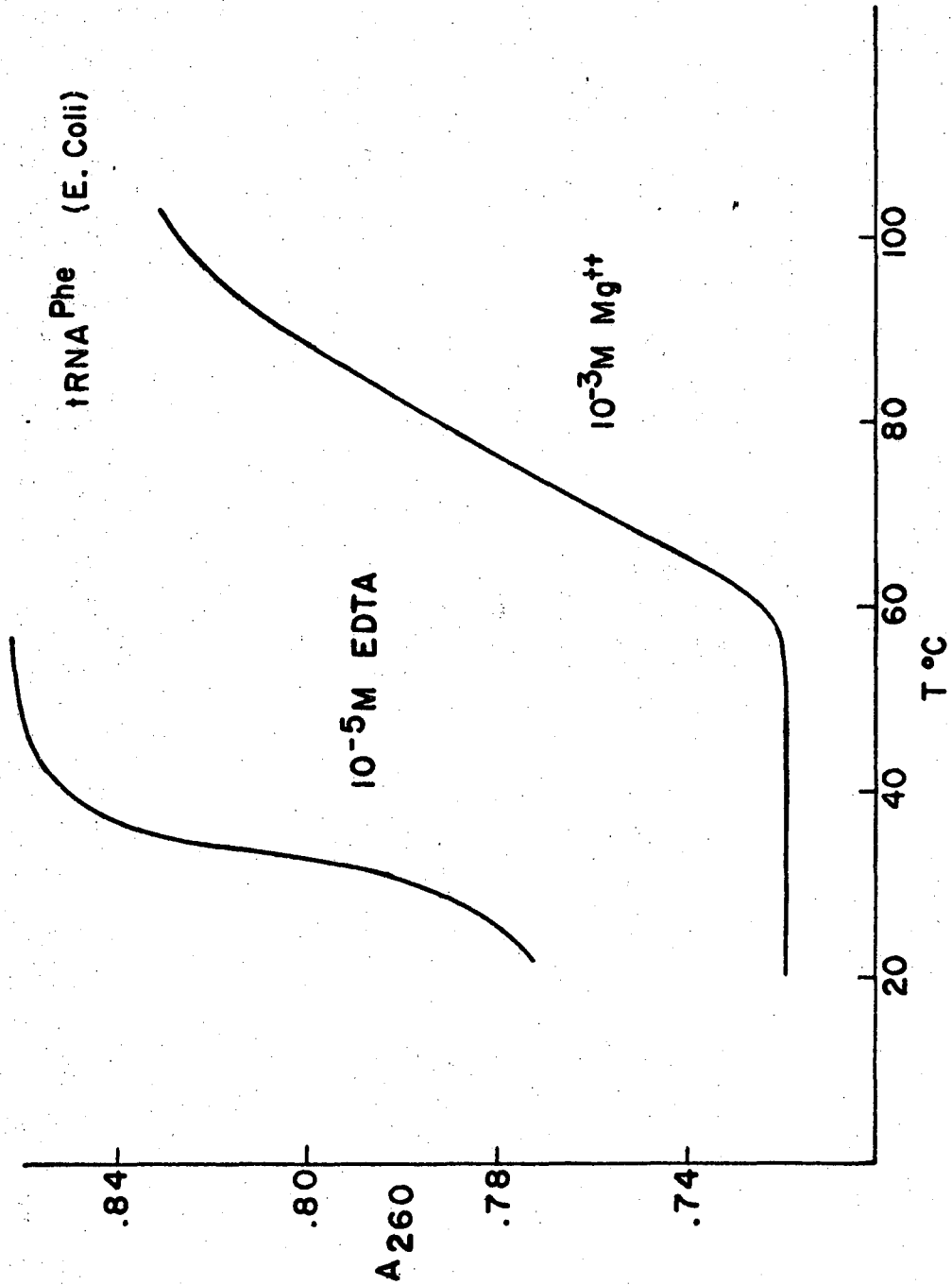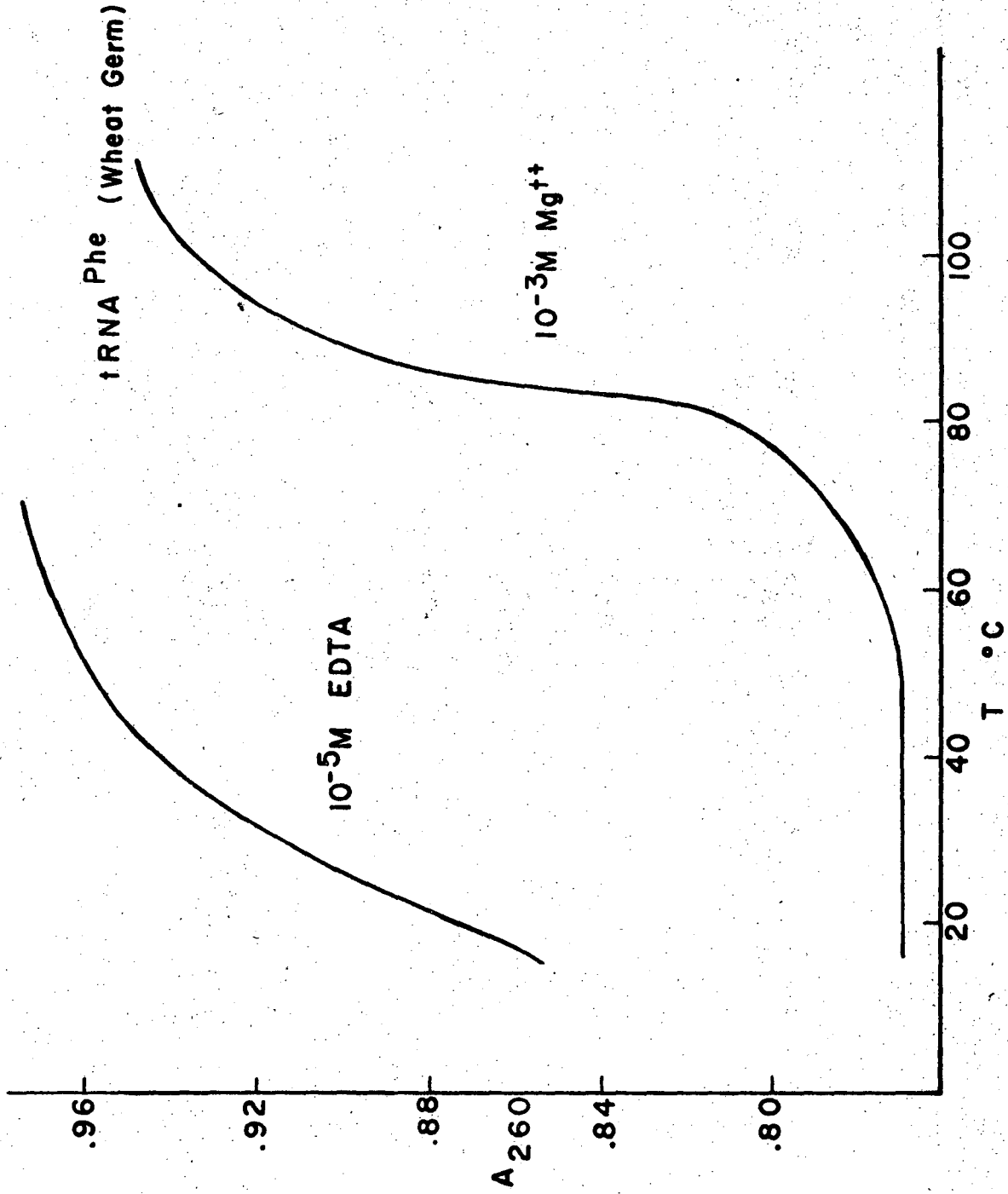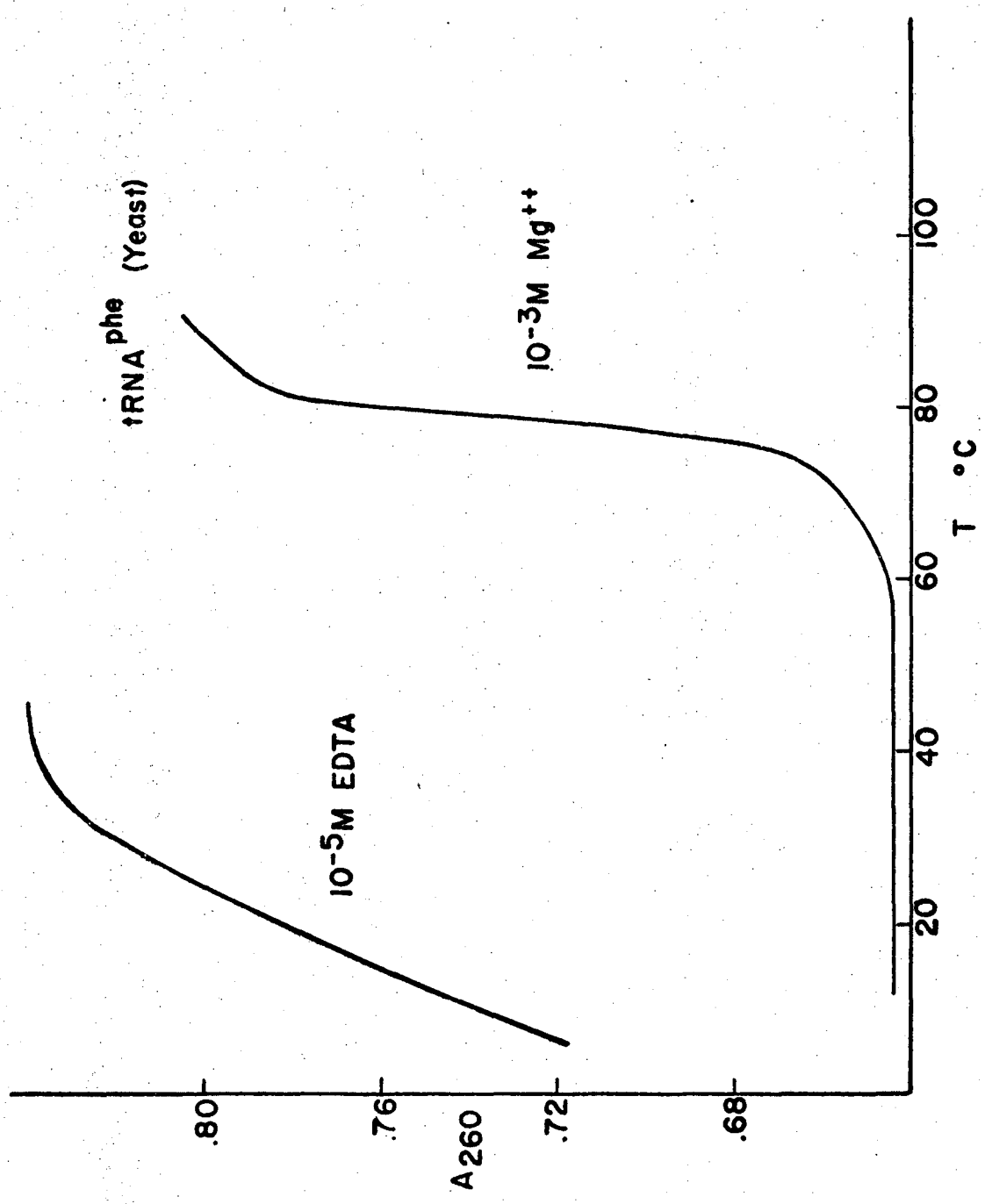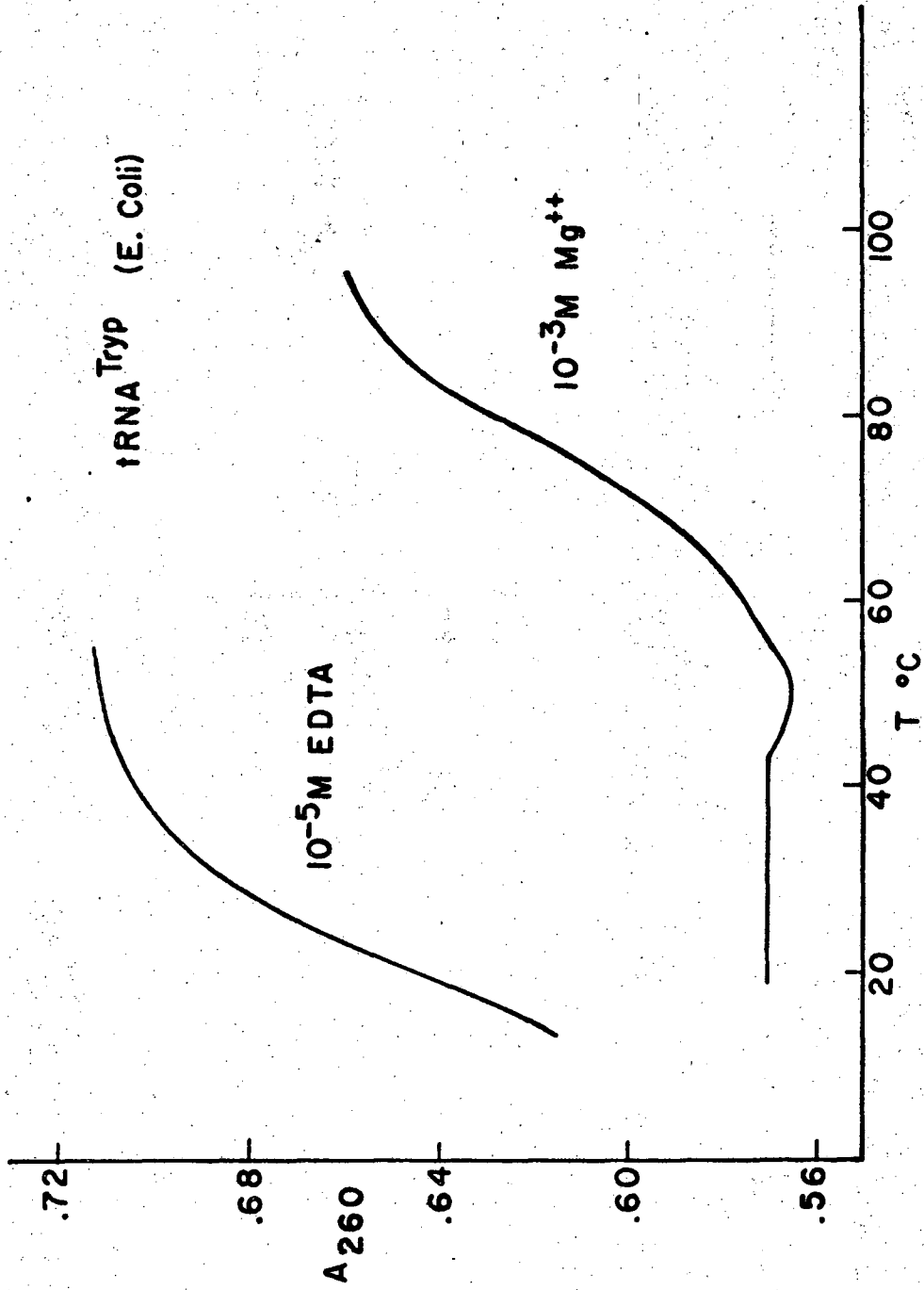
Figure 4-4

Figure 4-5

Figure 4-6
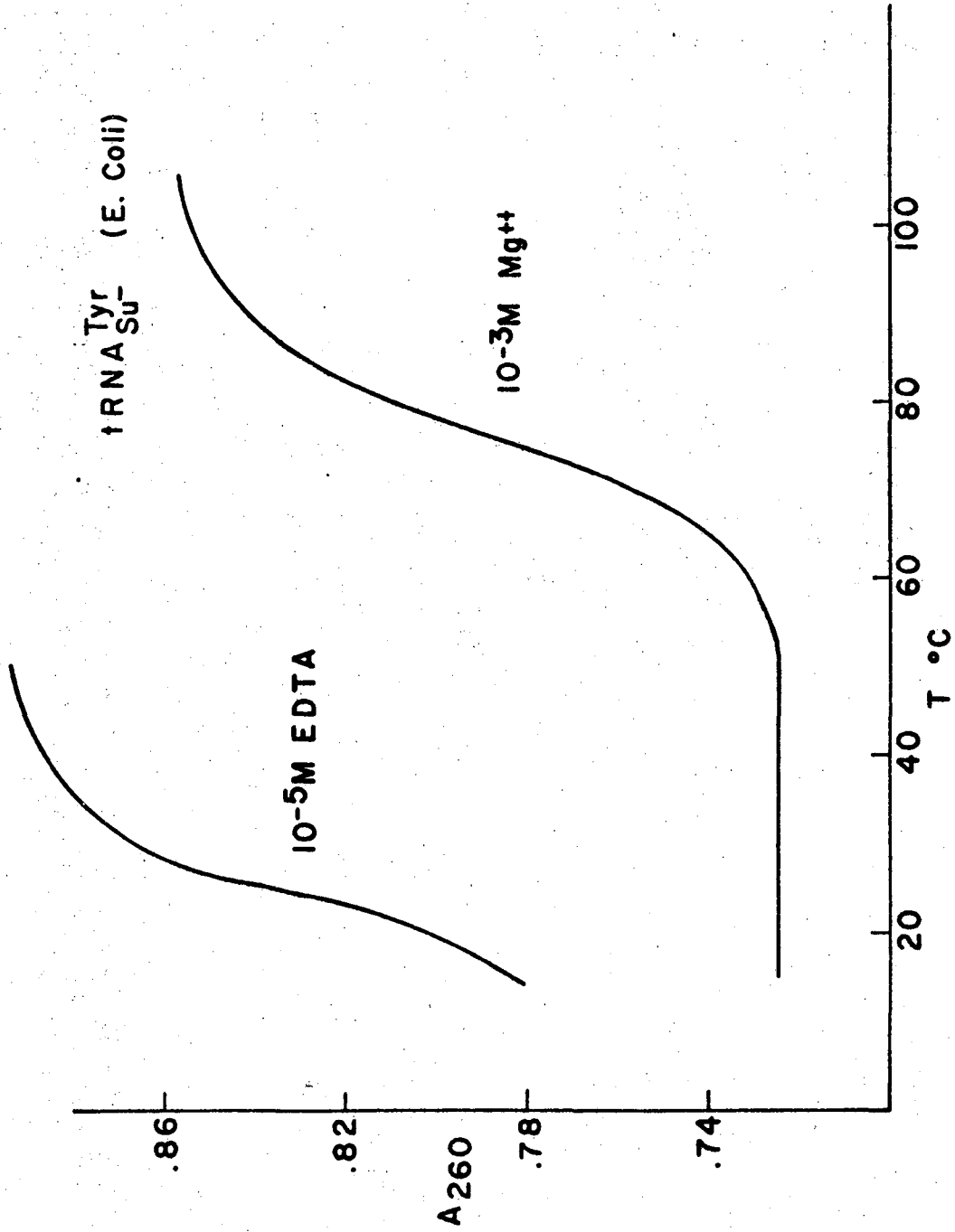
Figure 4-7
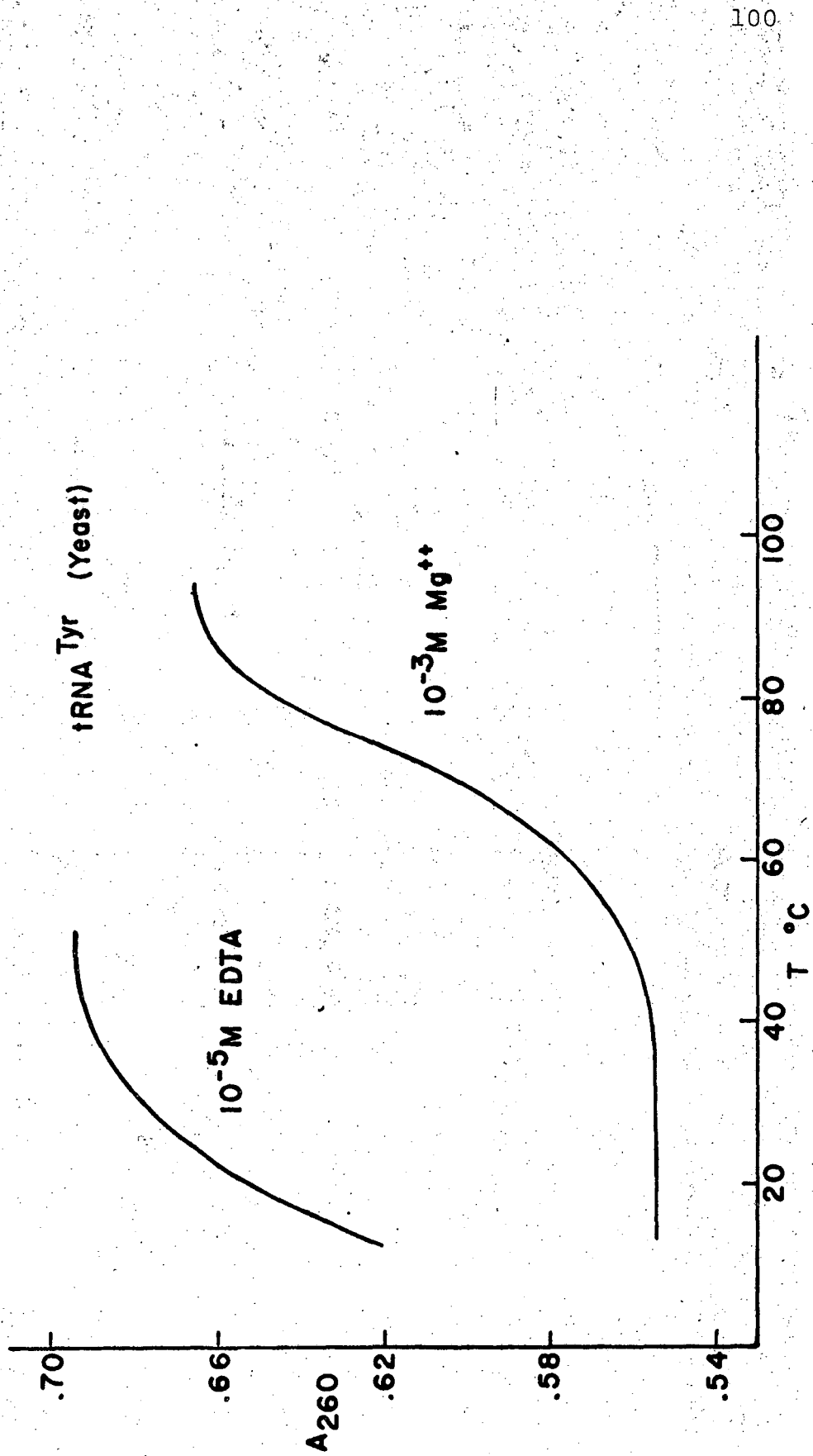
Figure 4-8
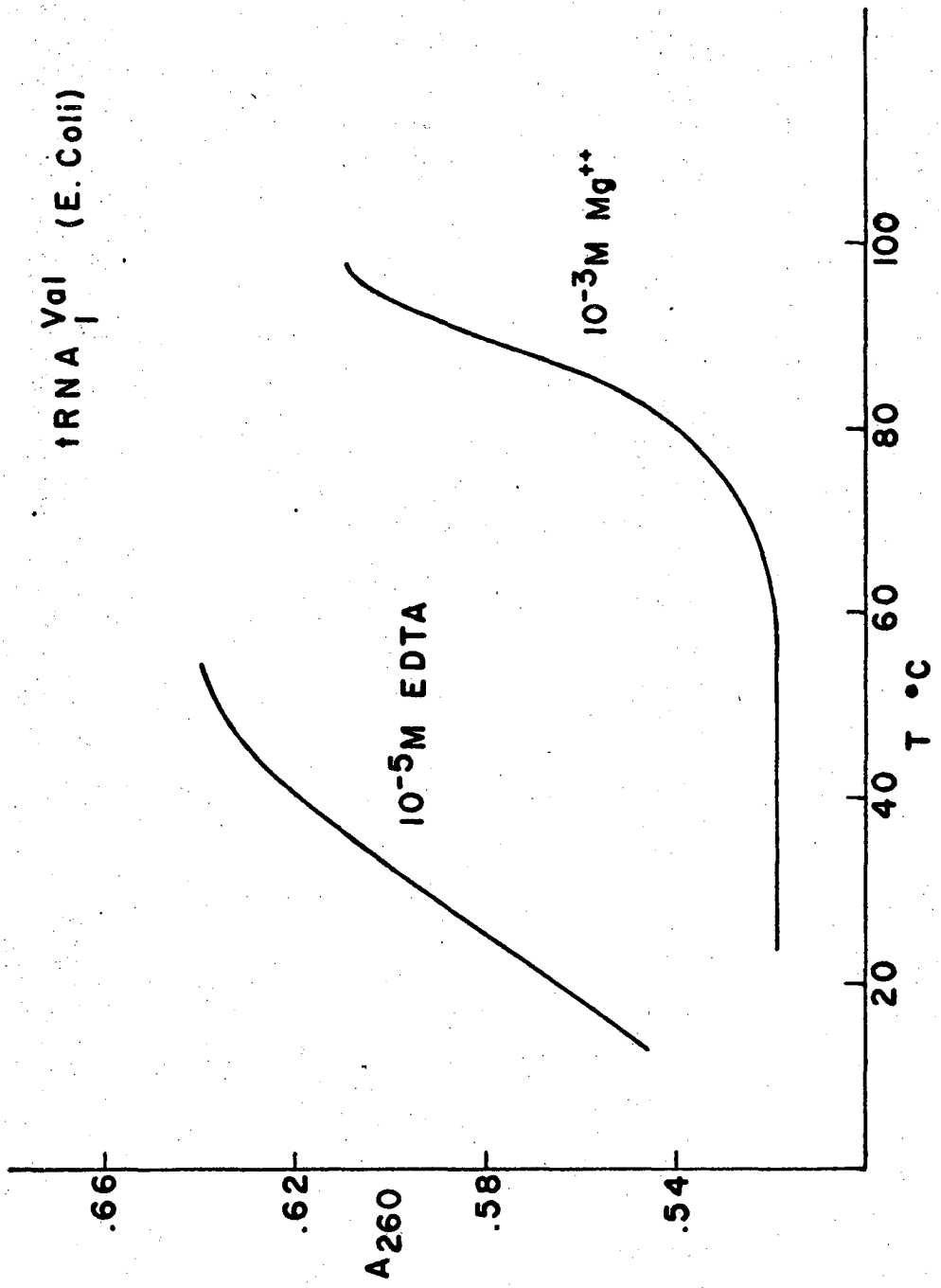
Figure 4-9

A.   Choice of a Temperature at Which to Study
     The Differences between Native and Single
     Stranded tRNA

These nine sets of curves (Figs. 4-1 to 4-9)
in the presence and absence of Mg^{++} were obtained in
order to find a temperature at which the low salt form
of the tRNA is mostly single stranded and the structure
of the native molecule is still intact. At this tempera-
ture the difference in properties between the native
and single strand forms of the tRNA are attributed to
the formation of secondary and tertiary structure.

Figures 4-1 to 4-9 show that most of the change
in absorption of the single strand tRNA has occurred
by 40°C. In the case of tRNA$^{F.Met}$ (E. coli) which
contains an unusually large number of G:C base pairs,
the corresponding temperature is 50°C. The absorption
of the native tRNA molecule in the presence of Mg^{++}
has not yet begun to increase at this temperature in
any case.

For several of the single strand melting curves
there is some change in the absorption above 40°C.
However, this change is less than 10% of the total
absorption change and may be attributed to unstacking
or the breaking of a very few base pairs. At 40°C
(or 50°C for tRNA$^{F.Met}$), the properties of the tRNAs
in 10^{-5} M EDTA are those of a molecule that is mostly

single stranded, and the properties of the tRNA in

1 mM Mg^{++} are those of the native molecule.

B. Parameters Describing Changes in Absorption

with Temperature

Curves showing the change in absorption of a
nucleic acid with temperature are called melting curves.
The bases in RNA have strong absorption bands in the
UV near 260 mμ. The magnitude of this absorption
depends upon the local environment of the bases. The
extinction coefficient of a free nucleotide in solution
is greater than that of a nucleotide in RNA. Absorption
of the base in a polymer will increase with temperature
or other denaturing conditions, and will approach that
of the free nucleotides at high temperatures. Breaking
of hydrogen bonds in double strand regions, unstacking
of the bases, and alteration of the tertiary structure
cause the observed change in the absorption of the RNA.

The melting temperature (T_m) of a nucleic acid is
defined as the temperature at which half the total change
between the low and high temperature limits of the
melting curves has occurred. The low temperature limit
of the melting curve of tRNA in the presence of Mg^{++}
is well defined. However, the high temperature limit
for several species of tRNA is difficult to determine.
There is probably some magnesium catalysed hydrolysis
of the tRNA at temperatures above 70°C (1). The T_m of

several of the native tRNAs must be approximated from the shape of the melting curve. The melting temperatures of the nine species of tRNA in 1 mM Mg^{++} vary between 73° and 90°C as listed in Table 4-1.

In the absence of Mg^{++}, the high temperature limits may be obtained readily, but the low temperature limits are not well defined. Thus the melting temperatures in the absence of Mg^{++} listed in Table 4-1 are only approximate. However, it should be noted that upon the addition of Mg^{++} there is an increase of at least 50°C in the melting temperature of all the species of tRNA being studied. This change reflects a major structural change in the molecule.

It should be noted that for most of the tRNAs studied here, the melting curve in the absence of Mg^{++} has a greater upper limit than does the melting curve in 1 mM Mg^{++}. This difference may also be observed in the melting curves of mixed yeast tRNA obtained by Fried (1). It suggests that even at quite high temperatures there is interaction between Mg^{++} and the tRNA. Apparently the Mg^{++} somewhat alters the geometry of the bases or the overall structure of the tRNA, even at 90°C. It would be interesting to compare the upper limit for the melting of single strand and double strand oligomers in the presence and absence of Mg^{++} to see if their structure is also sensitive to Mg^{++} at high temperatures, and to see if any of the optical properties of monomers change in the presence of magnesium.

Table 4-1

Melting Temperature and Percent Hyperchromicity of Nine tRNAs

	T_m in 10^{-5} M EDTA	T_m in 1 mM Mg	% Hyperchromicity
F. Met (E. coli)	27 ± 5°	90 ± 2°	24
Leu (Yeast)	10 ± 5°	78 ± 2°	27
Phe (E. coli)	30 ± 5°	79 ± 5°	22
Phe (Wheat)	21 ± 5°	85 ± 2°	20
Phe (Yeast)	10 ± 7°	79 ± 2°	27
Tryp (E. coli)	20 ± 6°	79 ± 3°	17
Tyr (E. coli)	25 ± 3°	79 ± 2°	18
Tyr (Yeast)	16 ± 5°	73 ± 3°	21
Val (E. coli)	33 ± 5°	88 ± 2°	18

Melting behavior is further characterized by the hyperchromicity or the increase in absorption upon melting relative to the low temperature absorption limit. Hyperchromicity may be calculated from:

$$\% \ h \ = \ \left(\frac{A_m}{A_p} - 1\right) \ 100 \qquad (4-1)$$

where A_m is the absorption limit at high temperatures, and A_p is the polynucleotide absorption at low temperature limit. The percent hyperchromicity of the tRNAs in the presence of Mg^{++} are listed in Table 4-1.

There is a large change in the melting behavior of all nine tRNAs upon the addition of Mg^{++}. The shape and position of these curves are different for different species of tRNA. Work is in progress in this laboratory to relate the characteristics of the melting curves of various tRNAs to the sequence of these RNAs (12).

2. CD Spectra of Native tRNAs at 25°C

A. Different Species of tRNA Have Different CD Spectra

Although it was shown that 40°C was a better temperature to study tRNA than 25°C, most other studies have been carried out at 25°C, so we will begin by presenting our results at 25°C.

The CD spectra of nine tRNAs at 25°C are shown in Figs. 3-10 to 3-12. The extrema and crossovers of these spectra are tabulated in Table 4-2. The first observation that may be made on the basis of these spectra is that different species of tRNA do exhibit

Table 4-2

Comparison of CD of Experimental and Calculated Native tRNA at 25°C

		λ_{min}	$[\theta]_{min}$ $(\times 10^{-4})$	λ_{max}	$[\theta]_{max}$ $(\times 10^{-4})$	λ_c	λ_{max}	$[\theta]_{max}$ $(\times 10^{-4})$	Fit
F. Met (E. coli)	exp	295	-.17	267	2.31	245	226	-.41	
	cal	299	-.10	270	1.76	250	221	-.04	.395
Leu (Yeast)	exp	---	----	263	2.58	242	222	-.16	
	cal	300	-.08	268	1.63	249	221	+.10	.465
Phe (E. coli)	exp	297	-.01	262	2.32	239	226	-.05	
	cal	299	-.10	269	1.55	248	221	-.02	.542
Phe (Wheat)	exp	296	-.15	264	1.98	245	227	-.50	
	cal	298	-.17	268	1.55	248	221	+.13	.411
Phe (Yeast)	exp	295	-.19	263	2.19	246	226	-.31	
	cal	300	-.13	268	1.64	248	221	+.16	.397
Tryp (E. coli)	exp	299	-.04	265	2.02	242	225	-.43	
	cal	299	-.10	270	1.61	247	235	-.44	.410
Tyr (E. coli)	exp	---	----	264	2.28	243	224	-.16	
	cal	301	-.06	271	1.86	249	221	+.03	.452
Tyr (Yeast)	exp	---	----	264	2.04	239	225	+.04	
	cal	298	-.11	270	1.53	250	221	+.04	.489
Val (E. coli)	exp	301	-.04	267	2.13	243	226	-.40	
	cal	300	-.10	269	1.59	245	221	-.08	.291

NATIVE tRNA at 25°C

F. Met (E. coli)
Leu (Yeast)
Phe (E. coli)

$[\theta] \times 10^{-4}$

LAMBDA IN MILLIMICRONS

Figure 4-10

NATIVE TRNA AT 25 DEG

Phe (Wheat)
Phe (Yeast)
Tryp (E. coli)

[θ] x 10⁻⁴

LAMBDA IN MILLIMICRONS

Figure 4-11

NATIVE tRNA AT 25°C

Tyr (E. coli)
Tyr (Yeast)
Val (E. coli)

$[\theta] \times 10^{-4}$

LAMBDA IN MILLIMICRONS
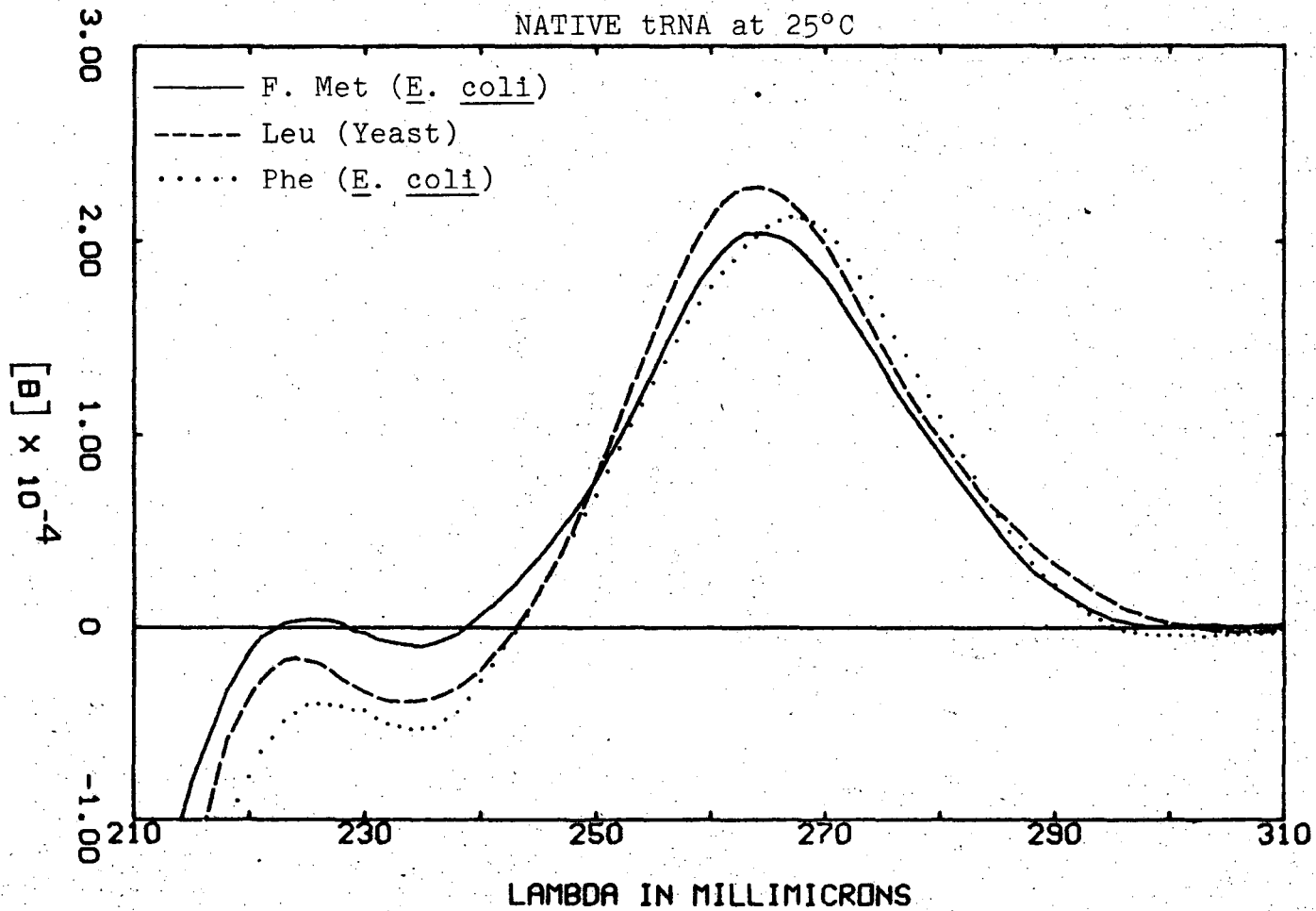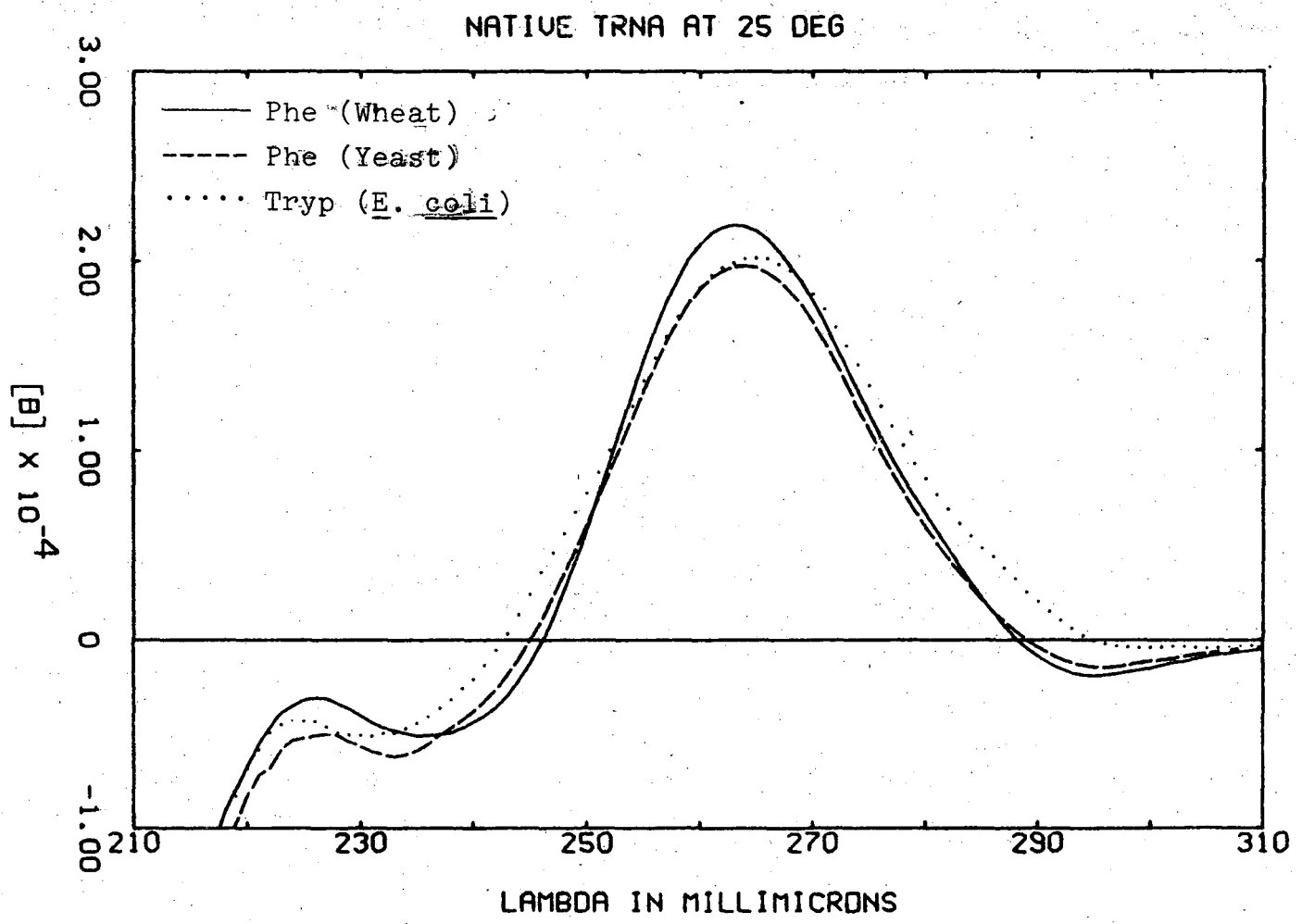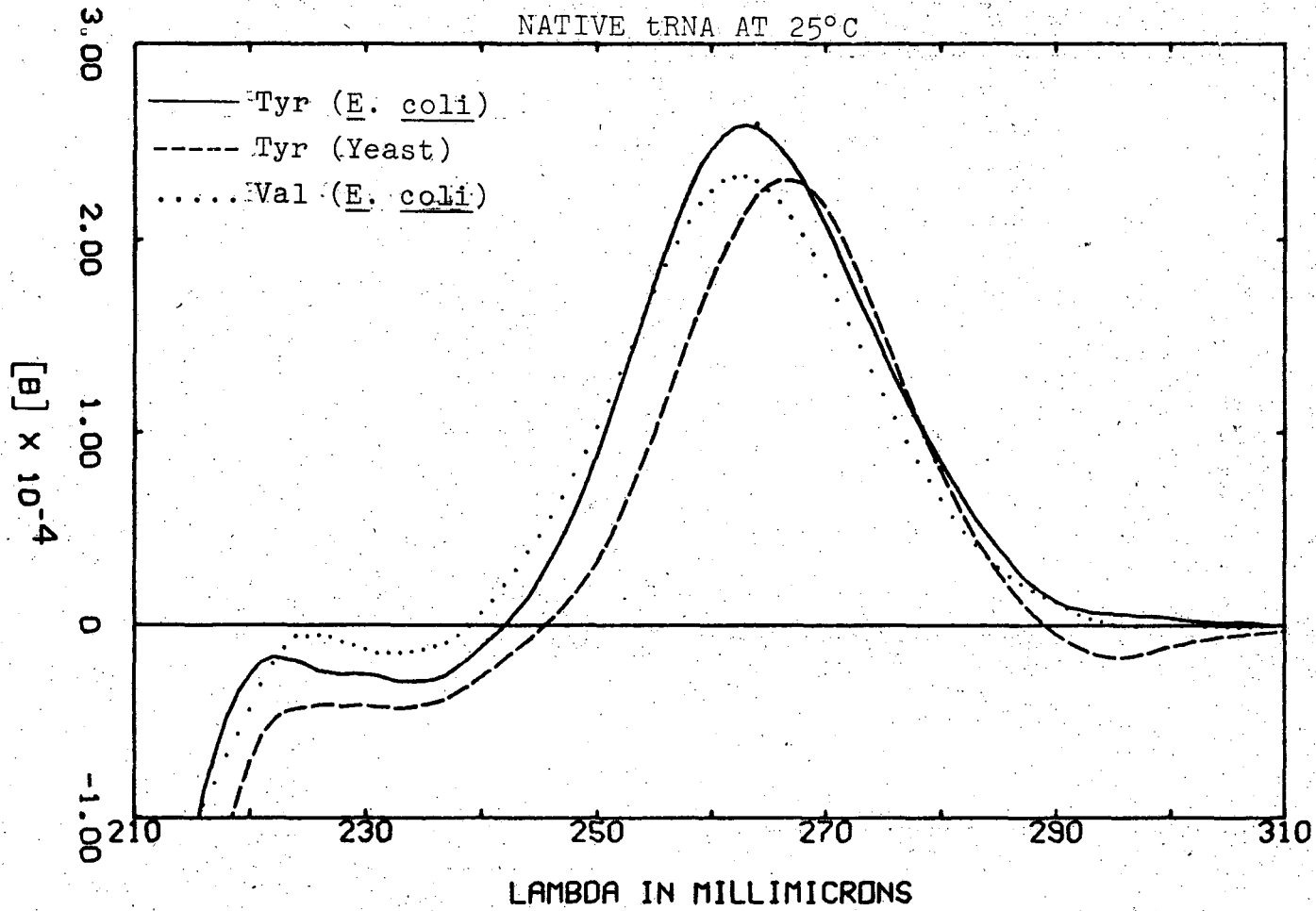
Figure 4-12

different CD behavior.

This study includes tRNA^{Phe} from three organisms, and tRNA^{Tyr} from two. If a common tertiary structure is assumed for tRNAs from these organisms, the observed differences in the CD spectra of the tRNAs may be explained by variation in the primary and secondary structure. Figure 4-12 shows the CD of tRNA^{Tyr} from yeast and E. coli. The shape and crossovers of these two spectra are similar although their magnitudes are somewhat different. The larger magnitude of the peak at 264 mµ and smaller magnitude at 225 mµ observed in tRNA^{Tyr} (E. coli) may be attributed to additional base pairing in the variable length region of this tRNA (Fig. 1-3). The spectra of tRNA^{Phe} from wheat germ and yeast are also quite similar as shown in Fig. 4-11. The larger magnitude of tRNA^{Phe} (yeast) is probably due to the larger number of A:U pairing interactions in this tRNA. tRNA^{Phe} (E. coli) has a fairly different primary sequence and CD spectrum from the other two Phe tRNAs.

In Figure 4-10 the spectra of tRNA$^{F \cdot Met}$ and tRNA^{Phe} from E. coli are quite different from each other, reflecting differences in percent A:U and G:C interactions in these tRNAs. The same species of tRNA from different organisms can have quite similar CD and different species of tRNA from the same organism may have relatively large differences in their CD spectra.

These similarities and differences may qualitatively
be related to the sequence and pairing interactions
of the tRNA. Thus the observation that tRNAs from
different organisms have similar structure is confirmed
by CD spectra.

B. Comparison of Calculated and Experimental
   tRNA Spectra at 25°C

The experimental spectra of native tRNA at 25°C
may be approximated by sums of monomer, dimer, and
double strand polymer spectra using Equation 3-11 and
setting (T) equal to zero. The extrema of these
calculated spectra and the "Fit" with the experimental
spectra are listed in Table 4-2. "Fit" is a measure of
the normalized root mean square deviation between the
two curves as defined in Equqtion 3-17. This gives a
quantiative measure of how well calculated and experi-
mental spectra agree. The calculated and experimental
spectra at 25°C for the three species of tRNA that
were purified as part of this work are shown in Figs
4-13 to 4-15.

Agreement between the calculated and experimental
spectra is qualitative only. The main peak and cross-
over of the calculated spectra are shifted about 5 mμ
to higher wavelengths than those experimentally observed.
Also, the magnitude of this large positive peak is
decreased in the calculated spectra. Examination of

Figures 4-13 to 4-15. Comparison of experimental
native CD spectra of three tRNAs at 25°C and spectra
calculated from sum of dimer basis spectra and
double strand polymer spectra using Equation 3-11.

NATIVE YEAST PHENYLALANINE TRNA 25 DEG

EXPERIMENTAL SPECTRUM

------ CALCULATED SPECTRUM

LAMBDA IN MILLIMICRONS

Figure 4-13

114
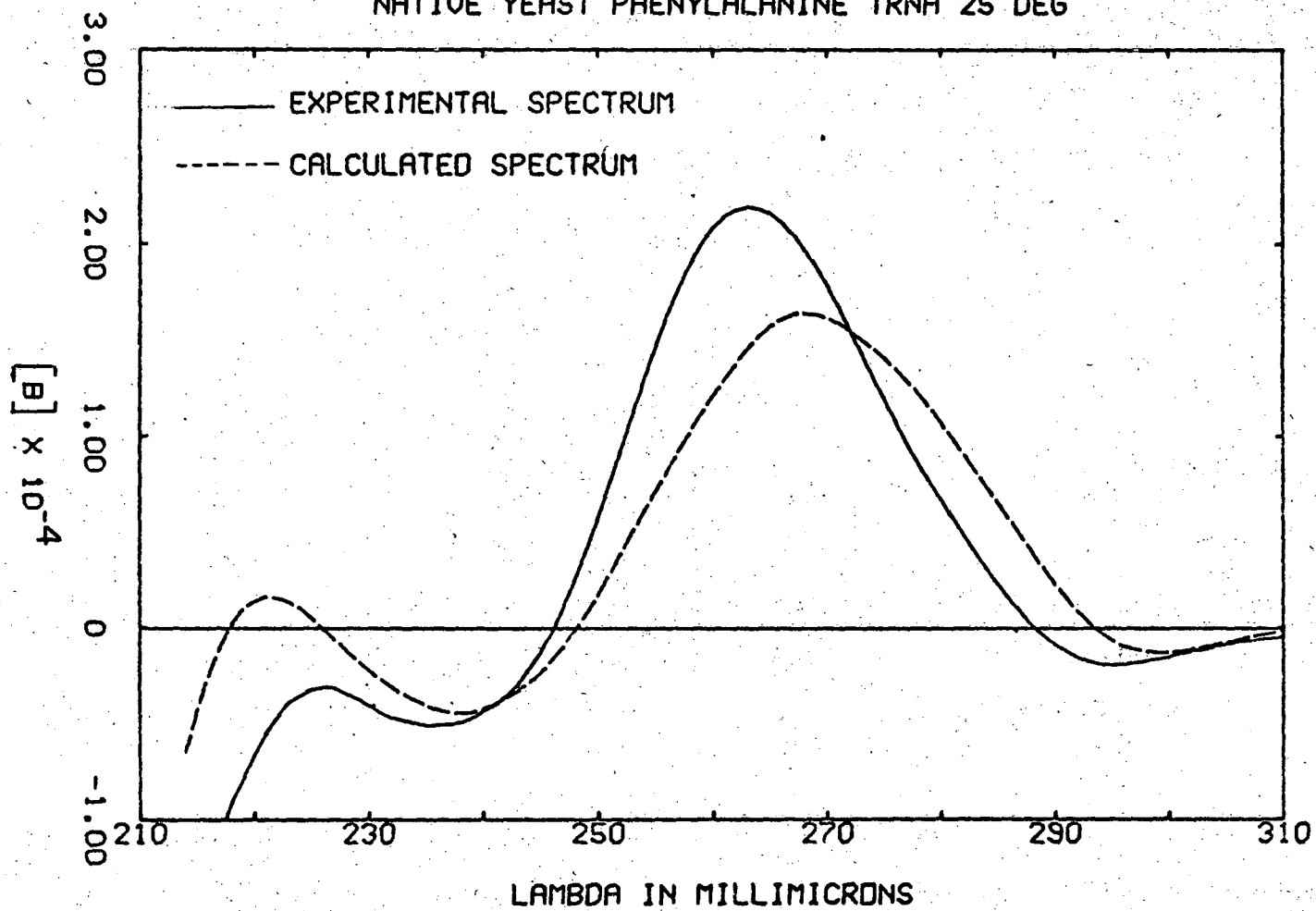
NATIVE E.COLI TRYPTOPHAN TRNA 25 DEG

Figure 4-14

LAMBDA IN MILLIMICRONS

EXPERIMENTAL SPECTRUM

CALCULATED SPECTRUM

$[\theta] \times 10^{-4}$

NATIVE YEAST TYROSINE TRNA AT 25 DEG

—— EXPERIMENTAL SPECTRUM

----- CALCULATED SPECTRUM

LAMBDA IN MILLIMICRONS

$[\theta] \times 10^{-4}$
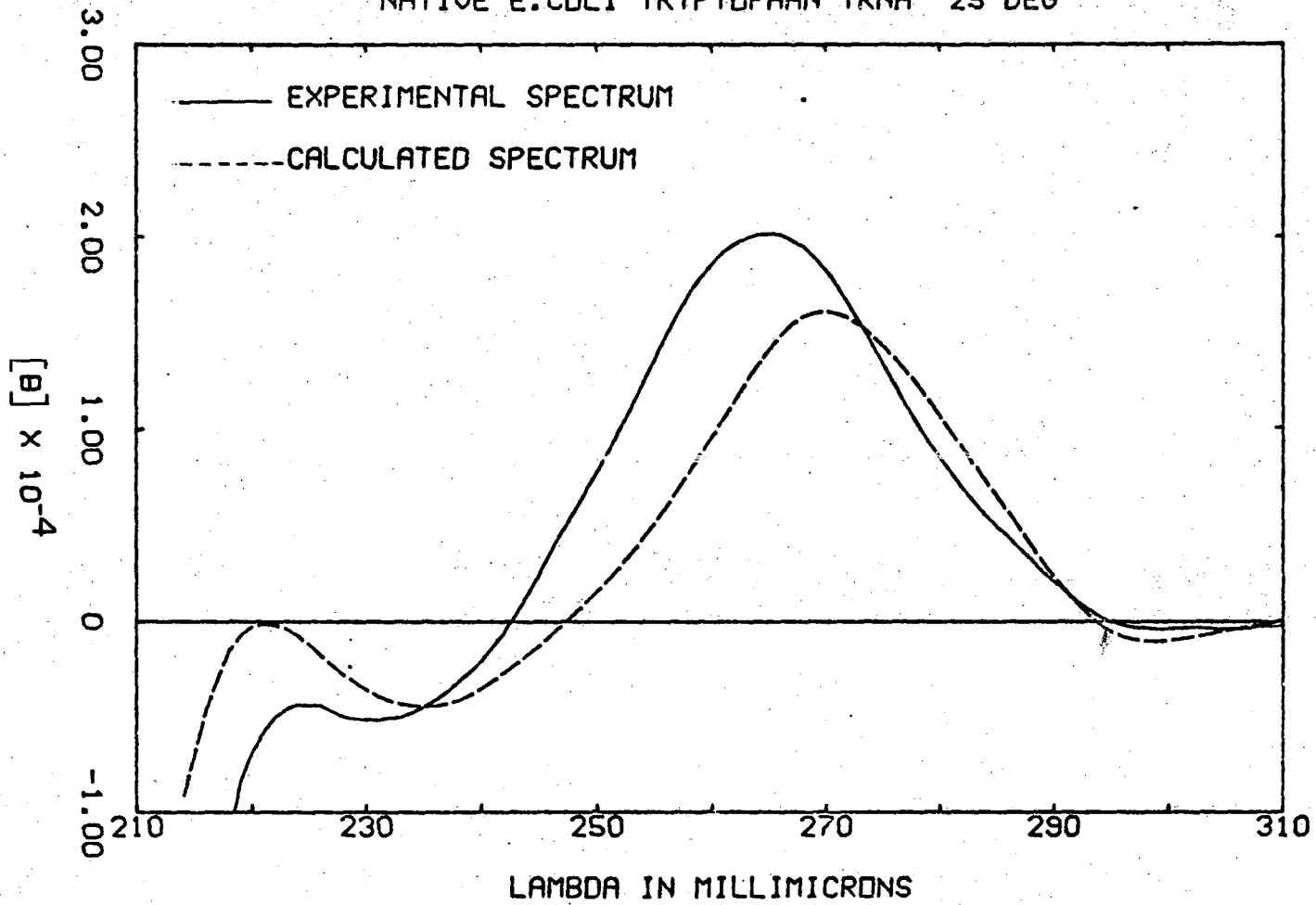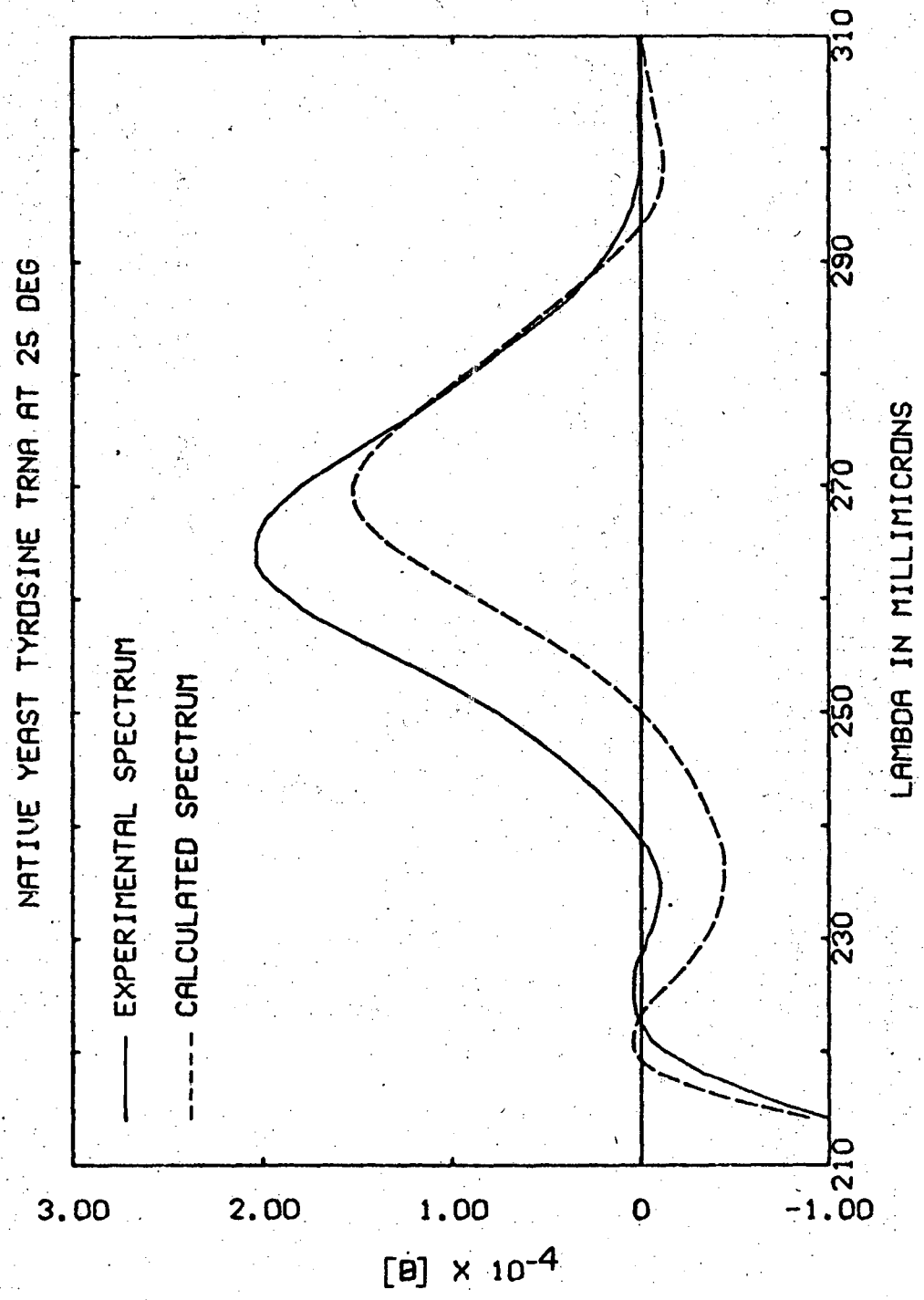
Figure 4-15

Fig. 3-1 shows that this sort of change corresponds to more single strand character in an RNA. This suggests that the native structure of tRNA may have more paired bases than is predicted by the Holley cloverleaf. These could be part of the tertiary structure of the molecule.

Other possible causes of this discrepancy are that the single strand basis spectra, the double strand polymers, or both are not good models for the nucleotides in tRNA. To investigate this, we will consider separately how well the dimers basis spectra and double strand polymers spectra will fit experimental CD data.

3. CD Spectra of Single Stranded tRNA at 40°C

Single stranded tRNA was prepared by dialysing the tRNA to reduce Mg^{++} concentration to less than 10^{-5} M and heating to 40°C in the presence of 10^{-5} M EDTA. Examination of the melting curves in Figs. 3-1 to 3-9 shows that at this temperature most of the secondary structure has melted. The extrema of the CD of the experimental single strand spectra are tabulated in Table 4-3. The band at 295 mμ has completely disappeared and the large peak is shifted to the red and diminished in magnitude relative to the native tRNA at 25°C.

According to the nearest neighbor approximation,

118

these experimental spectra should be similar to an
appropriate sum of dimer basis spectra. Single strand
spectra for the nine tRNAs were calculated from Equation 3-6 using the 20 dimer and 5 monomer spectra
listed in Appendix 1, and the nearest neighbor frequencies listed in Table 3-2. Extrema of these spectra
are tabulated in Table 4-3. The experimental and
calculated single strand spectra are compared for
three species of tRNA in Figs. 4-16 to 4-18. The
calculated spectra are shifted to the red relative to
the experimental single strand spectra. The position
of the low wavelength peak is accurately predicted in
all cases. However, the magnitude of the calculated
spectra is usually too low. "Fit" values are slightly
larger than those for native tRNA at 25°C indicating
a somewhat worse agreement between experimental and
calculated CD.

As previously discussed, about 2% of the bases in
these tRNAs are modified bases whose spectral properties
are not known. These bases may be responsible for
part of the discrepancy observed. An attempt was
made to improve the "Fit" by using an experimental
spectrum of TψCG measured by Dr. Carl Formoso (2) at
40°C in the place of the dimers. Unfortunately, this
did not result in any better agreement.

Figure 3-3 shows that when calculated ORD of
homopolymers is compared with the experimental spectra,

Table 4-3

Comparison of CD of Experimental and Calculated Single Strand tRNA at 40°C

		λ_{max}	$[\theta]_{max}$ $(\times 10^{-4})$	λ_c	λ_{min}	$[\theta]_{min}$ $(\times 10^{-4})$	λ_{max}	$[\theta]_{max}$ $(\times 10^{-4})$	Fit
F. Met (E. coli)	exp	274	1.37	254	237	-.46	222	-.12	.372
	cal	277	1.31	259	241	-.82	221	+.11	
Leu (Yeast)	exp	271	1.58	252	237	-.33	221	+.17	.582
	cal	275	1.22	260	246	-.80	220	+.17	
Phe (E. coli)	exp	276	1.13	245	231	-.31	222	-.04	.639
	cal	276	1.17	259	241	-.74	221	+.09	
Phe (Wheat)	exp	271	1.38	250	235	-.43	221	-.18	.613
	cal	275	1.12	260	242	-.80	220	+.16	
Phe (Yeast)	exp	274	1.08	252	237	-.40	219	-.08	.576
	cal	275	1.14	260	244	-.79	220	+.16	
Tryp (E. coli)	exp	274	1.37	250	233	-.43	219	-.08	.511
	cal	277	1.21	260	241	-.79	219	+.14	
Tyr (E. coli)	exp	271	1.75	249	235	-.3	221	+.18	.561
	cal	276	1.45	259	241	-.85	221	+.16	
Tyr (Yeast)	exp	273	1.27	249	237	-.22	221	+.14	.638
	cal	276	1.14	260	242	-.76	219	+.15	
Val (E. coli)	exp	273	1.73	247	236	-.32	221	+.15	.598
	cal	276	1.20	259	240	-.93	221	+.04	

Figures 4-16 to 4-18. Spectra of "single stranded"
tRNA at 40°C in 10^{-5} M EDTA are compared with sums
of 20 dimer spectra calculated using Equation 3-6.

SINGLE STRAND YEAST PHE TRNA AT 40 DEG

Figure 4-16

LAMBDA IN MILLIMICRONS

121

SINGLE STRAND E.COLI TRYPTRNA 40 DEG

—— EXPERIMENTAL SPECTRUM

------ CALCULATED SPECTRUM

LAMBDA IN MILLIMICRONS

$[\theta] \times 10^{-4}$
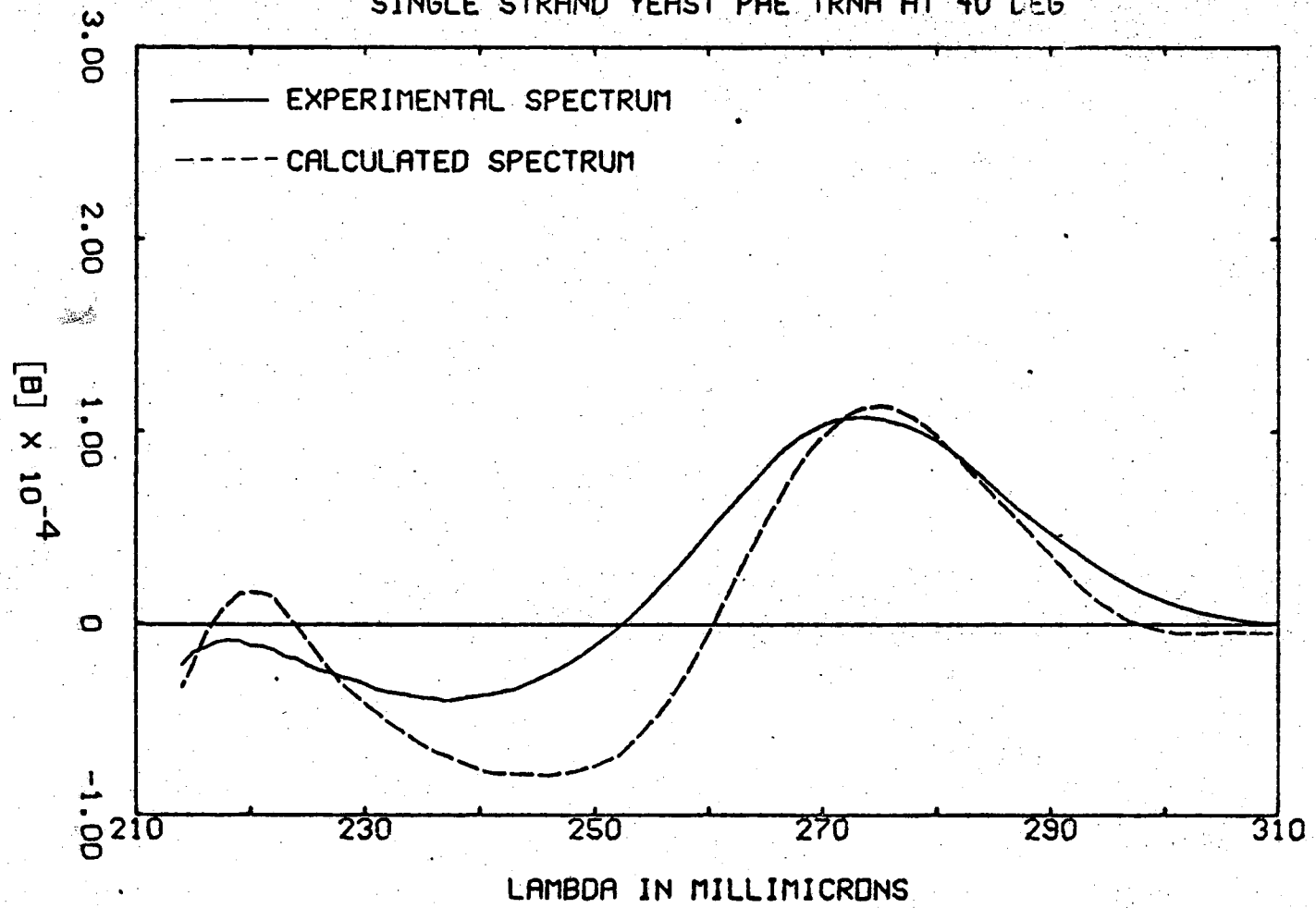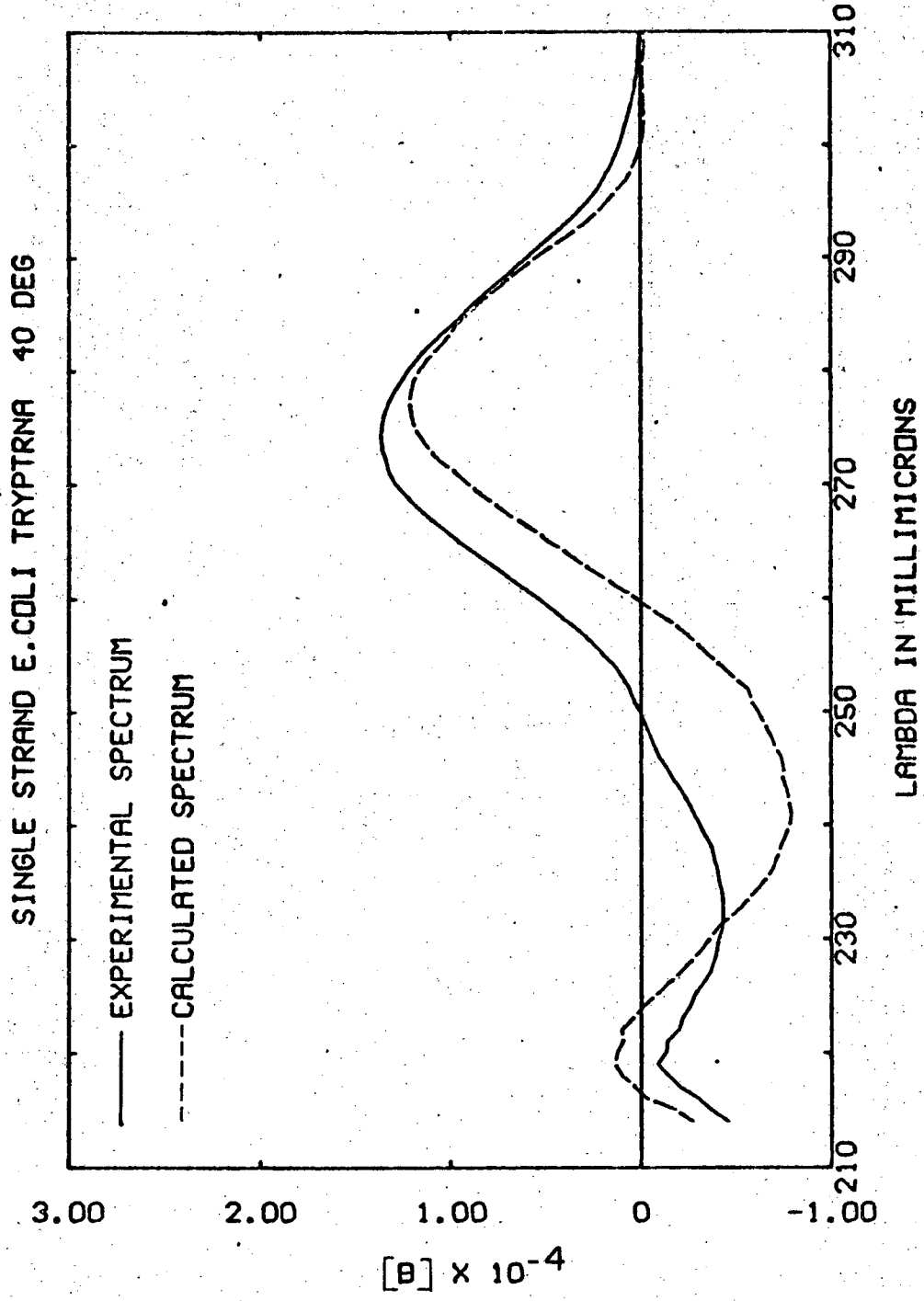
Figure 4-17

SINGLE STRAND YEAST TYR TRNA AT 40 DEG

EXPERIMENTAL SPECTRUM

CALCULATED SPECTRUM

$[\theta] \times 10^{-4}$

LAMBDA IN MILLIMICRONS
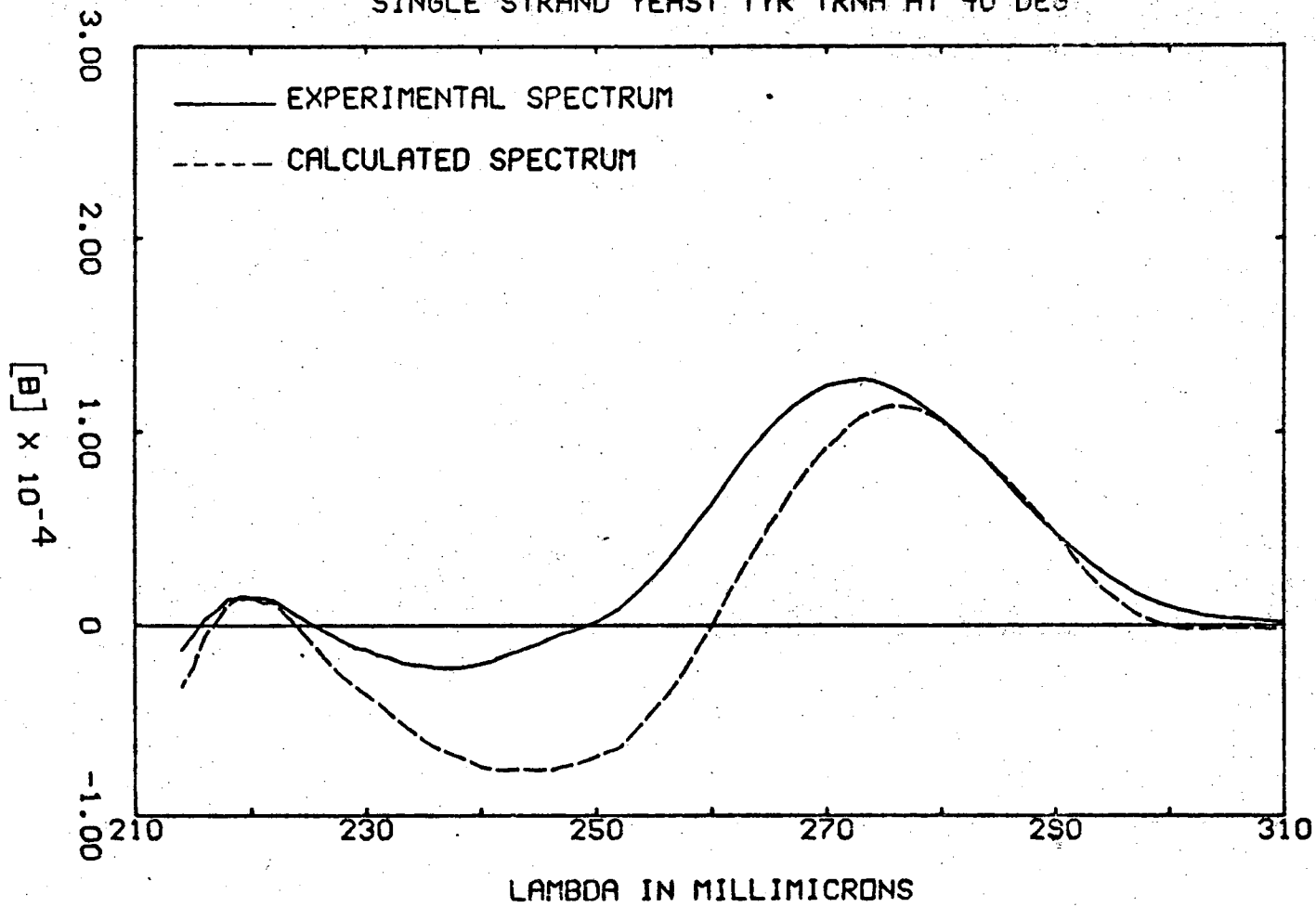
Figure 4-18

there is a similar red shift of the calculated ORD.
This lack of agreement was originally thought to be
due to long range symmetry in homopolymers (3). Obser-
vation of a similar shift for all nine tRNAs suggests
that dimers are not a good model for polymers.

We must conclude that the nearest neighbor
approximation is only qualitatively useful in predict-
ing the spectra of single strand tRNAs.

4. CD Spectra of Native tRNAs at 40°C

A. There is a Large Difference between the CD
of Native and Single Stranded tRNA at 40°C

The addition of 1 mM Mg^{++} to single stranded tRNA
results in a large change in the CD spectra as shown
in Figs. 3-19 to 3-21. The addition of 1 Mg^{++} for
each two bases is sufficient to produce this change (4).
The position of the maximum shifts about 10 mµ to lower
wavelengths and its magnitude increases markedly. For
some tRNAs there is now a band at 295 mµ. These
large changes parallel the 20% decreases in absorption
shown in Figs. 4-1 to 4-9.

The difference spectra corresponding to this change
were calculated for the tRNAs and their extrema are
tabulated in Table 4-4. The spectra for the three
species of tRNA that were purified as part of this
work are shown (Figs. 3-22 to 3-24) to provide examples
of the sorts of spectra obtained. These difference

YEAST PHE TRNA AT 40 DEG

---- NATIVE

—— SINGLE STRAND

$[\theta] \times 10^{-4}$

LAMBDA IN MILLIMICRONS

Figure 4-19

Figure 4-20

YEAST TYR TRNA AT 40 DEG

----- NATIUE

——— SINGLE STRAND

[θ] × 10⁻⁴

LAMBDA IN MILLIMICRONS
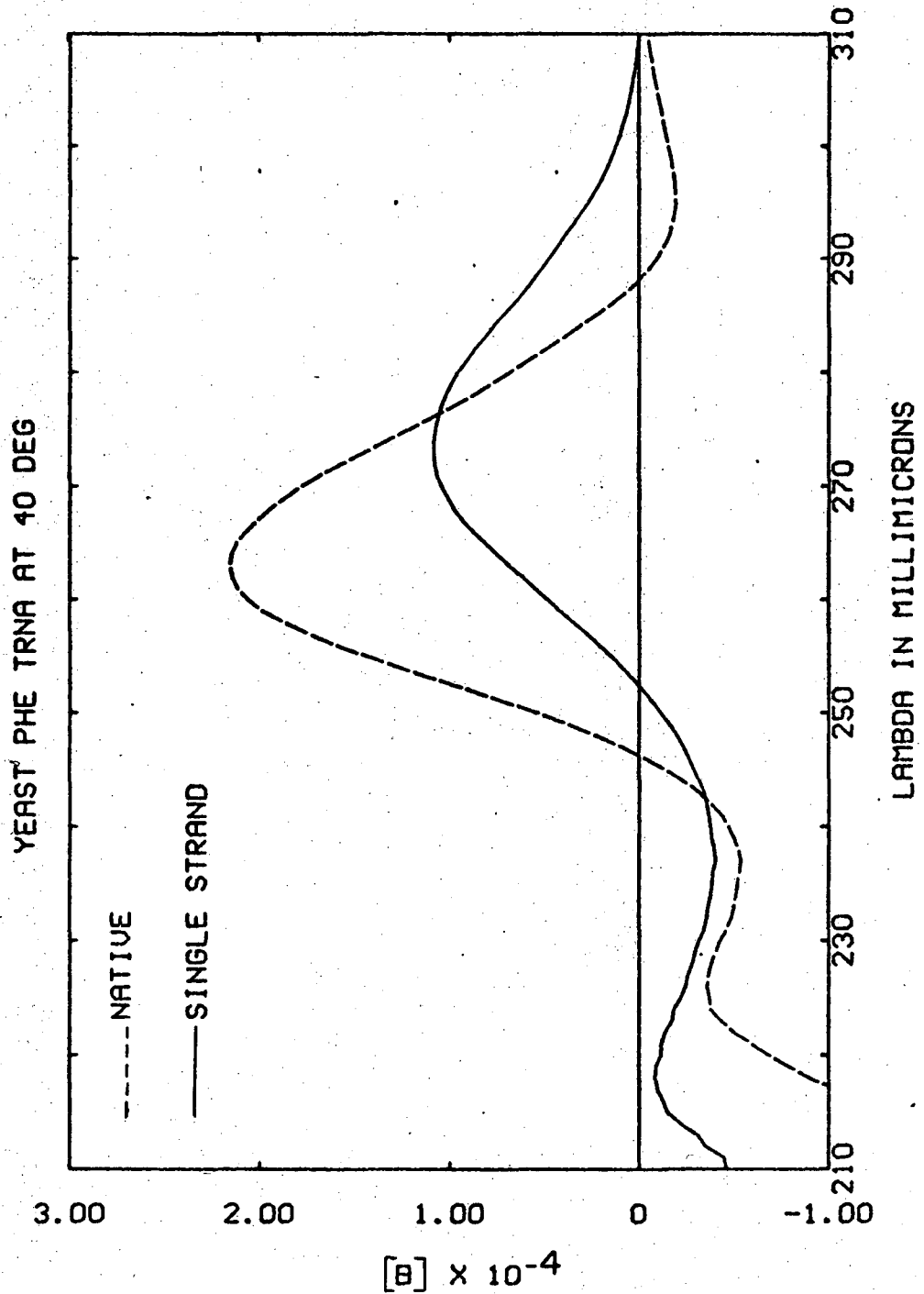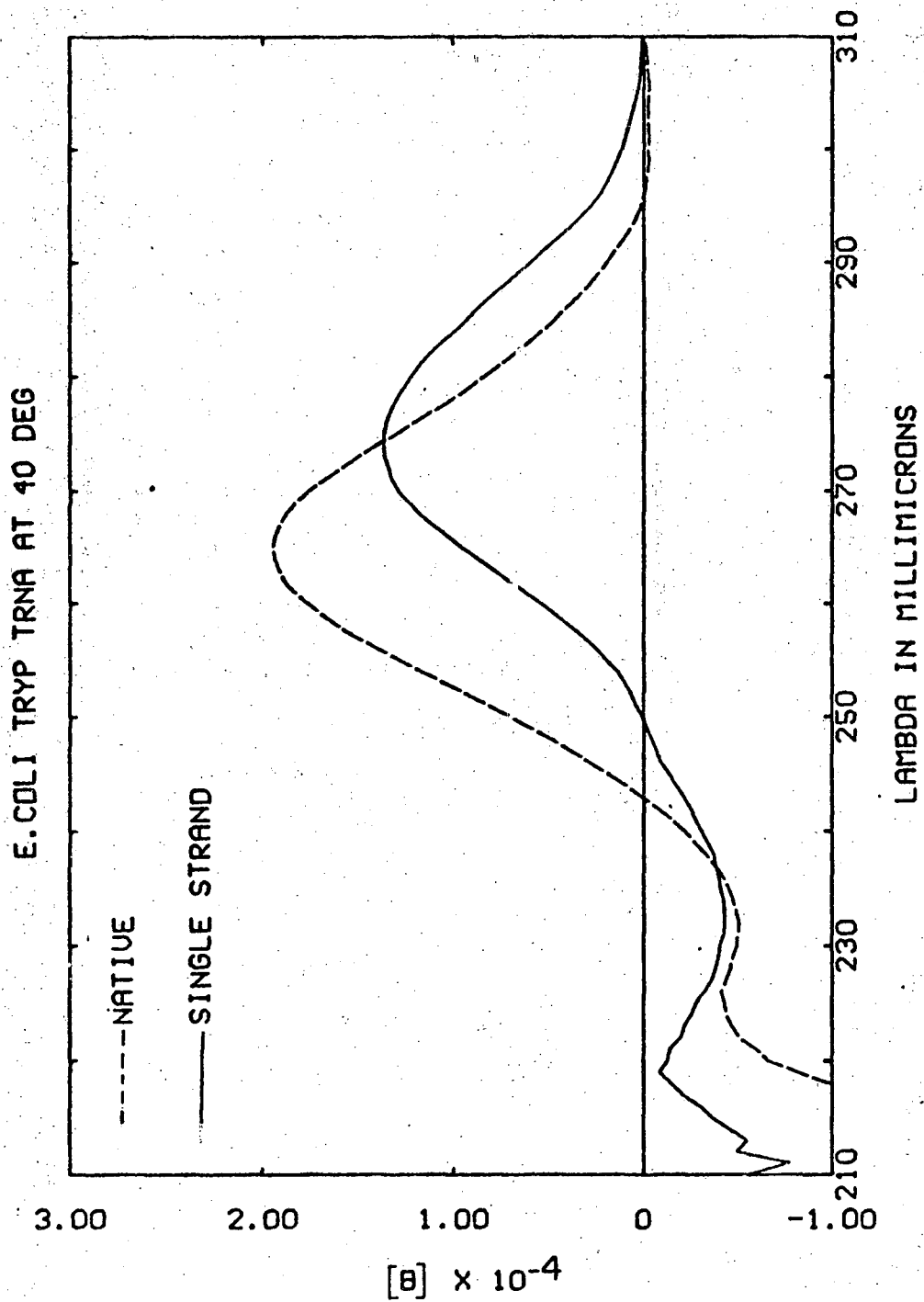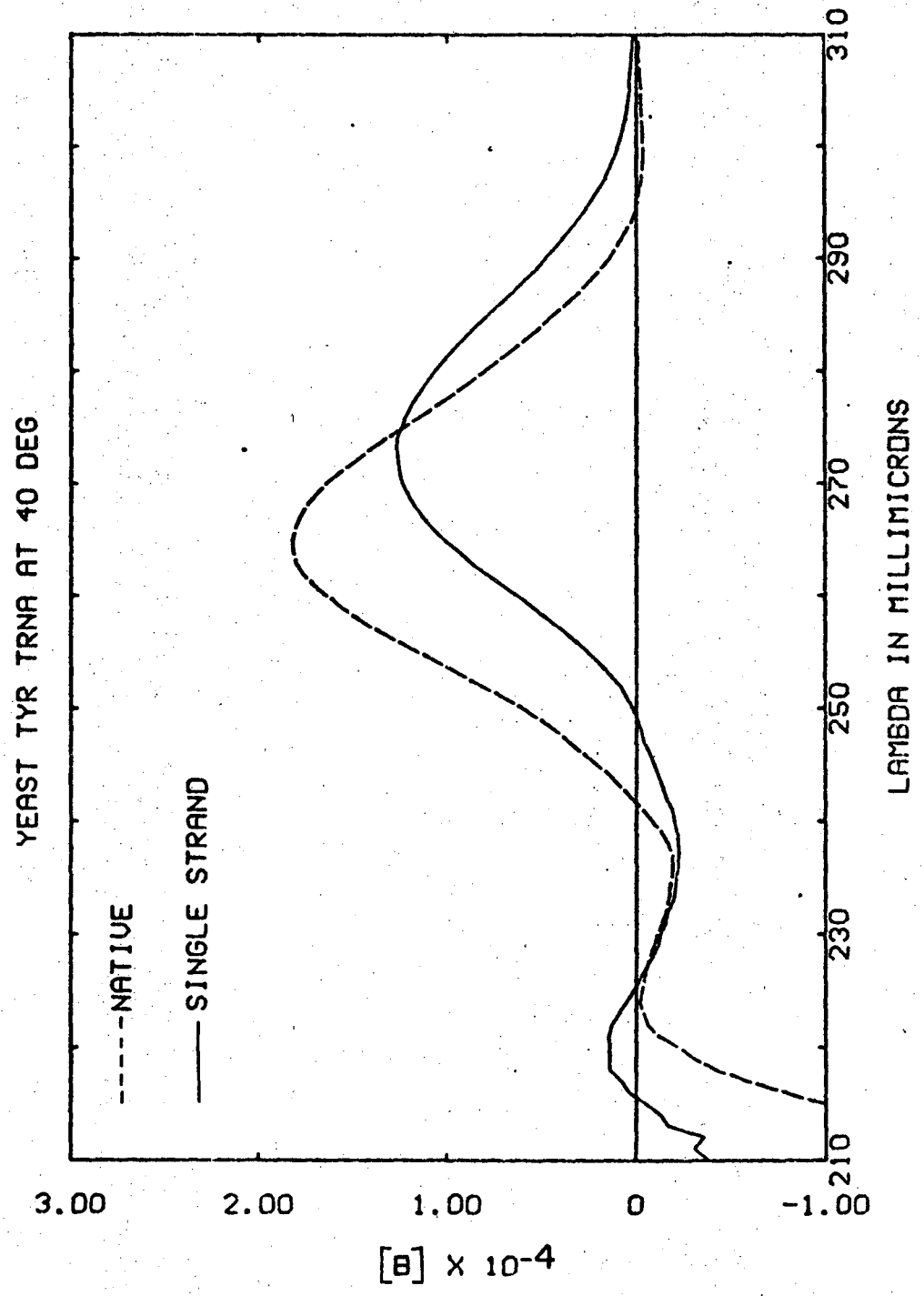
Figure 4-21

Table 4-4

Comparison of Difference Between CD of Native and Single Strand
tRNA with the Sum of Double Strand Pairing Interactions at 40°C

		λ_{min}	$[\theta]_{min}$ $(\times 10^{-4})$	λ_c	λ_{max}	$[\theta]_{max}$ $(\times 10^{-4})$	λ_c	Fit
F. Met (E. coli)	exp	286	-.58	276	261	1.26	229	
	cal	285	-.51	274	264	.65	-234	.401
Leu (Yeast)	exp	286	-.39	275	258	1.73	233	
	cal	288	-.11	277	257	1.15	223	.357
Phe (E. coli)	exp	285	-.48	275	260	1.68	223	
	cal	285	-.36	275	258	.80	233	.455
Phe (Wheat)	exp	286	-.52	274	259	1.19	238	
	cal	285	-.30	275	260	.99	237	.252
Phe (Yeast)	exp	290	-.56	276	260	1.58	242	
	cal	285	-.14	276	258	1.11	222	.406
Tryp (E. coli)	exp	285	-.46	274	260	1.23	237	
	cal	285	-.36	275	258	.80	233	.307
Tyr (E. coli)	exp	281	-.45	272	258	1.17	240	
	cal	285	-.25	276	257	.80	232	.441
Tyr (Yeast)	exp	286	-.35	275	259	1.02	227	
	cal	285	-.41	275	260	.80	234	.197
Val (E. coli)	exp	285	-.48	274	259	1.03	242	
	cal	284	-.29	275	257	.89	232	.455

Figures 4-22 to 4-24. A comparison of the difference between native and single strand tRNA CD spectra at 40° with a sum of double strand pairing interactions as defined in Equation 3-14 corresponding to the double strand regions shown in Figures 1-1 to 1-3.

NATIVE-SS YEAST PHE TRNA AT 40 DEG

EXPERIMENTAL SPECTRUM

CALCULATED SPECTRUM

[B] x 10⁻⁴

LAMBDA IN MILLIMICRONS

Figure 4-22

130.

NATIVE-SS E.COLI TRYP TRNA AT 40 DEG

—— EXPERIMENTAL SPECTRUM

----- CALCULATED SPECTRUM

LAMBDA IN MILLIMICRONS

$[\theta] \times 10^{-4}$
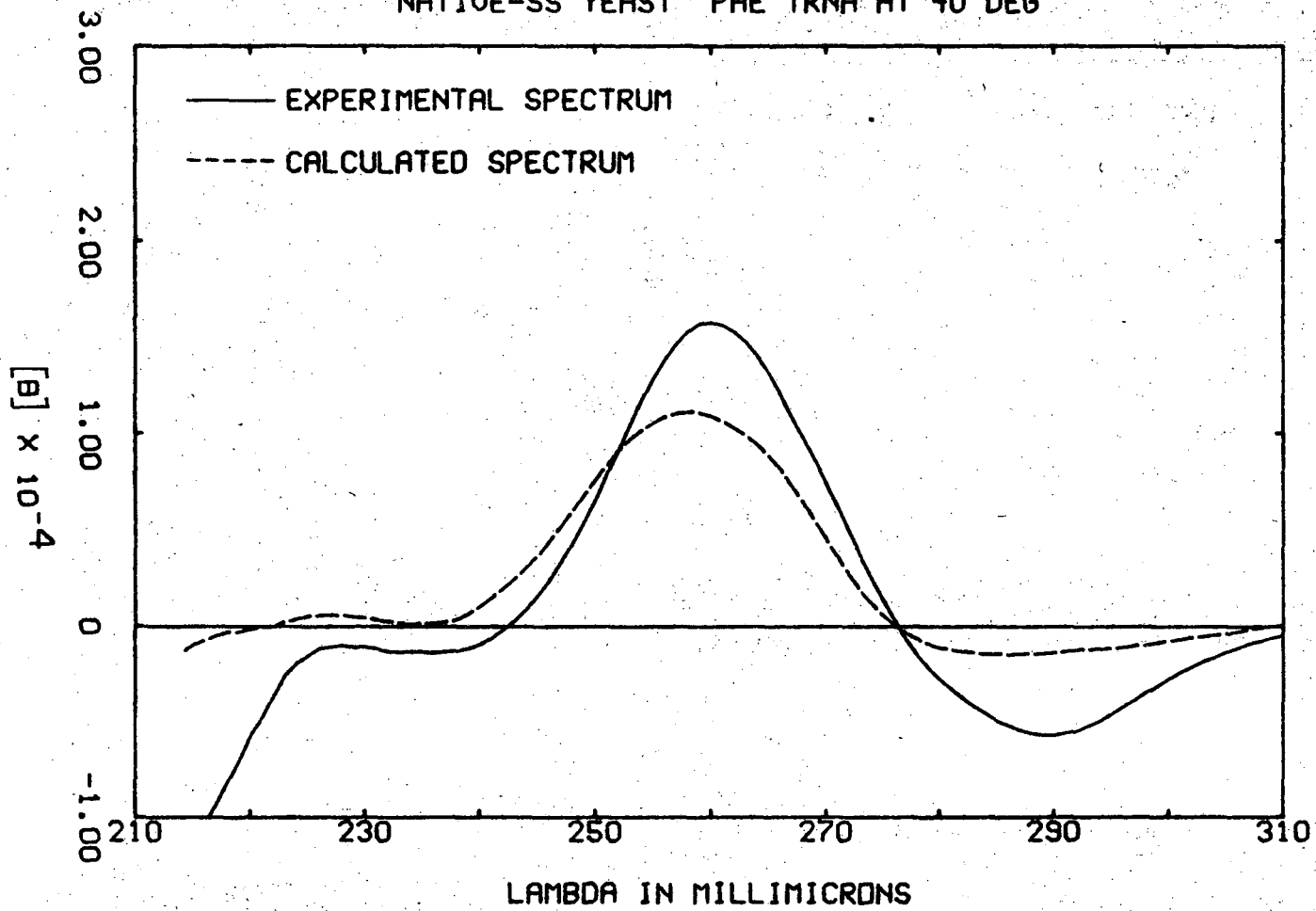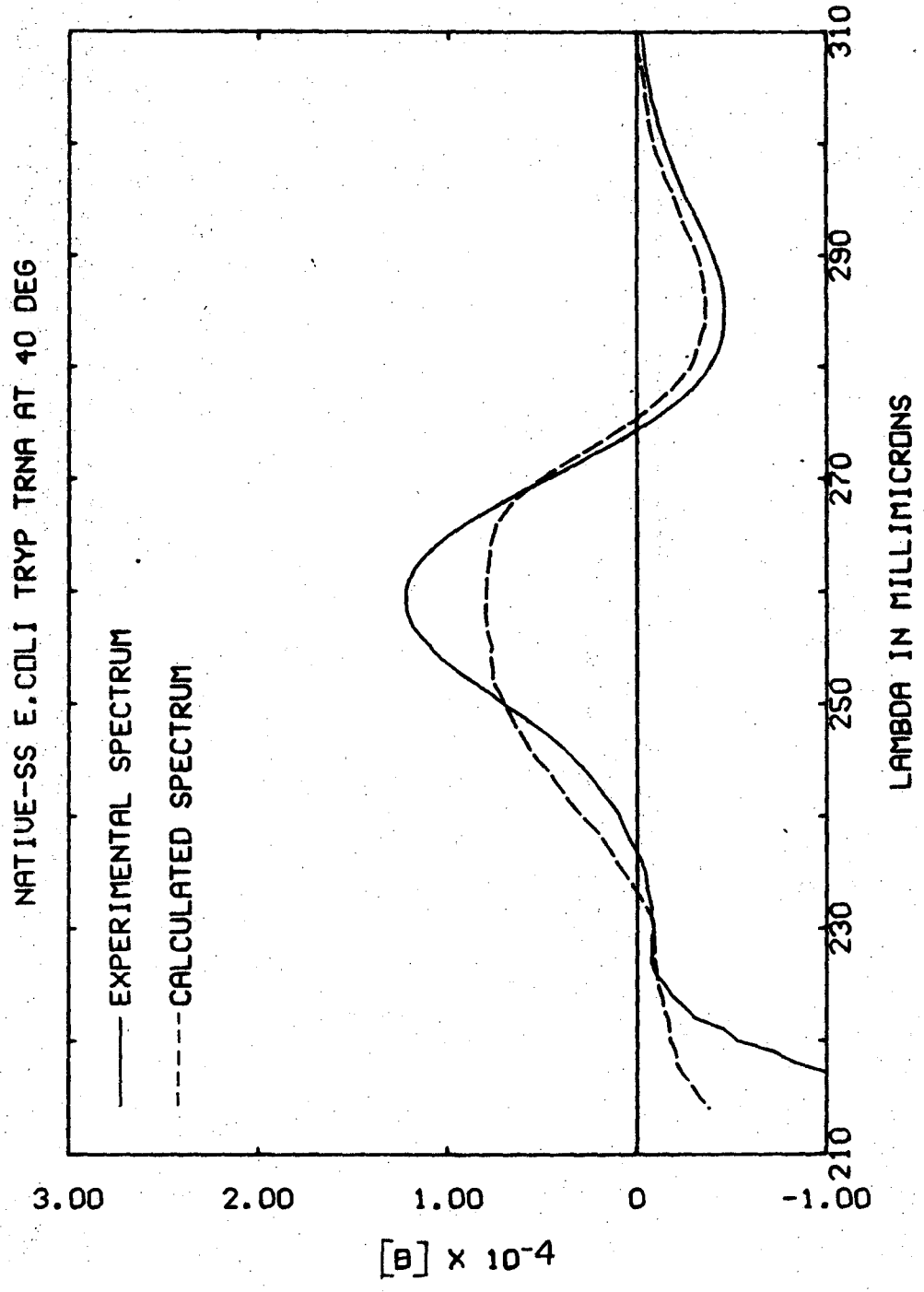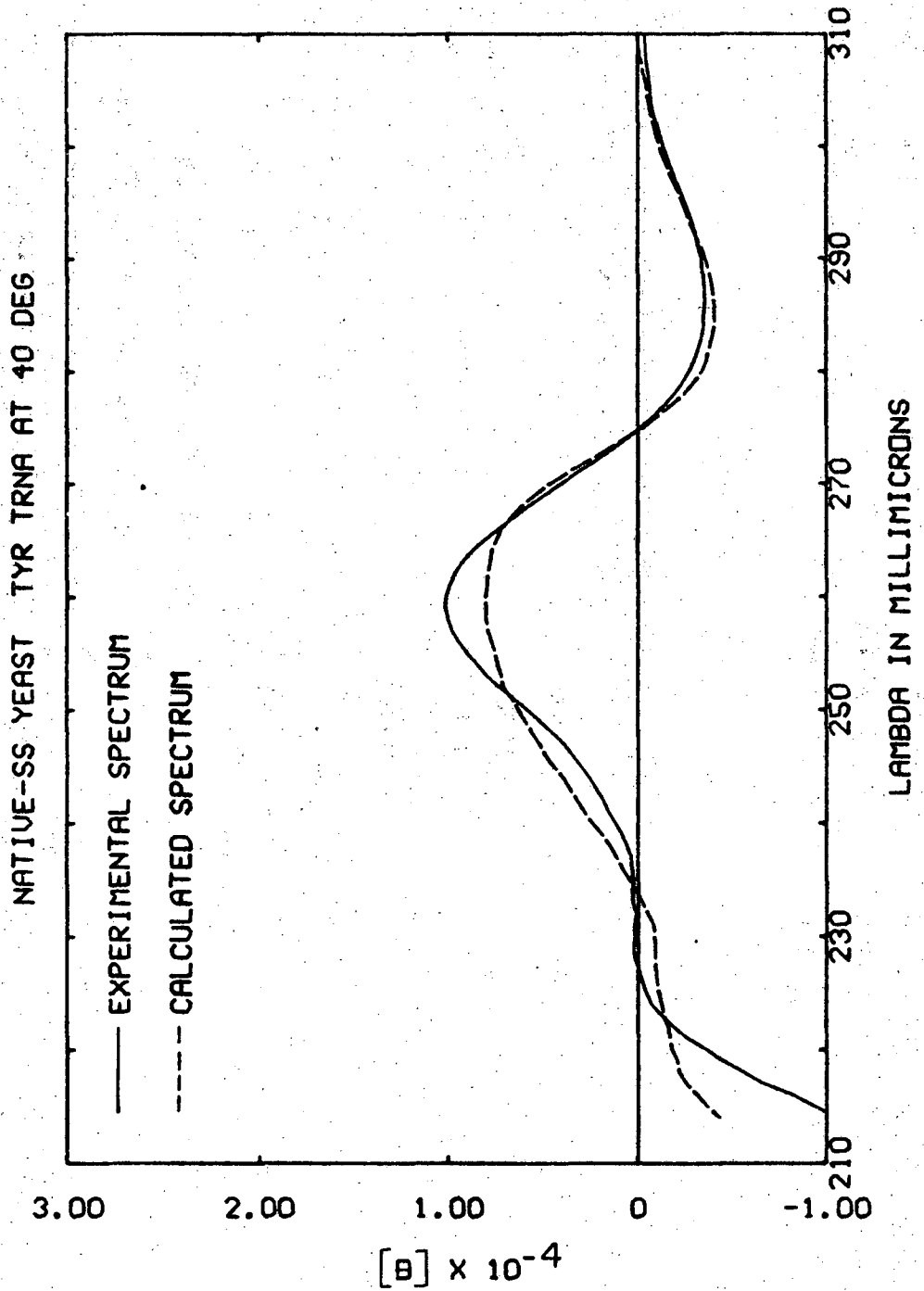
Figure 4-23

Figure 4-24

spectra correspond to the change in the structure of molecule upon the formation of secondary and tertiary structure.

This change was approximated with a sum of polymer pairing basis spectra as defined by Equation 3-14. The spectral properties and "Fit" of these calculated difference spectra are also listed in Table 4-4. Agreement is fairly good. "Fit" is seen to be better than in either of the previous cases. Still the magnitude of the experimental curve is greater than that of the calculated curve.

This difference is probably due to the double strand polymers not being a really good model for the short double strand regions in tRNA. Another possibility is that more double strand interactions are needed to fit the data. Several models for the tertiary structure of tRNA suggest additional base pairs.

B. Calculation of Native tRNA Spectra at 40°C

The agreement between calculated and experimental CD spectra of double strand regions of tRNA is better than for single strand regions. Thus, the major source of the large error in the calculation of native tRNA at 25°C appears to lie in the nearest neighbor approximation that the dimers are good models for single strand tRNA.

To avoid this difficulty, the experimental single strand at 40°C may be used to calculate the CD spectra

of native tRNA at 40°C:

$$(\text{tRNA,native})_{40°} = (\text{tRNA, single strand})_{40°} + \sum_{P=1}^{6} F_p \{P\}$$

$$(4-2)$$

where F_p is the frequency of the double strand pairing
interaction {P} defined by Equation 3-14 and the sum
is taken over the six polymers in Appendix 2.

The extrema of these calculated curves are com-
pared with the experimental spectra in Table 4-5.
Figures 4-25 to 4-27 show examples of relatively bad,
average, and good agreement. The "Fit" is much improved
from that involving the dimers instead of the experi-
mental single strand spectra. In general positions
and magnitudes agree reasonably well with the experi-
mental curves.

The reason for this fit may be qualitatively
understood by comparing the base composition and CD
curves of some of these tRNAs with the calculated
curves in Chapter III.

The position of the maximum of the large positive
band of the native tRNA varies from 262 to 267 mμ.
There is some correlation between the position of this
band and the base composition of the tRNAs. Table 4-6
lists the base composition, percent A and U, and per-
cent G and C in these tRNAs. With the exception of
tRNA^{Phe} (E. coli) which has a very low λ_{max}, the posi-

Table 4-5

Comparison of CD of Experimental Native tRNA at 40°C and Single
Strand Plus Base Pairing Interactions at 40°C

		λ_{min}	$[\theta]_{min}$ $(\times 10^{-4})$	λ_{max}	$[\theta]_{max}$ $(\times 10^{-4})$	λ_c	λ_{max}	$[\theta]_{max}$ $(\times 10^{-4})$	Fit
F. Met (E. coli)	exp	297	-.12	267	2.19	244	230	-.37	
	cal	298	-.05	268	1.77	242	222	-.33	.244
Leu (Yeast)	exp	---	----	263	2.57	242	223	-.16	
	cal	---	----	266	2.14	243	221	+.11	.216
Phe (E. coli)	exp	---	----	263	2.26	239	226	-.08	
	cal	300	-.02	268	1.60	238	222	-.20	.315
Phe (Wheat)	exp	296	-.15	264	2.07	244	226	-.40	
	cal	300	-.04	265	2.05	244	222	-.23	.139
Phe (Yeast)	exp	295	-.19	263	2.15	246	226	-.35	
	cal	---	----	265	1.69	244	218	-.11	.276
Tryp (E. coli)	exp	299	-.02	265	1.95	243	226	-.41	
	cal	----	----	268	1.83	240	219	-.29	.177
Tyr (E. coli)	exp	---	----	264	2.20	244	224	-.22	
	cal	---	----	268	2.21	239	221	+.01	.209
Tyr (Yeast)	exp	299	-.04	265	1.83	242	236	-.19	
	cal	298	-.02	267	1.80	239	221	-.02	.103
Val (E. coli)	exp	298	-.06	267	2.16	243	225	-.46	
	cal	---	----	268	2.15	240	222	+.03	.217

Figures 4-25 to 4-27. A comparison of CD spectra
of native tRNAs at 40°C with a sum of experimental
single strand spectra and double strand pairing
interaction spectra as defined in Equation 3-13.

NATIVE YEAST PHENYLALANINE TRNA 40 DEG

—— EXPERIMENTAL SPECTRUM
--- CALCULATED SPECTRUM

LAMBDA IN MILLIMICRONS

$[\theta] \times 10^{-4}$
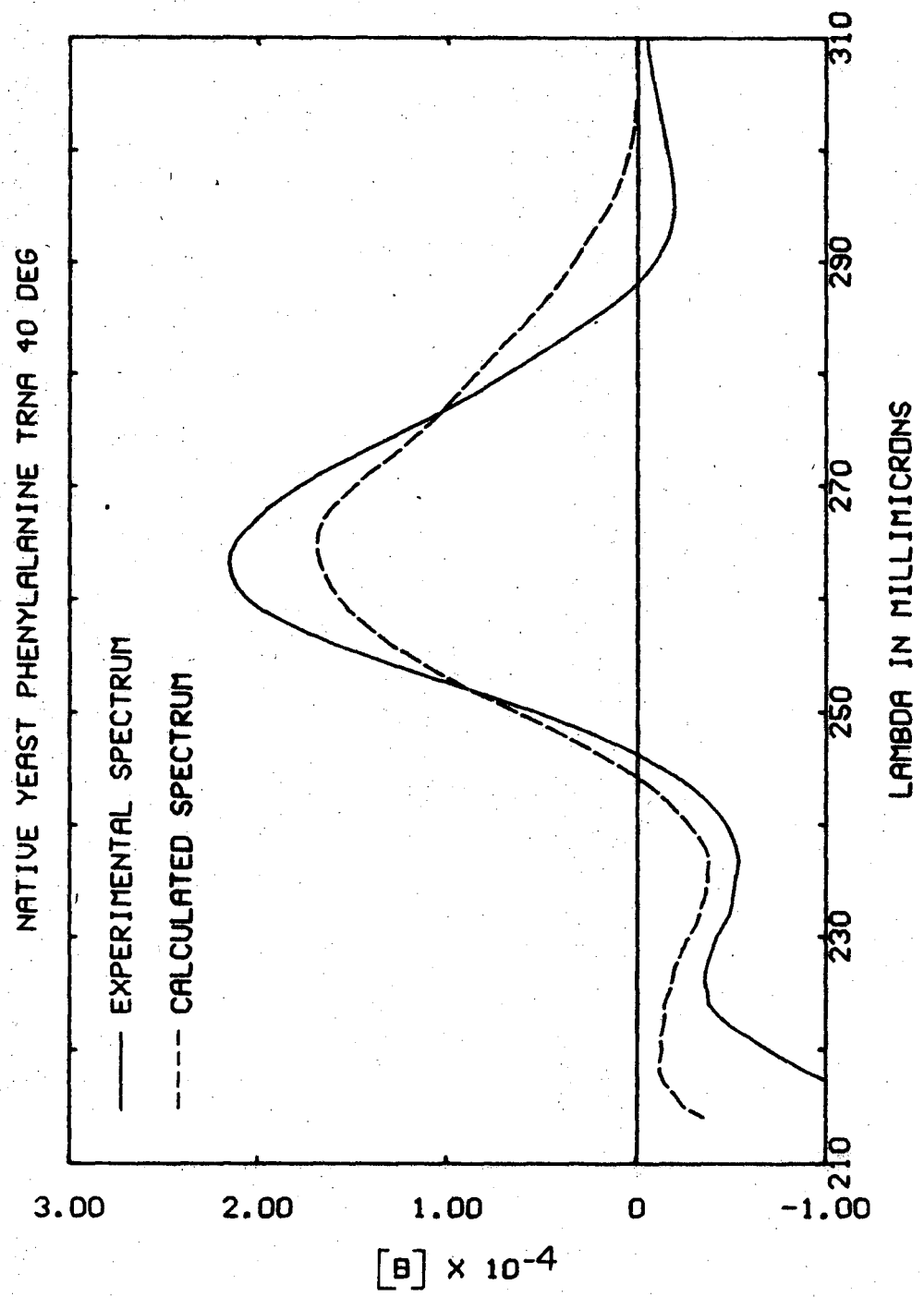
Figure 4-25

NATIVE E.COLI TRYPTOPHAN TRNA   40 DEG

——— EXPERIMENTAL SPECTRUM

– – – CALCULATED SPECTRUM

$[\theta] \times 10^{-4}$

LAMBDA IN MILLIMICRONS

Figure 4-26

138

NATIVE YEAST TYROSINE TRNA AT 40 DEG

EXPERIMENTAL SPECTRUM

CALCULATED SPECTRUM

[θ] × 10⁻⁴

LAMBDA IN MILLIMICRONS
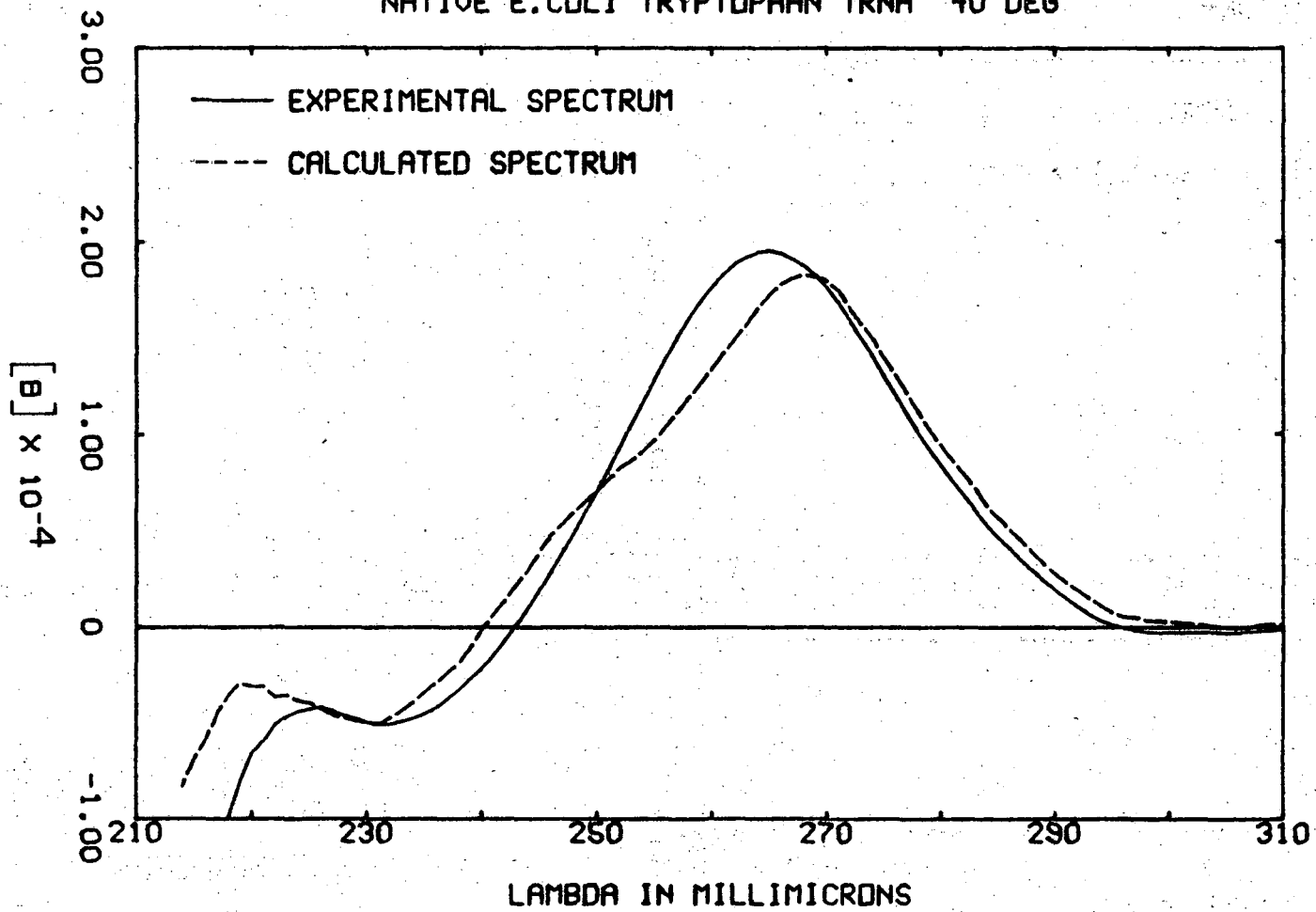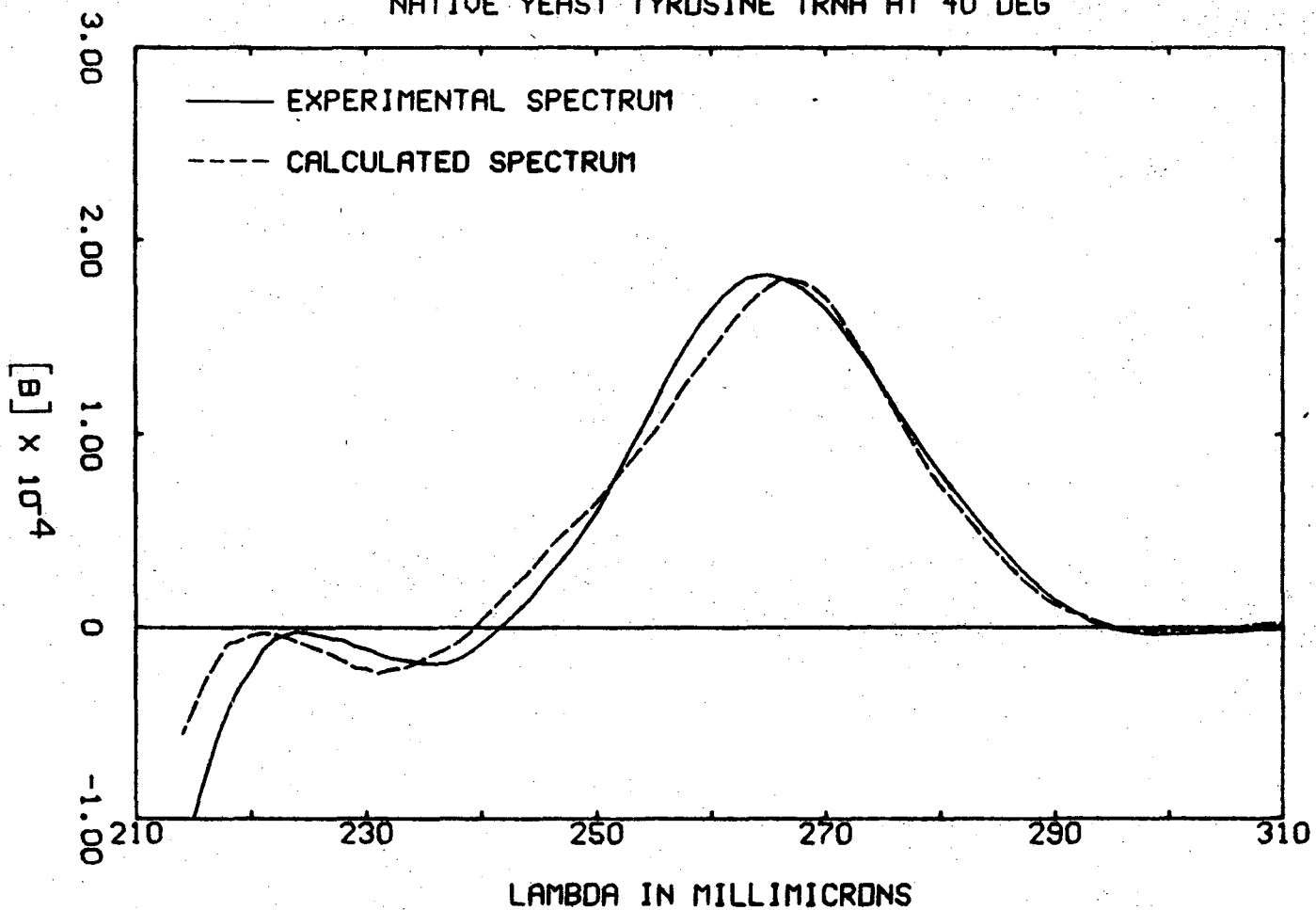
Figure 4-27

Table 4-6

Base Composition of Nine Species of tRNA

	A	U	C	G	D	Total Number of Bases	% A,U	% G,C
F. Met (E. coli)	14	11	26	25	1	77	34	66
Leu (Yeast)	21	19	20	23	2	85	49	51
Phe (E. coli)	15	12	23	24	2	76	37	63
Phe (Wheat)	18	12	20	24	2	76	42	58
Phe (Yeast)	19	15	17	23	2	76	47	53
Tryp (E. coli)	15	14	21	23	3	76	42	58
Tyr (E. coli)	19	16	28	22	-	85	41	59
Tyr (Yeast)	17	12	21	22	6	78	45	55
Val (E. coli)	16	13	23	23	1	76	40	60

tion of λ_{max} decreases with a decrease in percent G and C. This is the result that would be predicted from examination of Figs. 3-5 and 3-6.

The negative band at about 298 mµ is a variable feature that is found in six of the nine species of tRNA. The absence of this band in the two species of tRNA^{Tyr}, and in tRNA^{Leu} can be explained by differences in the sequence or the structure of these three species of tRNA. Examination of double strand interaction frequencies in Table 3-2 shows that these three tRNAs contain more of the interaction $\left(\begin{smallmatrix} A A \\ U U \end{smallmatrix}\right)$ than do most of the other tRNAs. Figure 3-6 indicates that the magnitude of the band at 295 mµ decreases with an increase in A:U pairing interactions.

The double strand polymers are a fairly good model for the double strand regions in tRNA in spite of the many approximations discussed in Chapter III. Thus, the CD of tRNA at 40°C may be calculated from a sum of double strand polymer interactions and the spectrum of the single strand tRNA at this temperature.

5. Applications

Examples of the sorts of information about the structure of RNA that may be obtained from RNA CD spectra will be given.

A. Native and Denatured tRNAs

Certain species of tRNA exist in two conformations
that are stable at room temperature, only one of
which is biologically active (5-9). It is customary
to call the form that will accept the correct amino
acid the native form, (N), and the inactive form, the
denatured form, (D). To denature the native form of
these tRNAs, it is necessary to heat it to some temper-
ature T in the presence of 1 mM EDTA for 10 minutes
and then cool it. This denatured tRNA is stable until
heated to T for 10 minutes in the presence of 10 mM
Mg^{++}. This process results in the renaturation of the
fully active tRNA:

$$\text{Native} \underset{Mg^{++}, T^\circ}{\overset{EDTA, T^\circ}{\rightleftharpoons}} \text{Denatured} \qquad (4-3)$$
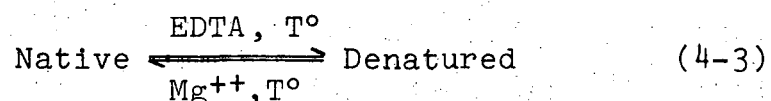
Two of the nine tRNAs being studied in this
work, $tRNA^{Leu}$ (Yeast) and $tRNA^{Tryp}$ (E. coli), exist
in two such forms. The temperature for interconversion
of forms is 50°C for $tRNA^{Tryp}$ and 60°C for $tRNA^{Leu}$.
As long as the temperature is kept below 40°C there will
be no interconversion and both forms will be stable in
the same solvent. It is of interest to consider what
sort of structural difference in these two forms is
responsible for the loss of biological activity of the
denatured molecule. This should provide some insight
into the nature of the specificity of the recognition

of the tRNA by the aminoacyl synthetase.

A number of studies have probed this difference in structure between the native and denatured forms of these tRNAs. Hydrodynamic studies on tRNA^{Leu} suggest that the denatured form has a volume about 25% larger than does the native form (7). Also, the denatured form is much more sensitive to pancreatic RNase (8). From the increase in UV absorption in the denatured molecule relative to the native, it has been suggested that the structural change between the two forms involves a loss in about four base pairs in the denatured molecule (7).

It is of interest to see if this result is also obtained from an analysis of the CD spectra of the two forms. Since CD is more sensitive than UV to molecular conformation, it should be able to provide more information about the nature of this change. CD spectra of the native and denatured forms of tRNA^{Tryp} and tRNA^{Leu} are shown in Figs. 4-28 and 4-29. For each tRNA the spectra of the native and denatured forms were measured in the Cary 6001 consecutively without moving the cell. First the spectrum of the denatured tRNA in the presence of 10 mM Mg^{++} was recorded. Then the sample was heated to 50 or 60°C for 10 minutes, cooled, and the spectrum of the native form was recorded. Doing the measurement without moving the cell allowed the difference spectra for the change

144

E.COLI TRYP TRNA AT 5 DEG

- - - - NATIVE
———— DENATURED

$[θ] × 10^{-4}$

LAMBDA IN MILLIMICRONS

Figure 4-28

YEAST LEUCINE TRNA AT 5 DEG

--- NATIVE

—— DENATURED

$[\theta] \times 10^{-4}$

LAMBDA IN MILLIMICRONS
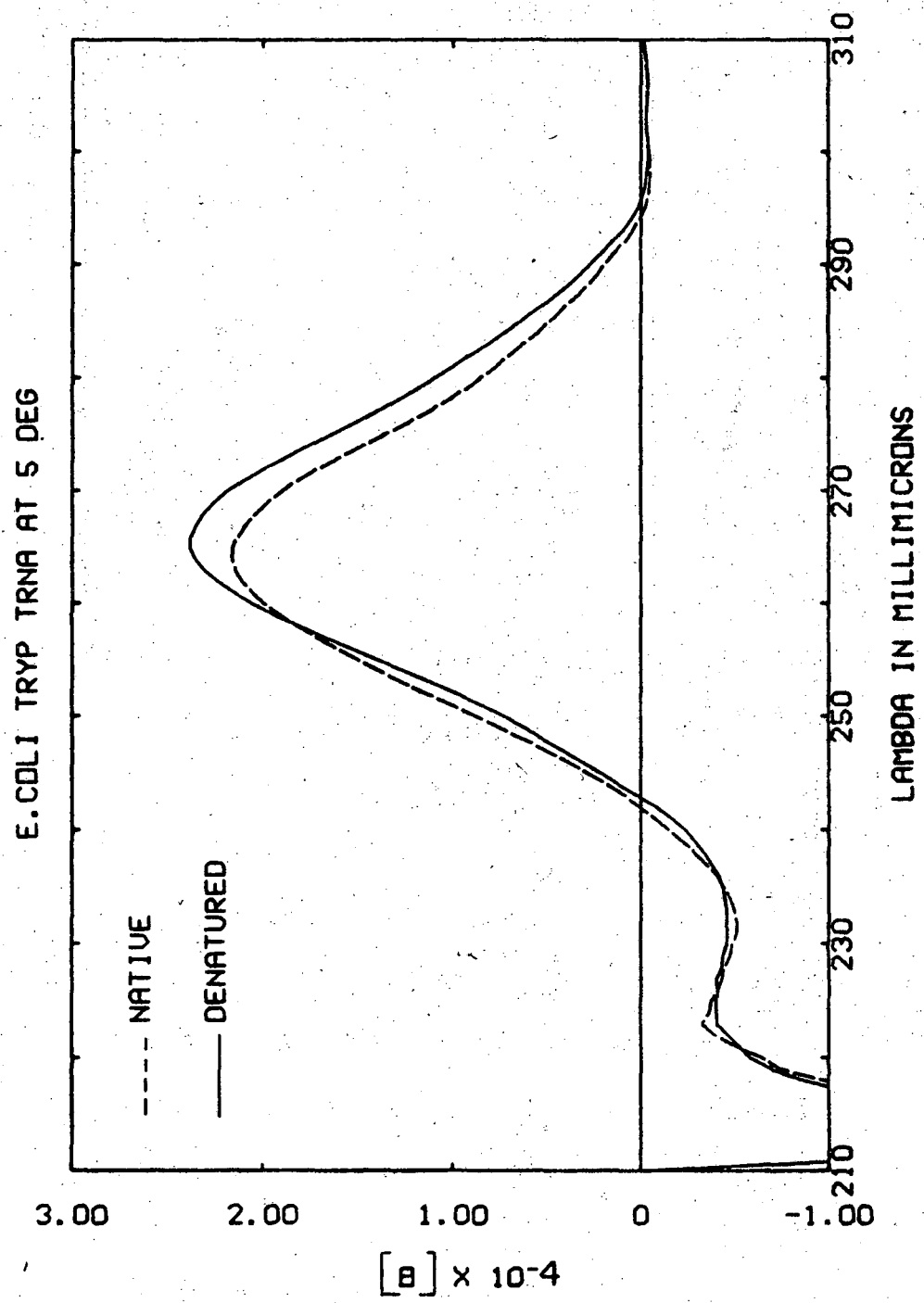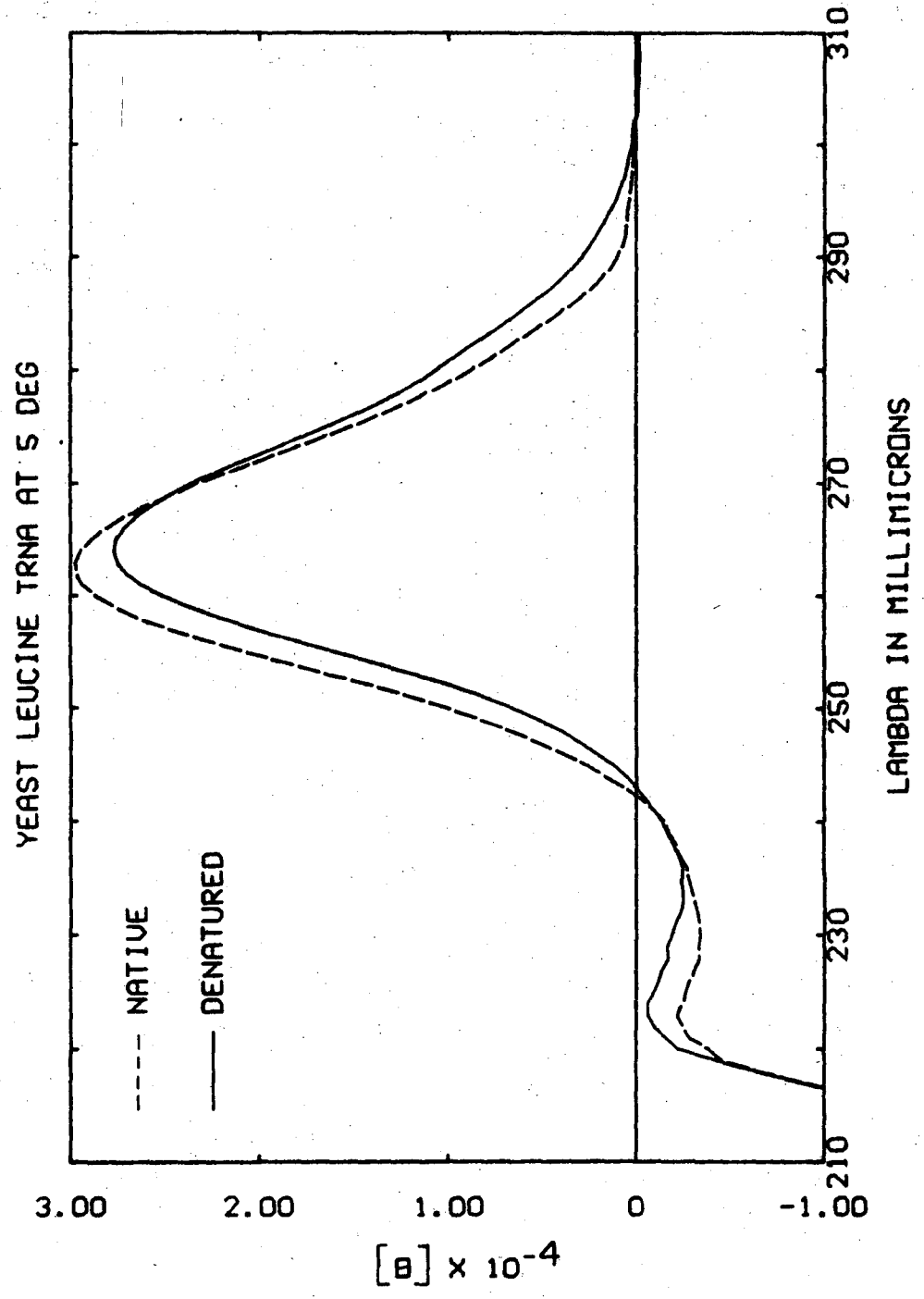
Figure 4-29

between the two forms to be determined with consider-
able accuracy.

The extrema of these spectra are listed in Table
4-6 along with the UV extinction coefficients. The
denaturation of tRNA^{Leu} results in an increase in
absorption and a decrease in the magnitude of the CD
maximum accompanied by a red shift of 2 mμ. All these
changes suggest the loss of base pairing interactions.
For tRNA^{Tryp}, denaturation is also accompanied by an
increase in absorption, and a slight red shift of the
CD maximum. However, the magnitude of the CD increases
upon denaturation. This result is somewhat surprising
and seems contradictory at first. However, the change
from 60 to 100% single strand RNA in Fig. 3-1 provides
a model for this sort of phenomena. In that case,
there is also an increase in absorption accompanied by
an increase in the magnitude of the CD maximum.

The difference spectra between the native and
denatured tRNAs, N-D, are shown in Figs. 4-30 and 4-31.
Using the double strand pairing spectra at 25°C, the
change in CD accompanying the opening up of the various
double strand regions in these tRNAs may be approxi-
mated. This comparison is shown in Figs. 4-30 and 4-31.

The CD of the four regions are in both cases quite
different, and theoretically we should be able to dis-
tinguish between the various double strand regions of
the tRNA. There is fairly good agreement between the

Figures 4-30 and 4-31. Comparison of difference between the CD of native and denatured tRNA^{Leu} (Yeast) and tRNA^{Tryp} (E. coli) with sum of double strand pairing interactions corresponding to various helical regions of the H model shown in Figs. 1-1 to 1-3. Experimental difference spectrum (———). Base pairs in D helix (·····). Base pairs in anticodon helix (-------). Base pairs in ACC helix (— — — —). Base pairs in TψC helix (——— ———).

NATIVE MINUS DENATURED LEU TRNA

Figure 4-30

148

NATIVE MINUS DENATURED TRYP TNA

LAMBDA IN MILLIMICRONS
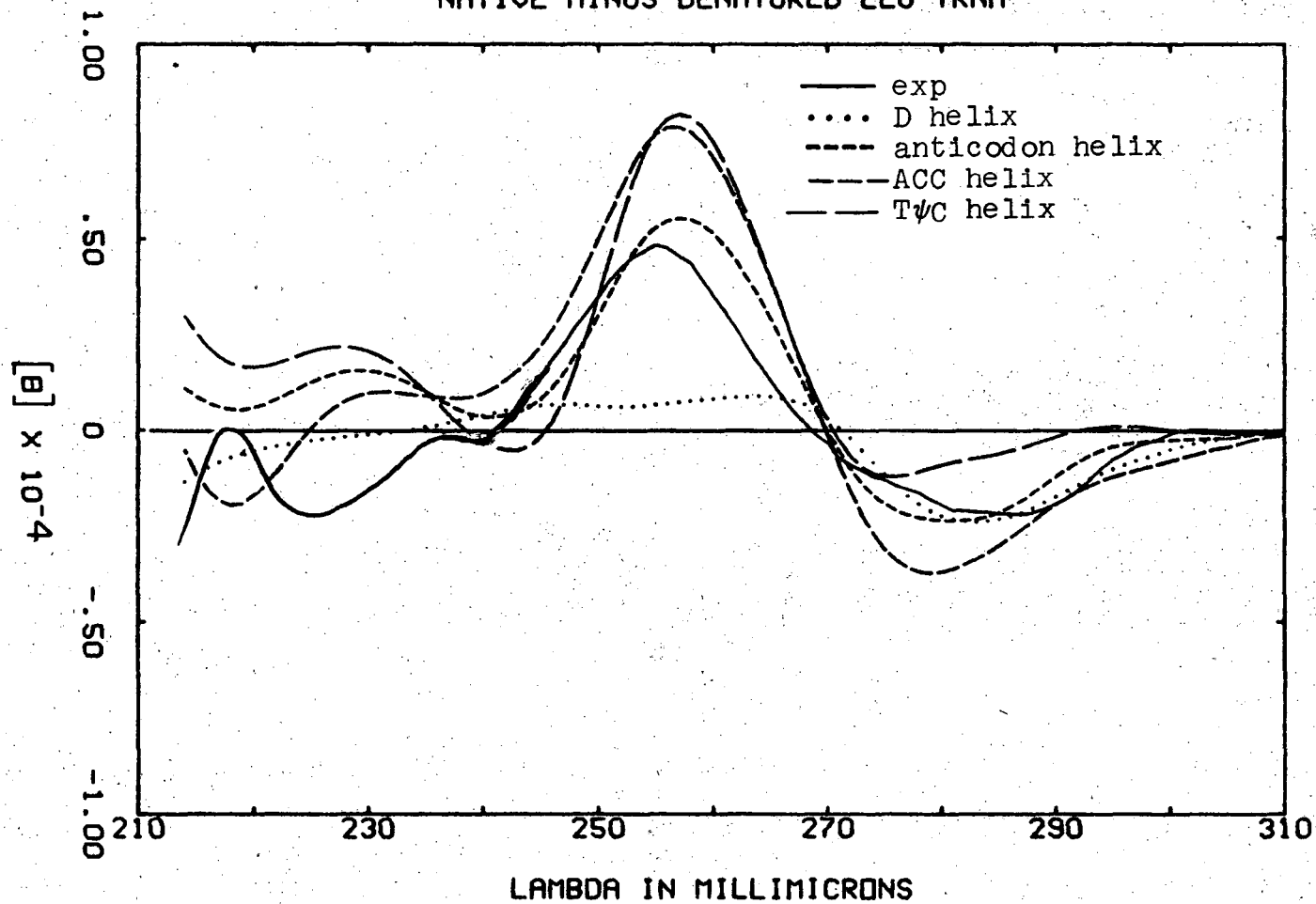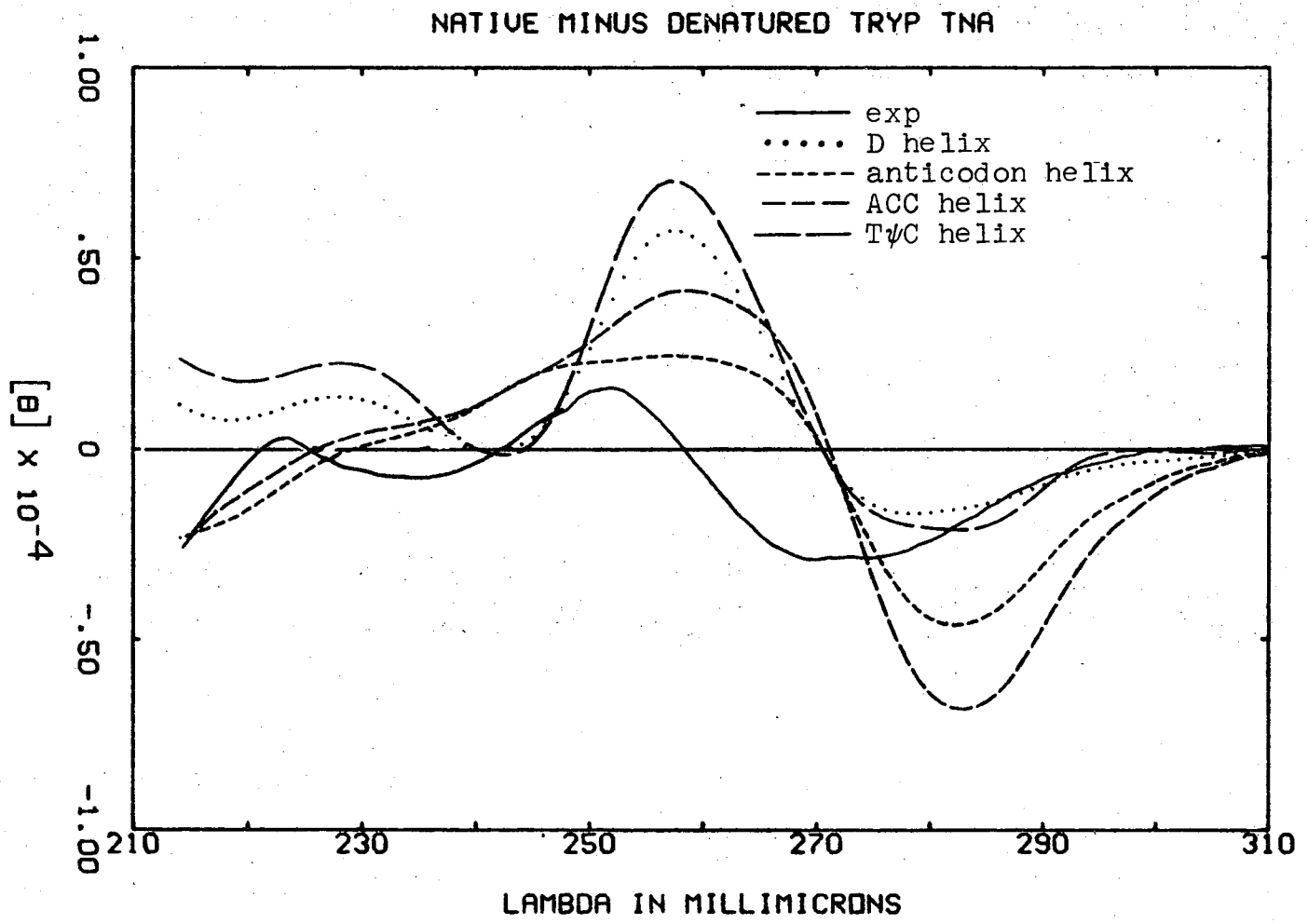
Figure 4-31

difference spectrum for tRNA^{Leu} and the opening of the helix that closes the anticodon loop (Fig. 4-30). Comparison of the difference spectra for tRNA^{Leu} with average double strand spectra corresponding to different numbers of base pairs indicates that the difference between native and denatured tRNA corresponds to the loss of four base pairing interactions or five base pairs.

Similar comparisons involving tRNA^{Tryp} do not work so well (Fig. 4-31). The somewhat anomalous increase in the CD upon denaturation leads to a difference spectrum with the crossover shifted so far to the blue that it will not fit well with any combination of double strand polymers. This suggests a structural rearrangement upon denaturation of tRNA^{Tryp} that is different form than observed in tRNA^{Leu}. It should be noted that the native to denatured change occurs at temperatures lower than the T$_m$ of the tRNAs (Figs. 4-2 and 4-6).

There is evidence that the change in denatured tRNA^{Tryp} does involve base pairing in the helix of the D loop. A supressor tRNA^{Tryp} (E. coli) has been isolated and sequenced which does not exist in a denatured form (13). The only sequence difference between this tRNA and the wild type is that a mismatched G in a G:U base pair in the D loop helix is changed to an A resulting in an A:U base pair that stabilizes the double strand region. It is possible that this change is also

involved in tertiary structure in some manner, but
it is strongly suggested that the helix of the D loop
is implicated in the change. However, the CD change
upon the loss of these base pairs is quite different
from the observed native-denatured difference (Fig.
4-31).

B. The A and B Forms of 5S RNA

Two forms of E. coli 5S RNA which are similar in
some respects to the native and denatured forms of tRNA
have been observed (10). The forms, called the A
form and the B forms, may be separated from one another
by chromatography on Sephadex G-100 or methylated albumin
silicic acid. The B form does not bind to the 5S RNA
binding site on the 50S ribosome subunit. B form can
be converted by heating in the presence of Mg^{++} to a
form that will bind to the ribosome and has the same
optical and chromatographic properties as the A form.

The optical properties of these two forms have
been studied (11), and found to be different. A has
a slightly larger hyperchromism than B suggesting that
B contains fewer base pairs than A. The magnitude of
the CD maximum is much greater for the B form, which
suggests greater stacking. Dr. Jim Lewis gave us the
samples of 5S RNA whose CD spectra are shown in Fig.
4-32. The maximum of the B forms is shifted about 2 mμ
to higher wavelengths relative to the A form as would
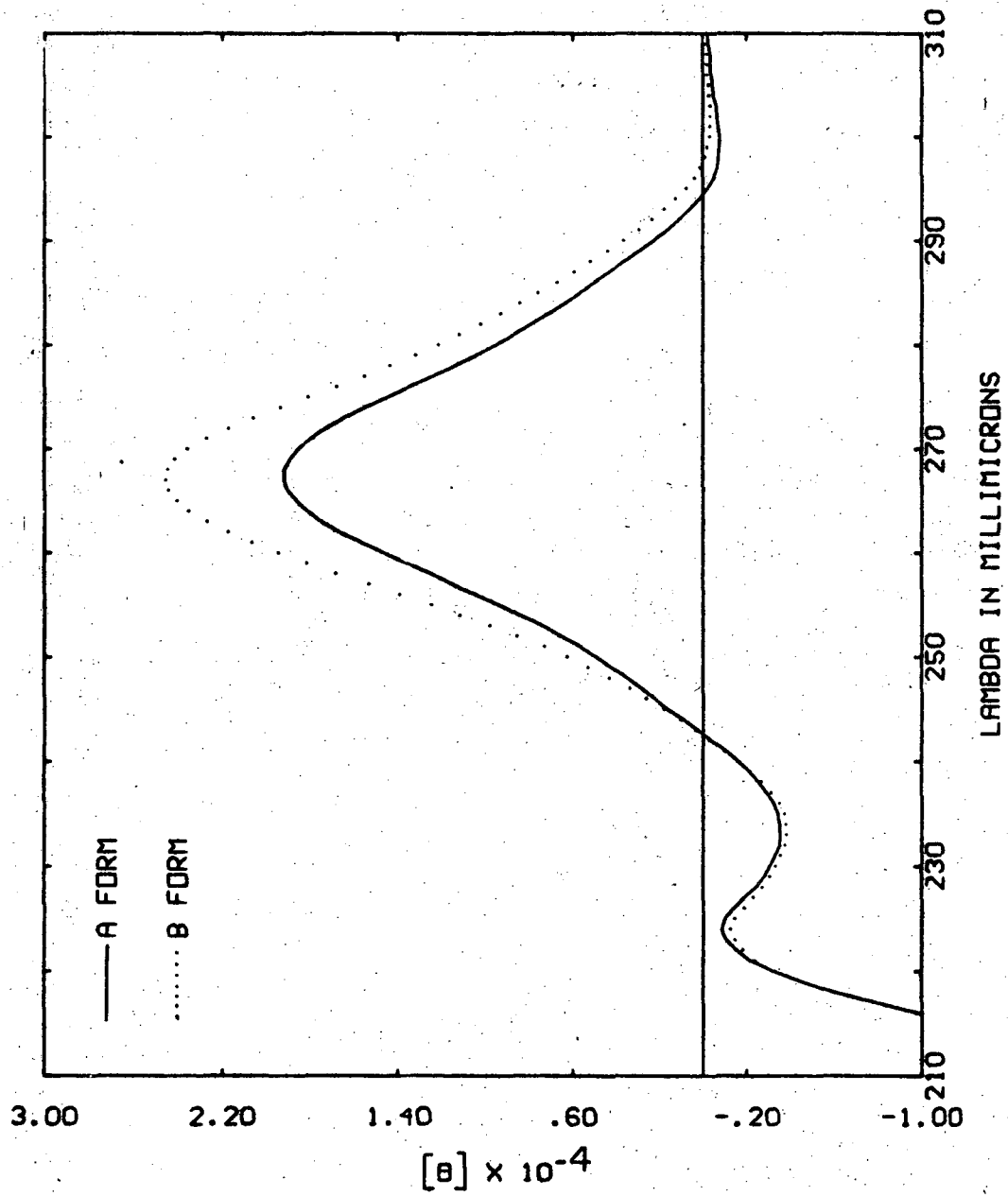
Figure 4-32

be expected upon the loss of double strand regions. However, there is a large increase in magnitude. This behavior is similar to that observed during the native to denatured transition in E. coli T tRNA^{Tryp} (E. coli).

The experimental CD of both forms of 5S RNA were compared with a series of calculated curves of RNAs with the same base composition as E. coli 5S RNA. These comparisons suggest that the A form is about 50% double stranded and the B form is about 60% double stranded. This result does not agree with the greater hyperchromicity of the A form. Further study of the physical differences between these two forms of 5S RNA should be interesting as it might help explain the anomalous optical properties of E. coli 5S RNA.

Dr. C. R. Cantor suggested that native 5S RNA was about 70% double stranded based on comparison of experimental and calculated ORD and UV curves (14). The discrepancy between our result and his result is probably due to the different basis spectra used in these two studies. Also the properties of the A form of 5S RNA are somewhat different from those of the native molecule (11).

REFERENCES TO CHAPTER IV

1. V. A. Freid, Thesis, University of Oregon (1970).

2. C. J. Formoso, Thesis, University of California, Berkeley (1970).

3. S. R. Jaskunas, Thesis, University of California, Berkeley (1968).

4. K. Javaherian and A. Blum, Biochemistry, submitted for publication.

5. T. Ishida and N. Sueoka, Proc. Natl. Acad. Sci. U.S., 58, 1081 (1967).

6. W. J. Gartland and N. Sueoka, Proc. Natl. Acad. Sci. U.S., 55, 948 (1966).

7. D. Henley, T. Lindahl, and J. Fresco, Proc. Natl. Acad. Sci. U.S., 55, 191 (1966).

8. A. Adams, T. Lindahl, and J. Fresco, Proc. Natl. Acad. Sci. U.S., 57, 1685 (1967).

9. T. Lindahl, A. Adams, M. Geroch, and J. Fresco, Proc. Natl. Acad. Sci. U.S., 57, 178 (1967).

10. M. Aubert, J. Scott, M. Renier, and R. Monier, Proc. Natl. Acad. Sci. U.S., 61, 292 (1968).

11. J. F. Scott, R. Monier, M. Aubert, and M. Reynier, Biochem. Biophys. Res. Commun., 33, 5 (1968).

12. M. Levine, personal communication.

13. D. Hirsh and L. Gold, J. Mol. Biol., 58, 459 (1971).

14. C. Cantor, Proc. Natl. Acad. Sci. U.S., 59, 478 (1968).

CHAPTER V

DISCUSSION AND SUMMARY

> "If seven maids with seven mops
> Swept it for half a year
> Do you suppose the Walrus said
> That they could get it clear?"
> "I doubt it," said the carpenter.
> And shed a bitter tear."   (1)

1. ## Calculated RNA Spectra Provide Models for Interpreting Changes in tRNA Spectra

In Chapter III, spectra are calculated that show the variation of the CD of RNAs with base composition, sequence, and percent double strand. Methods for obtaining these spectra are presented. Single strand regions are calculated using the nearest neighbor approximation and the spectra of 20 dimers. It is assumed that the spectra of the unusual nucleosides that account for about 10 percent of the bases in the tRNA are the same as those of the analogous unmodified nucleosides.

The CD of the double strand regions is calculated using 5 double strand polymer spectra. Since there are 10 double strand interactions, a number of approximations are necessary. Still, this calculation should be more accurate than previous ones which were based on only two double strand spectra, those of G:C and A:U (2,3).

It is assumed that the CD spectrum of tRNA may

be divided into contributions from bases in single strand, and double strand regions, and from tertiary structure. Methods of calculating these contributions are discussed in some detail. Examples of the variation of single and double strand RNA CD spectra with percent AU and GC, and with sequence of equimolar single strand RNA show the sensitivity of CD to primary structure of RNA. Changes in the spectrum of equimolar RNA as it changes from all single stranded to all double stranded show how CD is affected by secondary structure of tRNA. These changes may be used to help understand changes in the experimental spectra of tRNAs.

2. Experimental CD of Native tRNAs May be Fit Fairly Well with Appropriate Sums of Other RNA Spectra

In Chapter IV, we considered the manner in which the experimental spectra of nine native tRNAs could best be fit by calculated spectra. First we compared the spectra of the native tRNA at 25°C with a sum of dimer and monomer CD representing the single strand regions and polymer CD representing the double strand regions. Tertiary structure was set equal to zero. The fit was only qualitative.

Then we asked if the poor fit was due to lack of agreement between calculated and experimental spectra in single or double strand regions. The spectrum of

tRNA under salt and temperature conditions such that it was single stranded was compared with a sum of single strand basis spectra. Agreement was not very good. Then the change in the CD upon the formation of base pairs was compared with a sum of double strand pairing basis spectra. Agreement was much better in the latter case than in the former suggesting that the source of error in the original attempt to fit the spectra of native tRNA at 25°C was mostly in the calculation of the single strand regions. The conclusion that the CD of dimers is only a qualitative model for polymer CD agrees with previous comparisons between the ORD of dimers and polymers (2).

The experimental spectra of the native tRNAs at 40°C was then compared with a sum of the experimental single strand spectrum and double strand base pairing spectra. Agreement was quite good in most cases suggesting that double strand polymers are a fairly good model for the short double strand regions of the tRNAs. Much of the CD of the tRNAs could be accounted for on the basis of the double strand polymers although in most cases the calculated spectra were lower in magnitude than the experimental spectra.

3. Suggestions for Improvement

The agreement between the experimental and calculated CD is much better for some tRNAs such as tRNA^{Tyr}

(Yeast) than for others such as tRNA^{Phe} (Yeast) as shown in Figs. 4-27 and 4-25. At present we do not know if this difference indicates structural variation between the two tRNAs or merely poor calculated spectra. The least valid of the many approximations used in the calculation of the tRNA spectra was probably the construction of the spectrum of poly rGA:poly rCU. Since the double strand regions of tRNA^{Phe} (Yeast) contain more of this interaction than of any other (see Table 3-3), the calculated spectrum for this tRNA is certainly open to doubt. A good experimental CD spectrum of poly rAG:rUC should improve all of the tRNA calculated spectra, particularly that of tRNA^{Phe} (Yeast).

In general, the calculated spectra have somewhat lower magnitude than the experimental spectra. This might be because the double strand polymers are not good models for the short helical regions of tRNA. Presently, work is in progress in this laboratory to obtain a library of CD spectra of the 10 double strand interactions based upon the CD of a set of RNA oligomers. A preliminary result is the CD of the interaction $\overset{\displaystyle\longleftarrow}{\underset{\displaystyle\longrightarrow}{\genfrac{}{}{0pt}{}{AA}{UU}}}$ which was obtained by Mr. Phil Borer (4). Figure 5-1 compares this spectrum with the spectrum of poly rA:poly rU which was used to represent the interaction in this work. The oligomer spectrum is seen to have considerably greater magnitude than the polymer spectrum. The reason for this is presently unknown.
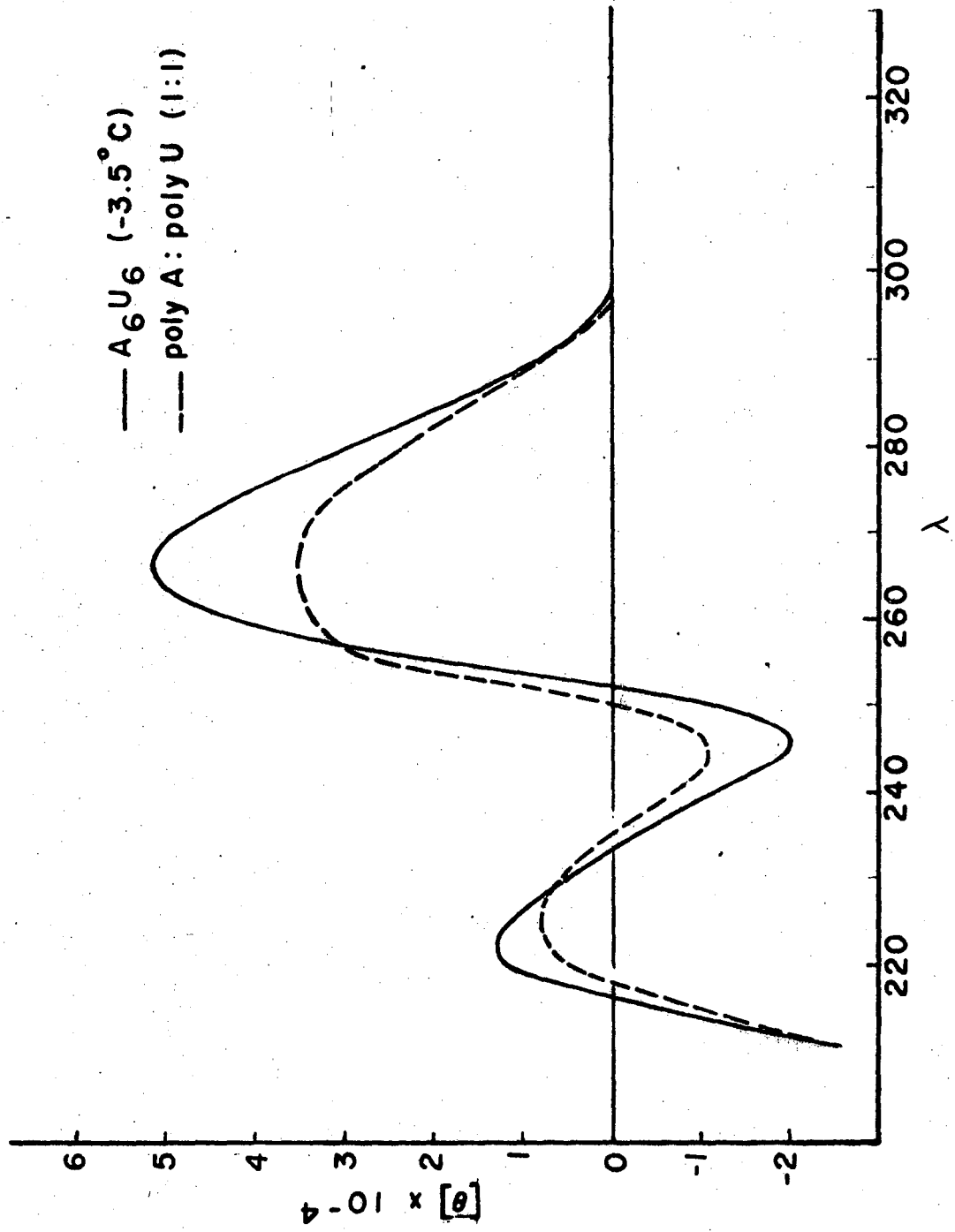
Figure 5-1

If this were a general phenomena, applicable to the
other double strand polymers, it might explain the
difference between the calculated and experimental CD.
When the CD of the 10 double strand interactions are
available, it should be possible to calculate the
CD of the double strand regions of tRNA with greater
accuracy and fewer approximations.

Single strand spectra calculated from a sum of
dimer basis spectra are not a very good model for
single strand tRNA or single strand homopolymers. To
avoid this problem, we used the experimental tRNA
single strand in our calculations. However, it would
be very useful to have a suitable model for the single
strand regions of tRNA. Such single strand basis
spectra could be constructed from an appropriate set
of polymer and oligomer spectra.

It would also be quite useful to have a library
of the 4 single strand homopolymers and the 8 alternat-
ing polymers at 40°C to be used in calculating the
double strand pairing interaction in Equation 3-14.

The base ψ accounts for 2% of the nucleotides
in tRNA. Knowledge of the CD behavior of ψ and some
of the other more exotic basis such as 4tU and A_i
would be very useful. CD spectra of the dimers $A\psi$, AA_i
and $A_i A$ have been measured and found to be quite
different from those of their unmodified analogues (5).
The CD of $A\psi$ is opposite in sign from that of ApU.
This work suggests that this is not generally true for

single strand interactions involving ψ.

Further information could also be obtained by measuring both basis spectra and experimental spectra between 185 and 350 mμ rather than between 210 and 310 as was done in this work. For example, using tRNA solutions of A_{260} = 30 in .5 mm pathlength cells, CD spectra have been obtained down to 200 mμ (6). However, it is likely that the tRNA is aggregated at this concentration (7). The 4tU CD present in many E. coli tRNAs at about 335 mμ may also be studied using concentrated solutions in a 1 cm pathlength cell. This base is in a region of the molecule that may change conformation upon charging of the tRNA (8), and a detailed study of its CD should prove interesting.

Another reason why the magnitude of the calculated CD is lower than that of the experimental spectrum may be that the native molecule has extra base pairs that stabilize the tertiary structure of the tRNA in addition to those predicted by the Holley model. This has been suggested in many of the models for the tertiary structure of tRNA that were discussed in Chapter I.

It is of interest to calculate the spectra of the tRNAs including the extra base pairs stabilizing tertiary structure to see if the CD predicted for these structures fits the experimental spectra any better than does the H model. Unfortunately, this procedure is not straightforward as many of the proposed interactions are triple strand or involve non-Watson-Crick base

pairs such as A:A and G:A. There is presently no model for the CD of these sorts of interactions. Furthermore, many of the suggested interactions involve only one or two consecutive base pairs, and as the method of calculating being used counts interactions rather than base pairs, it is difficult to properly represent these very short regions. Still it is possible to roughly approximate the contribution of extra base pairs required by the tertiary structure models proposed by Levitt (9) and Cramer (10). The "Fit" of these models with the experimental CD spectrum of native tRNA at 40°C are compared with that of the H model in Table 5-1.

The model of Levitt is approximated as involving three additional double strand pairing interactions, and that of Cramer as having six more such interactions. Thus, in cases where the calculated CD is too low assuming only the double strand regions predicted by the H model, both these models give improved agreement. Unfortunately, it is not presently known if the double strand pairing interactions predicted from polymers are too low in magnitude as suggested by Fig. 5-1. Thus, on the basis of comparison of these calculated CD spectra we tentatively suggest that the correct structure of tRNA contains more double strand inter- actions than are predicted by the H model. The number of additional base pairs needed for a better

Table 5-1

"Fit"[*] of CD Spectra of Native tRNAs
with CD Spectra Calculated Assuming
Various Models for Tertiary Structure
of the tRNAs

	H model	Levitt model	Cramer model
F. Met (E. coli)	.244	.176	.130
Leu (Yeast)	.216	.178	.129
Phe (E. coli)	.315	.248	.193
Phe (Wheat)	.139	.156	.173
Phe (Yeast)	.276	.251	.225
Tryp (E. coli)	.177	.148	.143
Tyr (E. coli)	.209	.213	.216
Tyr (Yeast)	.103	.106	.170
Val (E. coli)	.217	.234	.253

$$[*]\text{Fit} = \left(\frac{\sum\limits_{i=1}^{N} (E_i - C_i)^2}{\sum\limits_{i=1}^{N} (E_i)^2} \right)^{1/2}$$

where E_i is the value of the experimental curve at
the i-th wavelength, C_i is the value of the calcu-
lated CD curve at this same wavelength, and the
sum is taken over N wavelengths.

value of "Fit" varies for the different tRNAs. In
general, though, the experimental CD agrees best with
a calculated spectrum containing from two to four more
base pairing interactions than are predicted by the
H model.

4.   What CD Has Told Us about the Structure of tRNA

In this work, a large difference between the opti-
cal properties of nine purified species of tRNA in the
presence and absence of Mg^{++} at 40°C has been observed.
The difference between the CD spectra of these two forms
may be fit with a sum of the base pairing interaction
spectra based on the H model shown in Figs. 1-1 to 1-3.
An additional three or four base pairing interactions
will improve this fit. The comparison of calculated
and experimental spectra was made quantitatively at
many wavelengths, rather than by just considering the
extrema of the CD curves.

The general shape of the CD curves of the native
and single stranded tRNA suggest that the bases of
these two forms may have different relative geometry.
X-ray studies of RNA fibers show double stranded RNA to
be similar to the A form of DNA with bases tilted from
the helix axis (11). It is likely that bases in the
double strand regions of tRNA are also in this A form.
This is substantiated by comparing native and single
strand RNA spectra as shown in Figs. 4-19 to 4-21 with

CD spectra of DNA films in the A and B forms that have been measured by Schneider and Maestre (12,13). It is seen that the CD of DNA in the A form is qualitatively similar to that of native tRNA. When the relative humidity of the film is increased the DNA assumes the B conformation with its bases perpendicular to the helix axis. The CD of the B form of DNA is qualitatively similar to that of single strand tRNA. This suggests that in the absence of Mg^{++} the single strand form has bases that are stacked are nearly planar. Furthermore, the change in the band at 220 mμ in single strand RNA with percent A and U, and G and C is very similar to that observed in DNA in the B form.

The sensitivity of CD to small changes in conformation makes it quite useful in studying such phenomena as the change between the native and denatured conformations of some tRNAs. Our studies suggest that the transition between the native and denatured forms of $tRNA^{Leu}$ (Yeast) involves the loss of about four base pairs. The change in $tRNA^{Tryp}$ (E. coli) seems to involve something more. Perhaps the structure of the whole molecule is being rearranged or the tertiary structure is changing. This same sort of CD behavior was observed for the native and denatured forms of 5S RNA.

Thus we see that CD studies can provide information about the structure of tRNA. Presently, CD is

most useful for investigation of conformational change.
Better basis spectra should lead to better fit agree-
ment between calculated and experimental CD spectra.
By subtracting spectra calculated on the basis of the
primary and secondary structure of the tRNAs from the
experimental spectra, a constant difference spectrum
might be obtained. This difference should correspond
to the CD of the tertiary structure of the tRNA.

     Another way of obtaining some measure of the
contribution of tertiary structure to the CD of tRNA
would be from the difference between the CD of native
tRNA and fragments such as two half molecules. In any
case, our work has shown that the contribution of
tertiary structure to the CD of tRNA is not large.

5. Yet Another Model for the Tertiary Structure of tRNA

     Presently only tentative conclusions may be drawn
from our CD results due to the many approximations
necessary for the calculation of the experimental
spectra as previously discussed. Nevertheless, having
used CD to study the conformation of tRNA, I would
like to suggest yet another model for the structure of
tRNA.

     On the basis of evidence summarized in the intro-
duction and presented here, preliminary conclusions
about the tertiary structure of tRNA may be drawn. A
good model should have a long continuous helical region
from the ACC to the TψC loop, and the other helices
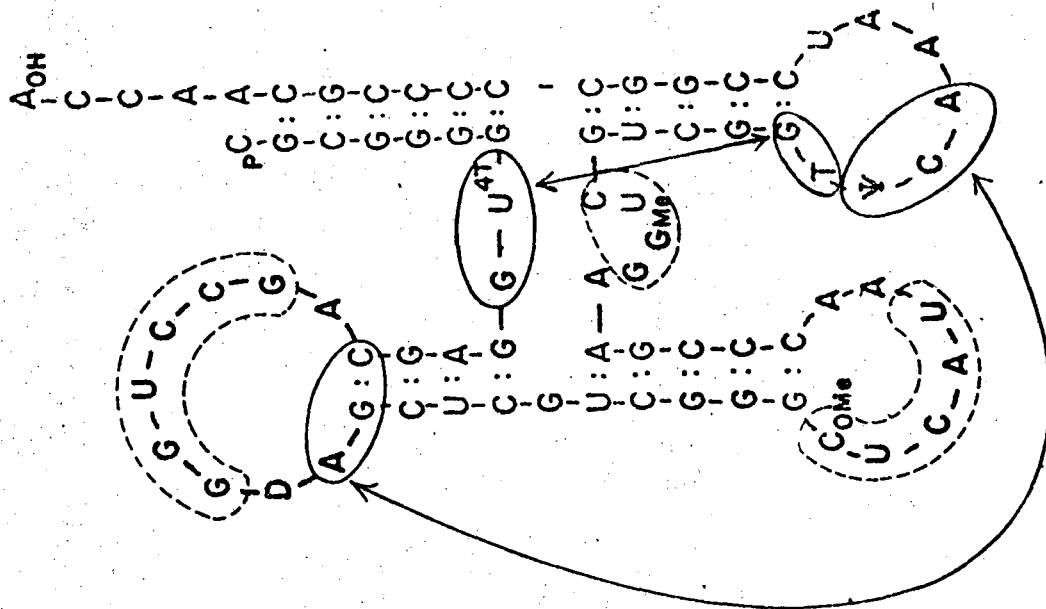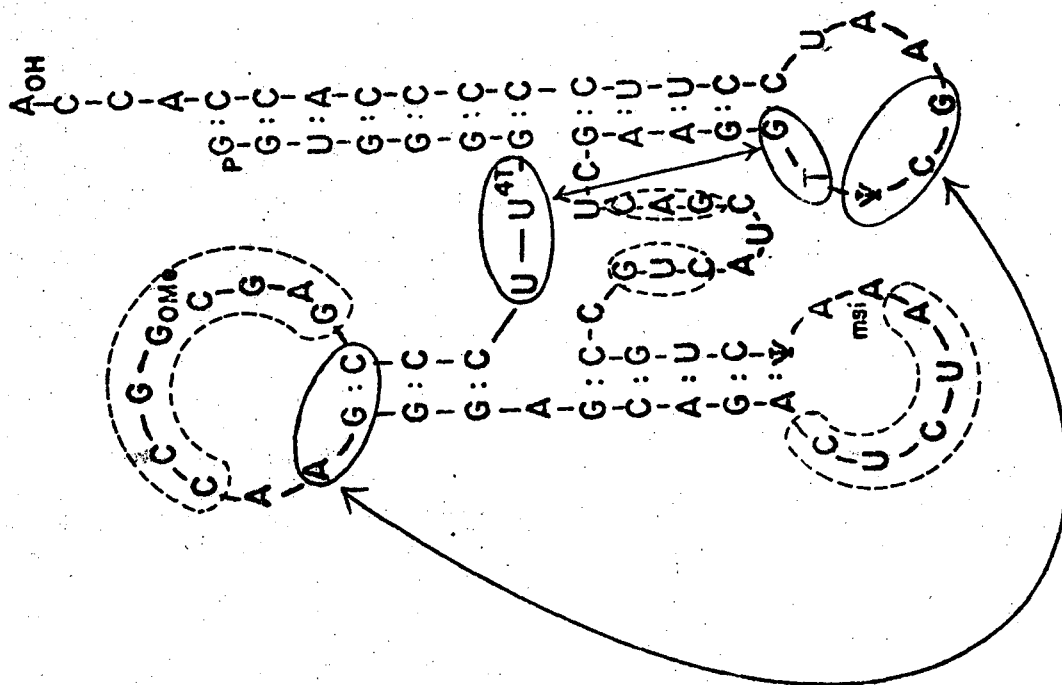
Figure 5-2. Regions of two tRNAs which will bind com-
plementary radioactive oligomers (-----) (from Refer-
ence 14). Areas in solid circles are assumed to inter-
act as described in text in proposed model for the
tertiary structure of tRNA.

parallel or nearly so to this helix. The TΨC loop

should be involved in tertiary structure in a manner

that makes it unavailable for chemical modification or

oligomer binding, perhaps by hydrogen bonding of some

sort with the bases in the part of the D loop. Resi-

dues 8 and 13 should be in close proximity. Our CD

results suggest that a good model should have about

three base pairing interactions in addition to those

due to the cloverleaf secondary structure.

Most of the models that have been proposed for

the tertiary structure of tRNA do not agree with the

oligomer binding results of Uhlenbeck (14) and the

methoxyamine reaction results of Cashmore and Brown

(15) as to which bases of the tRNAs are protected.

Dotted circles in Fig. 5-2 show the areas in two tRNAs

that will bind radioactive oligomers. It is assumed

that these areas are not directly involved in the

tertiary structure of the tRNA.

A refinement of the H model for the tertiary

structure of tRNA presented in Chapter I that does

agree with these results is also shown in Fig. 5-2.

The areas enclosed with solid lines are postulated to

interact with the other areas to which they are connec-

ted. The D loop bends over the TΨC loop and the bases

AGC in the D loop interact with the bases ΨCG in the

TΨC loop. The TG in the TΨC loop interacts with the

UU or the GU in the single strand region between the

stem and the D helix further stabilizing this inter-

action. This results in about three additional base

pairing interactions as suggested by the CD spectra.
With minor modification, this model will apply to all
the species of tRNA whose sequences are presently
known. The overall structure of this model is some-
what similar to that of Levitt (9).

As for more than speculation as to the tertiary
structure of tRNA, and how this molecule carries out
its many functions with such great specificity:

"We dance round in a ring and suppose
But the secret sits in the middle and knows."

Robert Frost

REFERENCES TO CHAPTER V

1. Lewis Carroll, Alice's Adventures in Wonderland, Whitney Co. (1945), p. 154.

2. C. R. Cantor, S. R. Jaskunas, and I. Tinoco, Jr., J. Mol. Biol., 20, 39 (1966).

3. C. R. Cantor, Proc. Natl. Acad. Sci. U.S., 59, 478 (1968).

4. P. Borer, personal communication.

5. M. P. Schweizer, R. Thedford, and J. Stama, Biochim. Biophys. Acta, 232, 217 (1971).

6. G. E. Willick and C. M. Kay, Biochemistry, 10, 2216 (1971).

7. D. B. Millar and R. F. Steiner, Biochemistry, 5, 2289 (1966).

8. K. Watanabe and K. Imahore, Biochem. Biophys. Res. Commun., 45, 488 (1971).

9. M. Levitt, Nature, 224, 759 (1969).

10. F. Cramer, H. Dapner, F. von der Haar, E. Schlimme, and H. Seidel, Proc. Natl. Acad. Sci. U.S., 61, 1384 (1968).

11. S. Arnott, S. D. Dover, and A. J. Wonacott, Acta Cryst., B25, 2192 (1969).

12. M. F. Maestre, J. Mol. Biol., 52, 543 (1970).

13. M. J. B. Tunis-Schneider and M. F. Maestre, J. Mol. Biol., 52, 521 (1970).

14. O. C. Uhlenbeck, J. Mol. Biol., submitted.

15. A. R. Cashmore and J. D. Smith, <u>J. Mol. Biol.</u>, in press (1971).

Appendix 1

Single Strand CD Basis Spectra

Basis spectra for 20 nearest neighbor interactions at 40°C are listed between 310 and 210 mμ. Ellipticity values listed are times 10^{-4}. These spectra were calculated from dimer and monomer spectra using Equation 3-4. The first 16 of these spectra were measured as part of this work in 1 mM MgCl, 10 mM tris HCl, pH 7.8. The last four dimer spectra involving D were measured by Dr. Carl Formoso. These 20 basis spectra were used to calculate the CD of single strand tRNA and double strand pairing interactions at 40°C.

AA EXPERIMENTAL SPECTRUM AT 40 DEG C

WAVELENGTH	ELLIPTICITY	WAVELENGTH	ELLIPTICITY	WAVELENGTH	ELLIPTICITY
310	.0245	276	2.3916	242	-1.8379
309	.0199	275	2.5646	241	-1.5404
308	.0258	274	2.7092	240	-1.2935
307	.0118	273	2.8208	239	-1.0539
306	.0067	272	2.9062	238	-.9192
305	.0024	271	2.9180	237	-.6076
304	-.0071	270	2.9234	236	-.4627
303	-.0171	269	2.8668	235	-.3127
302	-.0200	268	2.7430	234	-.1557
301	-.0339	267	2.5396	233	-.0456
300	-.0249	266	2.2557	232	.0267
299	-.0309	265	1.8901	231	.0709
298	-.0257	264	1.4437	230	.1522
297	-.0365	263	.9794	229	.2262
296	-.0325	262	.4331	228	.3529
295	-.0401	261	-.1685	227	.5187
294	-.0411	260	-.7995	226	.7689
293	-.0372	259	-1.4162	225	1.1138
292	-.0263	258	-1.9945	224	1.5088
291	-.0158	257	-2.4869	223	1.9017
290	.0009	256	-2.9481	222	2.2882
289	.0500	255	-3.2941	221	2.5044
288	.1221	254	-3.5856	220	2.6709
287	.1975	253	-3.7845	219	2.6046
286	.3029	252	-3.8516	218	2.2448
285	.4254	251	-3.8462	217	1.5586
284	.5977	250	-3.8095	216	.7794
283	.7798	249	-3.6920	215	-.2532
282	1.0018	248	-3.5205	214	-1.1140
281	1.2280	247	-3.3089	213	-2.2591
280	1.4867	246	-3.0678	212	-3.6679
279	1.7160	245	-2.7403	211	-4.0564
278	1.9470	244	-2.4437	I	I
277	2.1954	243	-2.1229	I	I

AU EXPERIMENTAL SPECTRUM AT 40 DEG C

WAVELENGTH	ELLIPTICITY	WAVELENGTH	ELLIPTICITY	WAVELENGTH	ELLIPTICITY
310	-.0276	276	.8383	242	-1.0279
309	-.0371	275	.9866	241	-.9594
308	-.0526	274	1.1224	240	-.8908
307	-.0671	273	1.2422	239	-.8260
306	-.0678	272	1.3360	238	-.7469
305	-.0734	271	1.3854	237	-.6610
304	-.0773	270	1.4146	236	-.5996
303	-.0869	269	1.4168	235	-.5351
302	-.0738	268	1.3810	234	-.4728
301	-.0797	267	1.2936	233	-.3951
300	-.0827	266	1.1807	232	-.3522
299	-.0995	265	1.0363	231	-.2899
298	-.1092	264	.8526	230	-.1893
297	-.1206	263	.6377	229	-.0943
296	-.1294	262	.3964	228	-.0081
295	-.1271	261	.1717	227	.1001
294	-.1251	260	-.0585	226	.2675
293	-.1266	259	-.3030	225	.4006
292	-.1192	258	-.5274	224	.4938
291	-.1183	257	-.7290	223	.5925
290	-.1114	256	-.8888	222	.6882
289	-.1195	255	-1.0160	221	.7621
288	-.1230	254	-1.1205	220	.8257
287	-.1260	253	-1.2161	219	.9126
286	-.1130	252	-1.2870	218	.8592
285	-.0938	251	-1.3449	217	.7469
284	-.0537	250	-1.3856	216	.5204
283	-.0004	249	-1.3537	215	.4288
282	.0676	248	-1.3496	214	.3790
281	.1582	247	-1.3338	213	.0606
280	.2733	246	-1.3198	212	-.2186
279	.3895	245	-1.2654	211	-.8486
278	.5241	244	-1.1928	I	I
277	.6786	243	-1.1042	I	I

AC   EXPERIMENTAL SPECTRUM AT 40 DEG C

WAVELENGTH	ELLIPTICITY	WAVELENGTH	ELLIPTICITY	WAVELENGTH	ELLIPTICITY
310	-.0483	276	2.5237	242	-1.8890
309	-.0587	275	2.5216	241	-1.9045
308	-.0594	274	2.4922	240	-1.9085
307	-.0623	273	2.4125	239	-1.8950
306	-.0537	272	2.3068	238	-1.8834
305	-.0455	271	2.1726	237	-1.9441
304	-.0405	270	2.0325	236	-1.7671
303	-.0362	269	1.8478	235	-1.6719
302	-.0176	268	1.6270	234	-1.5806
301	-.0169	267	1.3901	233	-1.4512
300	.0012	266	1.1234	232	-1.3114
299	.0125	265	.8630	231	-1.1491
298	.0378	264	.5726	230	-.9604
297	.0621	263	.2968	229	-.7535
296	.1049	262	.0199	228	-.5349
295	.1601	261	-.2511	227	-.2611
294	.2347	260	-.4987	226	.0464
293	.3135	259	-.7260	225	.3340
292	.4109	258	-.9121	224	.6068
291	.5223	257	-1.0755	223	.8201
290	.6486	256	-1.2235	222	1.0385
289	.7640	255	-1.3291	221	1.1602
288	.9081	254	-1.4388	220	1.2055
287	1.0429	253	-1.5137	219	1.1289
286	1.1755	252	-1.5971	218	.9044
285	1.3135	251	-1.6289	217	.7779
284	1.4595	250	-1.7131	216	.5434
283	1.6082	249	-1.7669	215	.1738
282	1.7865	248	-1.8025	214	-.1328
281	1.9520	247	-1.8243	213	-.3154
280	2.1118	246	-1.8454	212	-.5558
279	2.2584	245	-1.8476	211	-.8602
278	2.3715	244	-1.8668	I	I
277	2.4658	243	-1.8663	I	I

AG   EXPERIMENTAL SPECTRUM AT 40 DEG C

WAVELENGTH	ELLIPTICITY	WAVELENGTH	ELLIPTICITY	WAVELENGTH	ELLIPTICITY
310	-.0790	276	.6780	242	-.5539
309	-.0605	275	.5003	241	-.5155
308	-.0424	274	.3078	240	-.4764
307	-.0387	273	.0877	239	-.4175
306	-.0351	272	-.1620	238	-.3748
305	-.0366	271	-.4301	237	-.3042
304	-.0417	270	-.6740	236	-.2742
303	-.0535	269	-.9468	235	-.2578
302	-.0694	268	-1.2096	234	-.2272
301	-.0742	267	-1.4631	233	-.2668
300	-.0531	266	-1.6968	232	-.2440
299	-.0264	265	-1.8991	231	-.2757
298	-.0133	264	-2.0630	230	-.2657
297	.0324	263	-2.2190	229	-.2200
296	.0885	262	-2.3123	228	-.1869
295	.1270	261	-2.3979	227	-.1516
294	.1959	260	-2.4179	226	-.1254
293	.2446	259	-2.3931	225	-.0780
292	.2948	258	-2.3019	224	-.0194
291	.3655	257	-2.1962	223	-.0072
290	.4349	256	-2.0775	222	.0858
289	.5002	255	-1.9335	221	.1622
288	.5868	254	-1.7499	220	.2660
287	.6622	253	-1.6021	219	.3353
286	.7278	252	-1.4436	218	.4433
285	.7936	251	-1.2890	217	.6431
284	.8586	250	-1.1635	216	.6248
283	.8927	249	-1.0357	215	.3919
282	.9287	248	-.9094	214	.2317
281	.9341	247	-.7993	213	.0133
280	.9342	246	-.6939	212	.0461
279	.9227	245	-.6277	211	-2.0351
278	.8786	244	-.5830	I	I
277	.7844	243	-.5622	I	I

UA   EXPERIMENTAL SPECTRUM AT 40 DEG C

WAVELENGTH	ELLIPTICITY	WAVELENGTH	ELLIPTICITY	WAVELENGTH	ELLIPTICITY
310	-.0676	276	.4817	242	-.7979
309	-.0661	275	.5536	241	-.7724
308	-.0510	274	.6408	240	-.7422
307	-.0523	273	.6998	239	-.7720
306	-.0575	272	.7930	238	-.7811
305	-.0770	271	.8602	237	-.7704
304	-.0919	270	.9094	236	-.7750
303	-.1052	269	.9322	235	-.7976
302	-.1214	268	.9384	234	-.7922
301	-.1058	267	.9270	233	-.7839
300	-.0901	266	.8775	232	-.7653
299	-.0852	265	.8565	231	-.7813
298	-.0814	264	.7730	230	-.7485
297	-.0704	263	.6813	229	-.7161
296	-.0638	262	.5760	228	-.6957
295	-.0645	261	.4517	227	-.6844
294	-.0755	260	.3681	226	-.7100
293	-.0730	259	.2316	225	-.6996
292	-.0682	258	.1046	224	-.7532
291	-.0631	257	-.0539	223	-.7352
290	-.0566	256	-.1890	222	-.6558
289	-.0461	255	-.2892	221	-.5109
288	-.0492	254	-.4251	220	-.4019
287	-.0500	253	-.4927	219	-.2902
286	-.0314	252	-.5704	218	-.1327
285	.0001	251	-.6157	217	-.0349
284	.0217	250	-.6714	216	-.0070
283	.0634	249	-.7049	215	-.2290
282	.1000	248	-.7104	214	-.1432
281	.1492	247	-.7290	213	-.3072
280	.2135	246	-.7526	212	-.8558
279	.2771	245	-.7764	211	-1.2720
278	.3297	244	-.7594	I	I
277	.4058	243	-.7666	I	I

UU   EXPERIMENTAL SPECTRUM AT 40 DEG C

WAVELENGTH	ELLIPTICITY	WAVELENGTH	ELLIPTICITY	WAVELENGTH	ELLIPTICITY
310	-.0102	276	1.7252	242	-.9955
309	-.0183	275	1.8206	241	-.9922
308	-.0291	274	1.8844	240	-.9842
307	-.0335	273	1.9298	239	-.9617
306	-.0370	272	1.9398	238	-.9086
305	-.0437	271	1.9212	237	-.8578
304	-.0465	270	1.8822	236	-.8278
303	-.0486	269	1.8160	235	-.7622
302	-.0465	268	1.7261	234	-.7233
301	-.0454	267	1.6052	233	-.6882
300	-.0416	266	1.4566	232	-.6522
299	-.0388	265	1.3197	231	-.6131
298	-.0329	264	1.1617	230	-.5620
297	-.0370	263	.9956	229	-.5169
296	-.0313	262	.8223	228	-.4715
295	-.0131	261	.6587	227	-.3866
294	.0038	260	.4781	226	-.3048
293	.0301	259	.2896	225	-.2479
292	.0683	258	.1376	224	-.2056
291	.1108	257	-.0172	223	-.1496
290	.1589	256	-.1673	222	-.1258
289	.2188	255	-.3271	221	-.1203
288	.2990	254	-.4656	220	-.1713
287	.3919	253	-.5891	219	-.2055
286	.4963	252	-.7058	218	-.1751
285	.6059	251	-.8200	217	-.1966
284	.7306	250	-.8973	216	-.1693
283	.8592	249	-.9428	215	-.1866
282	.9980	248	-.9975	214	-.1534
281	1.1385	247	-1.0317	213	-.2380
280	1.2735	246	-1.0145	212	-.5320
279	1.4004	245	-1.0247	211	-.6264
278	1.5092	244	-1.0255	I	I
277	1.6261	243	-1.0185	I	I

UC EXPERIMENTAL SPECTRUM AT 40 DEG C

WAVELENGTH	ELLIPTICITY	WAVELENGTH	ELLIPTICITY	WAVELENGTH	ELLIPTICITY
310	.0227	276	2.1367	242	-.4747
309	.0260	275	2.1144	241	-.4980
308	.0257	274	2.0862	240	-.5056
307	.0244	273	2.0437	239	-.4937
306	.0201	272	1.9882	238	-.4825
305	.0160	271	1.8964	237	-.4728
304	.0097	270	1.8307	236	-.4783
303	.0075	269	1.7355	235	-.4650
302	.0125	268	1.6197	234	-.4235
301	.0247	267	1.4922	233	-.3721
300	.0352	266	1.3556	232	-.3082
299	.0525	265	1.2119	231	-.2572
298	.0787	264	1.0639	230	-.1848
297	.1006	263	.9246	229	-.1563
296	.1375	262	.8124	228	-.0934
295	.1891	261	.7101	227	-.0503
294	.2558	260	.6063	226	-.0420
293	.3332	259	.4968	225	-.0542
292	.4220	258	.4169	224	-.1132
291	.5276	257	.3155	223	-.1562
290	.6717	256	.2306	222	-.1895
289	.8105	255	.1316	221	-.3014
288	.9582	254	.0573	220	-.3775
287	1.0966	253	-.0283	219	-.4391
286	1.2750	252	-.1189	218	-.6011
285	1.3715	251	-.1618	217	-.7130
284	1.5056	250	-.2272	216	-.7963
283	1.6225	249	-.2756	215	-.6544
282	1.7582	248	-.3036	214	-.6822
281	1.8637	247	-.3556	213	-.7715
280	1.9700	246	-.4043	212	-.5102
279	2.0210	245	-.4193	211	-.5231
278	2.0812	244	-.4497	I	I
277	2.1082	243	-.4584	I	I

UG EXPERIMENTAL SPECTRUM AT 40 DEG C

WAVELENGTH	ELLIPTICITY	WAVELENGTH	ELLIPTICITY	WAVELENGTH	ELLIPTICITY
310	.0248	276	.6003	242	-.0014
309	.0160	275	.5087	241	-.0037
308	.0095	274	.4192	240	-.0178
307	.0034	273	.3491	239	-.0285
306	.0119	272	.2506	238	-.0313
305	.0100	271	.1481	237	-.0408
304	.0116	270	.0594	236	-.0521
303	.0156	269	-.0378	235	-.0648
302	.0278	268	-.1021	234	-.0485
301	.0433	267	-.2077	233	-.0589
300	.0570	266	-.2907	232	-.0724
299	.0718	265	-.3759	231	-.0532
298	.0925	264	-.4424	230	-.0592
297	.1047	263	-.5027	229	-.0410
296	.1346	262	-.5396	228	-.0291
295	.1788	261	-.5505	227	.0182
294	.2274	260	-.5535	226	.0598
293	.2682	259	-.5495	225	.0980
292	.3230	258	-.5015	224	.0798
291	.3718	257	-.4660	223	.1058
290	.4435	256	-.3966	222	.1234
289	.4985	255	-.3542	221	.0792
288	.5541	254	-.2788	220	.0423
287	.6136	253	-.2675	219	.0425
286	.6642	252	-.2124	218	.0940
285	.7184	251	-.1713	217	.0450
284	.7632	250	-.1455	216	-.0477
283	.7893	249	-.1040	215	-.0139
282	.8095	248	-.0648	214	.0535
281	.8151	247	-.0421	213	.2731
280	.8122	246	.0010	212	-.5755
279	.7744	245	-.0113	211	.1649
278	.7277	244	-.0025	I	I
277	.6692	243	.0054	I	I

CA   EXPERIMENTAL SPECTRUM AT 40 DEG C

WAVELENGTH	ELLIPTICITY	WAVELENGTH	ELLIPTICITY	WAVELENGTH	ELLIPTICITY
310	-.3331	276	1.8684	242	-1.3665
309	-.3456	275	1.9193	241	-1.4265
308	-.3450	274	1.9444	240	-1.4969
307	-.3481	273	1.9305	239	-1.5506
306	-.3547	272	1.8980	238	-1.6199
305	-.3553	271	1.8064	237	-1.6713
304	-.3411	270	1.7169	236	-1.7115
303	-.3494	269	1.5669	235	-1.7445
302	-.3238	268	1.3706	234	-1.7382
301	-.3117	267	1.1799	233	-1.7512
300	-.2834	266	.9931	232	-1.7550
299	-.2725	265	.7947	231	-1.7225
298	-.2466	264	.5994	230	-1.6860
297	-.2296	263	.4098	229	-1.5650
296	-.1936	262	.2060	228	-1.4684
295	-.1504	261	.0143	227	-1.3177
294	-.1125	260	-.1755	226	-1.1612
293	-.0471	259	-.3398	225	-.9430
292	.0450	258	-.4585	224	-.7096
291	.1354	257	-.5877	223	-.5179
290	.2576	256	-.7211	222	-.2777
289	.3644	255	-.7945	221	-.2278
288	.4902	254	-.8444	220	-.2957
287	.6158	253	-.8859	219	-.3873
286	.7455	252	-.9403	218	-.5100
285	.8612	251	-.9633	217	-.7723
284	.9911	250	-1.0385	216	-1.0116
283	1.1092	249	-1.0651	215	-1.4436
282	1.2443	248	-1.0997	214	-1.9038
281	1.3770	247	-1.1267	213	-2.4072
280	1.5026	246	-1.1426	212	-2.9260
279	1.6055	245	-1.1864	211	-2.9130
278	1.7122	244	-1.2696	I	I
277	1.7892	243	-1.2967	I	I

CU   EXPERIMENTAL SPECTRUM AT 40 DEG C

WAVELENGTH	ELLIPTICITY	WAVELENGTH	ELLIPTICITY	WAVELENGTH	ELLIPTICITY
310	.0217	276	2.7459	242	-.9237
309	.0218	275	2.7416	241	-.9672
308	.0169	274	2.7078	240	-1.0006
307	.0200	273	2.6323	239	-1.0423
306	.0261	272	2.5226	238	-1.0677
305	.0278	271	2.3976	237	-1.0966
304	.0277	270	2.2495	236	-1.1065
303	.0357	269	2.0777	235	-1.0970
302	.0485	268	1.8747	234	-1.0751
301	.0610	267	1.6790	233	-1.0429
300	.0760	266	1.4712	232	-.9859
299	.0897	265	1.2681	231	-.9271
298	.1195	264	1.0629	230	-.8593
297	.1484	263	.8946	229	-.7749
296	.1959	262	.7294	228	-.6780
295	.2685	261	.5871	227	-.5941
294	.3578	260	.4573	226	-.5198
293	.4624	259	.3302	225	-.4170
292	.6014	258	.2179	224	-.3074
291	.7550	257	.1019	223	-.2062
290	.9263	256	-.0112	222	-.1007
289	1.1077	255	-.1150	221	-.1186
288	1.2986	254	-.2097	220	-.1369
287	1.4794	253	-.2971	219	-.1467
286	1.6792	252	-.3883	218	-.2246
285	1.8581	251	-.4594	217	-.3792
284	2.0280	250	-.5232	216	-.4079
283	2.1808	249	-.5726	215	-.6044
282	2.3263	248	-.6268	214	-.7616
281	2.4601	247	-.6898	213	-.7965
280	2.5606	246	-.7299	212	-1.1502
279	2.6388	245	-.7967	211	-.5971
278	2.7008	244	-.8469	I	I
277	2.7382	243	-.8924	I	I

CC EXPERIMENTAL SPECTRUM AT 40 DEG C

WAVELENGTH	ELLIPTICITY	WAVELENGTH	ELLIPTICITY	WAVELENGTH	ELLIPTICITY
310	.0369	276	3.5617	242	-.1701
309	.0350	275	3.4073	241	-.2487
308	.0372	274	3.2238	240	-.3128
307	.0407	273	3.0134	239	-.3797
306	.0500	272	2.7856	238	-.4269
305	.0503	271	2.5232	237	-.5167
304	.0607	270	2.2630	236	-.5749
303	.0864	269	2.0041	235	-.6221
302	.1167	268	1.7566	234	-.6914
301	.1561	267	1.5255	233	-.7602
300	.2087	266	1.3254	232	-.7995
299	.2727	265	1.1413	231	-.8114
298	.3707	264	.9757	230	-.8081
297	.4788	263	.8333	229	-.7599
296	.6264	262	.7082	228	-.6948
295	.8444	261	.6095	227	-.6192
294	1.0774	260	.5206	226	-.5647
293	1.3173	259	.4410	225	-.4905
292	1.5822	258	.3900	224	-.4202
291	1.8561	257	.3677	223	-.3923
290	2.1404	256	.3393	222	-.3856
289	2.4232	255	.3109	221	-.4622
288	2.6812	254	.3011	220	-.5563
287	2.9132	253	.2840	219	-.5696
286	3.1290	252	.2517	218	-.7110
285	3.3133	251	.2403	217	-.7960
284	3.4895	250	.2214	216	-.8166
283	3.6401	249	.1998	215	-.9750
282	3.7409	248	.1713	214	-1.0746
281	3.7891	247	.1341	213	-1.0415
280	3.8037	246	.0965	212	-.6638
279	3.7851	245	.0386	211	-.8913
278	3.7577	244	-.0156	I	I
277	3.6780	243	-.0892	I	I

CG EXPERIMENTAL SPECTRUM AT 40 DEG C

WAVELENGTH	ELLIPTICITY	WAVELENGTH	ELLIPTICITY	WAVELENGTH	ELLIPTICITY
310	-.0142	276	1.0579	242	-.6539
309	-.0179	275	.9484	241	-.6511
308	-.0154	274	.8386	240	-.6738
307	-.0188	273	.7288	239	-.6886
306	-.0178	272	.6304	238	-.6803
305	-.0085	271	.5331	237	-.6764
304	.0041	270	.4213	236	-.6642
303	.0275	269	.3609	235	-.6316
302	.0490	268	.2702	234	-.6208
301	.0810	267	.1724	233	-.6266
300	.1235	266	.0935	232	-.6500
299	.1613	265	.0237	231	-.6494
298	.2153	264	-.0371	230	-.6341
297	.2673	263	-.1102	229	-.6238
296	.3378	262	-.1757	228	-.6226
295	.4301	261	-.2347	227	-.6133
294	.5296	260	-.2922	226	-.5495
293	.6470	259	-.3449	225	-.5090
292	.7770	258	-.3866	224	-.4712
291	.9074	257	-.4272	223	-.4241
290	1.0369	256	-.5071	222	-.3941
289	1.1534	255	-.5460	221	-.3572
288	1.2537	254	-.5599	220	-.3499
287	1.3419	253	-.6016	219	-.4160
286	1.4082	252	-.6365	218	-.5259
285	1.4401	251	-.6551	217	-.5950
284	1.4558	250	-.6716	216	-.6718
283	1.4663	249	-.6766	215	-.7469
282	1.4567	248	-.6872	214	-.9501
281	1.4296	247	-.6576	213	-1.0304
280	1.3911	246	-.6297	212	-.5529
279	1.3203	245	-.6217	211	-1.3077
278	1.2454	244	-.6449	I	I
277	1.1530	243	-.6405	I	I

GA   EXPERIMENTAL SPECTRUM AT 40 DEG C

WAVELENGTH	ELLIPTICITY	WAVELENGTH	ELLIPTICITY	WAVELENGTH	ELLIPTICITY
310	-.0318	276	.0200	242	-.5577
309	-.0379	275	.1441	241	-.5073
308	-.0424	274	.2874	240	-.4575
307	-.0523	273	.4287	239	-.4145
306	-.0611	272	.5730	238	-.3472
305	-.0682	271	.6905	237	-.3164
304	-.0725	270	.8236	236	-.3030
303	-.0849	269	.9214	235	-.2704
302	-.0982	268	.9850	234	-.2364
301	-.1094	267	1.0545	233	-.2388
300	-.1189	266	1.0536	232	-.2684
299	-.1296	265	1.0552	231	-.2411
298	-.1401	264	1.0244	230	-.2073
297	-.1578	263	1.0060	229	-.1776
296	-.1766	262	.9561	228	-.1787
295	-.1979	261	.8497	227	-.1422
294	-.2231	260	.7306	226	-.1035
293	-.2546	259	.5961	225	-.0700
292	-.2892	258	.4692	224	-.0540
291	-.3429	257	.3181	223	-.0364
290	-.3950	256	.1646	222	.0016
289	-.4498	255	.0657	221	-.0496
288	-.5069	254	-.0565	220	-.0850
287	-.5601	253	-.1723	219	-.1025
286	-.6057	252	-.2550	218	-.1609
285	-.6396	251	-.3008	217	-.0605
284	-.6465	250	-.3587	216	.0416
283	-.6333	249	-.4265	215	-.0081
282	-.5943	248	-.4928	214	.0369
281	-.5287	247	-.5465	213	-.1594
280	-.4541	246	-.5783	212	.6838
279	-.3535	245	-.5975	211	-.5907
278	-.2358	244	-.6189	I	I
277	-.1128	243	-.5952	I	I

GU   EXPERIMENTAL SPECTRUM AT 40 DEG C

WAVELENGTH	ELLIPTICITY	WAVELENGTH	ELLIPTICITY	WAVELENGTH	ELLIPTICITY
310	-.0088	276	.2123	242	.1480
309	-.0095	275	.1929	241	.1137
308	-.0050	274	.1710	240	.0996
307	-.0092	273	.1515	239	.0753
306	-.0057	272	.1324	238	.0563
305	-.0118	271	.1059	237	.0268
304	-.0210	270	.0806	236	.0091
303	-.0352	269	.0780	235	.0048
302	-.0434	268	.0783	234	.0015
301	-.0355	267	.0761	233	.0035
300	-.0352	266	.1025	232	.0056
299	-.0292	265	.1486	231	.0205
298	-.0256	264	.1912	230	.0428
297	-.0221	263	.2367	229	.0558
296	-.0127	262	.2712	228	.1021
295	-.0079	261	.3039	227	.1158
294	.0008	260	.3392	226	.1148
293	.0164	259	.3495	225	.1374
292	.0263	258	.3485	224	.1488
291	.0310	257	.3758	223	.1950
290	.0499	256	.3853	222	.2444
289	.0605	255	.4107	221	.2872
288	.0721	254	.4632	220	.3490
287	.0903	253	.4302	219	.3669
286	.1020	252	.4236	218	.4894
285	.1174	251	.4253	217	.5374
284	.1320	250	.4081	216	.5396
283	.1355	249	.3946	215	.6041
282	.1591	248	.3500	214	.7043
281	.1814	247	.3271	213	.6227
280	.1995	246	.2834	212	-.0817
279	.2110	245	.2469	211	-.0509
278	.2107	244	.2245	I	I
277	.2079	243	.1860	I	I

GC EXPERIMENTAL SPECTRUM AT 40 DEG C

WAVELENGTH	ELLIPTICITY	WAVELENGTH	ELLIPTICITY	WAVELENGTH	ELLIPTICITY
310	-.0430	276	.9989	242	-.0159
309	-.0423	275	1.0290	241	-.0534
308	-.0338	274	1.0494	240	-.1024
307	-.0263	273	1.0836	239	-.1242
306	-.0182	272	1.1012	238	-.1776
305	-.0195	271	1.1197	237	-.2342
304	-.0237	270	1.1291	236	-.2934
303	-.0177	269	1.1393	235	-.3508
302	-.0140	268	1.1478	234	-.4114
301	-.0007	267	1.1251	233	-.4528
300	.0140	266	1.1051	232	-.4835
299	.0341	265	1.0622	231	-.5226
298	.0566	264	1.0155	230	-.5455
297	.0853	263	.9543	229	-.5260
296	.1278	262	.8753	228	-.5322
295	.1715	261	.8169	227	-.4973
294	.2204	260	.7336	226	-.4567
293	.2816	259	.6571	225	-.4138
292	.3484	258	.5940	224	-.3480
291	.4056	257	.5197	223	-.3025
290	.4689	256	.4281	222	-.2371
289	.5154	255	.3390	221	-.2214
288	.5625	254	.2730	220	-.2019
287	.6107	253	.1662	219	-.1676
286	.6490	252	.0979	218	-.2169
285	.6801	251	.0739	217	-.3384
284	.7174	250	.0544	216	-.3974
283	.7520	249	.0696	215	-.3351
282	.7809	248	.0704	214	-.5959
281	.8280	247	.0915	213	-.5706
280	.8662	246	.1127	212	-.5009
279	.8963	245	.1125	211	-.1480
278	.9404	244	.0877	I	I
277	.9612	243	.0557	I	I

GG EXPERIMENTAL SPECTRUM AT 40 DEG C

WAVELENGTH	ELLIPTICITY	WAVELENGTH	ELLIPTICITY	WAVELENGTH	ELLIPTICITY
310	-.0904	276	-.7586	242	-2.3754
309	-.1176	275	-.7038	241	-2.4608
308	-.0884	274	-.8118	240	-2.4514
307	-.0206	273	-.7404	239	-2.2898
306	-.0106	272	-.7822	238	-2.1812
305	-.0144	271	-.8010	237	-2.0472
304	-.0284	270	-.6986	236	-1.8864
303	-.0556	269	-.5710	235	-1.6264
302	-.0958	268	-.4274	234	-1.3234
301	-.1336	267	-.2106	233	-.9072
300	-.1498	266	-.1082	232	-.5126
299	-.1310	265	.1542	231	-.0688
298	-.0826	264	.2980	230	.0153
297	-.0648	263	.5136	229	.0482
296	.0624	262	.5942	228	.0824
295	.0868	261	.6768	227	.1028
294	.0876	260	.6728	226	.1289
293	.1442	259	.7506	225	.1679
292	.2060	258	.6110	224	.1987
291	.3502	257	.5130	223	.2271
290	.3516	256	.5034	222	.2529
289	.3214	255	.4036	221	.2966
288	.2426	254	.0560	220	.3354
287	.1544	253	-.1444	219	.3544
286	.0888	252	-.5248	218	.3663
285	-.0166	251	-.6282	217	.4096
284	-.0938	250	-.8008	216	.4176
283	-.3082	249	-1.0650	215	.3713
282	-.4234	248	-1.3302	214	.3640
281	-.4424	247	-1.5570	213	.2939
280	-.4562	246	-1.9296	212	.2516
279	-.5048	245	-2.0786	211	-.1632
278	-.6176	244	-2.0944	I	I
277	-.6978	243	-2.2884	I	I

DD   EXPERIMENTAL SPECTRUM AT 40 DEG C

WAVELENGTH	ELLIPTICITY	WAVELENGTH	ELLIPTICITY	WAVELENGTH	ELLIPTICITY
310	.043R	276	.0392	242	-.0455
30q	.0416	275	.0395	241	-.0802
30R	.0336	274	.0547	240	-.0758
307	.0092	273	.0723	239	-.0703
306	-.0104	272	.0804	23R	-.0911
305	-.0148	271	.0805	237	-.0880
304	-.0120	270	.0776	236	-.0849
303	-.0240	269	.0842	235	-.0889
302	-.0216	268	.0893	234	-.0861
301	-.0264	267	.1146	233	-.0972
300	-.0479	266	.1218	232	-.0780
299	-.0384	265	.1450	231	-.0879
29R	-.035R	264	.1542	230	-.0926
297	-.0070	263	.1430	229	-.0792
296	-.0272	262	.1427	228	-.0844
295	-.0123	261	.1167	227	-.0821
294	-.0200	260	.0856	226	-.0963
293	-.0068	259	.0559	225	-.0976
292	-.0023	258	.0022	224	-.0832
291	-.0067	257	-.0225	223	-.0982
290	.0035	256	-.0467	222	-.1058
289	-.0018	255	-.0547	221	-.0980
288	.0075	254	-.0650	220	-.0758
287	.0089	253	-.0653	219	-.1518
286	.006R	252	-.0870	218	-.1264
285	.0199	251	-.1090	217	-.1222
284	.0320	250	-.0959	216	-.1270
283	.0376	249	-.1114	215	-.1749
282	.0418	248	-.1197	214	-.1702
281	.0363	247	-.1228	213	-.2186
280	.0251	246	-.1294	212	-.2099
279	.0392	245	-.1111	211	-.2251
278	.0426	244	-.1009	I	I
277	.0406	243	-.0877	I	I

AD   EXPERIMENTAL SPECTRUM AT 40 DEG C

WAVELENGTH	ELLIPTICITY	WAVELENGTH	ELLIPTICITY	WAVELENGTH	ELLIPTICITY
310	.0833	276	-1.1454	242	-.6046
309	.0486	275	-1.2741	241	-.5097
308	.0502	274	-1.3535	240	-.4488
307	.0245	273	-1.4773	239	-.3554
306	-.0103	272	-1.5492	238	-.3029
305	-.0548	271	-1.5947	237	-.2615
304	-.0723	270	-1.6581	236	-.1844
303	-.0829	269	-1.7319	235	-.1246
302	-.0931	268	-1.7242	234	-.0322
301	-.0939	267	-1.7761	233	.0284
300	-.0701	266	-1.8743	232	.1414
299	-.0856	265	-1.8824	231	.2713
29R	-.0984	264	-1.9575	230	.3571
297	-.0785	263	-1.9692	229	.4011
296	-.0835	262	-1.9292	228	.4186
295	-.1012	261	-1.9194	227	.4603
294	-.1342	260	-1.9316	226	.4470
293	-.1643	259	-1.9352	225	.4766
292	-.1774	258	-1.9115	224	.4920
291	-.1914	257	-1.9081	223	.4003
290	-.1907	256	-1.8324	222	.2050
289	-.1961	255	-1.8394	221	-1.3120
288	-.2072	254	-1.8222	220	1.0308
287	-.2240	253	-1.7364	219	2.8048
286	-.2623	252	-1.6754	218	3.8925
285	-.2969	251	-1.5964	217	3.3926
284	-.3462	250	-1.4842	216	4.5796
283	-.3920	249	-1.4030	215	3.0262
282	-.4701	248	-1.3405	214	4.2117
281	-.5771	247	-1.2201	213	4.7535
280	-.6589	246	-1.0992	212	4.7248
279	-.7234	245	-.9960	211	3.7039
278	-.8752	244	-.8355	I	I
277	-.9960	243	-.7209	I	I

DA   EXPERIMENTAL SPECTRUM AT 40 DEG C

WAVELENGTH	ELLIPTICITY	WAVELENGTH	ELLIPTICITY	WAVELENGTH	ELLIPTICITY
310	.7187	276	.8158	242	1.0094
309	.7344	275	.8740	241	.8843
308	.7486	274	.9475	240	.9521
307	.7501	273	1.0260	239	.9174
306	.7422	272	1.1124	238	.8808
305	.7428	271	1.1745	237	.8485
304	.7436	270	1.2185	236	.8012
303	.7338	269	1.2481	235	.7382
302	.7325	268	1.2643	234	.6850
301	.7380	267	1.2625	233	.6214
300	.7437	266	1.2392	232	.5531
299	.7600	265	1.2231	231	.5087
298	.7845	264	1.1974	230	.4781
297	.8178	263	1.1874	229	.4605
296	.8190	262	1.1850	228	.4430
295	.8202	261	1.1799	227	.4387
294	.8001	260	1.1887	226	.4354
293	.7845	259	1.1925	225	.3944
292	.7654	258	1.1994	224	.2888
291	.7442	257	1.2137	223	.0955
290	.7287	256	1.2194	222	-.0706
289	.7283	255	1.2052	221	-.2944
288	.7300	254	1.1712	220	-.5267
287	.7344	253	1.1516	219	-.7028
286	.7413	252	1.1272	218	-.8569
285	.7506	251	1.1098	217	-.9284
284	.7579	250	1.0844	216	-.9932
283	.7558	249	1.0702	215	-1.0477
282	.7465	248	1.0653	214	-.9795
281	.7338	247	1.0626	213	-.9108
280	.7283	246	1.0640	212	-.5738
279	.7274	245	1.0730	211	-.8272
278	.7350	244	1.0621	I	I
277	.7748	243	1.0409	I	I

GD   EXPERIMENTAL SPECTRUM AT 40 DEG C

WAVELENGTH	ELLIPTICITY	WAVELENGTH	ELLIPTICITY	WAVELENGTH	ELLIPTICITY
310	-.0518	276	-.5288	242	-.1732
309	-.0290	275	-.5249	241	-.0450
308	.0006	274	-.5336	240	.0533
307	.0198	273	-.5126	239	.1620
306	.0198	272	-.5282	238	.2092
305	.0202	271	-.5099	237	.2535
304	.0180	270	-.5033	236	.3140
303	-.0192	269	-.5207	235	.3668
302	-.0955	268	-.5338	234	.4308
301	-.1145	267	-.5394	233	.4762
300	-.1573	266	-.5538	232	.4836
299	-.1547	265	-.5293	231	.5124
298	-.1629	264	-.5250	230	.6514
297	-.1368	263	-.4632	229	.7501
296	-.1321	262	-.4766	228	.8510
295	-.1566	261	-.4688	227	.8786
294	-.1755	260	-.4761	226	.9671
293	-.2071	259	-.4183	225	.9702
292	-.2387	258	-.4350	224	.9844
291	-.2869	257	-.4570	223	.9626
290	-.3210	256	-.4868	222	.8636
289	-.3297	255	-.5133	221	.7438
288	-.3606	254	-.5235	220	.4901
287	-.3928	253	-.4712	219	.2709
286	-.4151	252	-.4080	218	.1314
285	-.3829	251	-.3374	217	-.0439
284	-.4165	250	-.3220	216	-.2078
283	-.4547	249	-.2879	215	.0861
282	-.4726	248	-.2562	214	.7434
281	-.5250	247	-.2172	213	.9092
280	-.5769	246	-.2123	212	.9879
279	-.5685	245	-.2006	211	.9668
278	-.5168	244	-.1947	I	I
277	-.4986	243	-.2124	I	I

Appendix II

Double Strand Polymer CD

CD spectra of six polymers at 25°C are listed between 310 and 210 mμ. Ellipticity values are times 10^{-4}. The poly A:poly U spectrum was measured by Dr. Dana Carroll; the poly G:poly C, poly AU:poly AU, poly GC:poly GC, and poly GU:poly CA were measured by Dr. Donald Grey. The poly GA:poly CU spectrum was constructed as described in the text. These polymer spectra were used to calculate basis spectra for double strand regions of tRNA.

POLY AA POLY UJ   EXPERIMENTAL SPECTRUM AT 25 DEG

WAVELENGTH	ELLIPTICITY	WAVELENGTH	ELLIPTICITY	WAVELENGTH	ELLIPTICITY
310	0.	276	2.6749	242	-1.6647
309	0.	275	2.8227	241	-1.4730
308	0.	274	2.9634	240	-1.2682
307	0.	273	3.1016	239	-1.0594
306	0.	272	3.2384	238	-.8586
305	0.	271	3.3711	237	-.6740
304	.0005	270	3.4940	236	-.5097
303	-.0013	269	3.6006	235	-.3685
302	-.0052	268	3.6867	234	-.2472
301	-.0083	267	3.7509	233	-.1434
300	-.0070	266	3.7914	232	-.0540
299	-.0006	265	3.8008	231	.0266
298	.0096	264	3.7713	230	.1022
297	.0243	263	3.7005	229	.1794
296	.0462	262	3.5919	228	.2648
295	.0782	261	3.4446	227	.3592
294	.1230	260	3.2532	226	.4640
293	.1830	259	3.0147	225	.5784
292	.2585	258	2.7296	224	.6957
291	.3486	257	2.4015	223	.8076
290	.4542	256	2.0267	222	.9017
289	.5774	255	1.6054	221	.9635
288	.7192	254	1.1437	220	.9790
287	.8753	253	.6480	219	.9528
286	1.0393	252	.1353	218	.8384
285	1.2075	251	-.3668	217	.6600
284	1.3783	250	-.8328	216	.3600
283	1.5503	249	-1.2429	215	0.
282	1.7223	248	-1.5762	214	-.4400
281	1.8914	247	-1.8177	213	-.8000
280	2.0540	246	-1.9568	212	-1.6000
279	2.2105	245	-1.9944	211	-2.6000
278	2.3649	244	-1.9470	I	I
277	2.5204	243	-1.8303	I	I

POLY GG POLYCC   EXPERIMENTAL SPECTRUM AT 25 DEG

WAVELENGTH	ELLIPTICITY	WAVELENGTH	ELLIPTICITY	WAVELENGTH	ELLIPTICITY
310	0.	276	1.1765	242	.4348
309	0.	275	1.2984	241	.2946
308	0.	274	1.4124	240	.1584
307	0.	273	1.5109	239	.0256
306	0.	272	1.5911	238	-.1027
305	0.	271	1.6488	237	-.2244
304	-.0029	270	1.6799	236	-.3376
303	-.0098	269	1.6828	235	-.4402
302	-.0175	268	1.6553	234	-.5309
301	-.0274	267	1.6009	233	-.6069
300	-.0407	266	1.5290	232	-.6669
299	-.0544	265	1.4504	231	-.7121
298	-.0628	264	1.3762	230	-.7470
297	-.0616	263	1.3162	229	-.7761
296	-.0474	262	1.2749	228	-.8017
295	-.0193	261	1.2529	227	-.8261
294	.0198	260	1.2483	226	-.8541
293	.0667	259	1.2560	225	-.8899
292	.1199	258	1.2719	224	-.9346
291	.1773	257	1.2896	223	-.9687
290	.2351	256	1.3023	222	-1.0508
289	.2880	255	1.3075	221	-1.1196
288	.3329	254	1.3073	220	-1.1927
287	.3727	253	1.3040	219	-1.2900
286	.4093	252	1.2977	218	-1.3600
285	.4431	251	1.2849	217	-1.4400
284	.4788	250	1.2599	216	-1.5200
283	.5227	249	1.2181	215	-1.6200
282	.5776	248	1.1564	214	-1.6800
281	.6457	247	1.0747	213	-1.7600
280	.7284	246	.9737	212	-1.8000
279	.8253	245	.8545	211	-1.9900
278	.9350	244	.7209	I	I
277	1.0533	243	.5786	I	I

POLYAU POLYAU   EXPERIMENTAL SPECTRUM AT 25 DEG

WAVELENGTH	ELLIPTICITY	WAVELENGTH	ELLIPTICITY	WAVELENGTH	ELLIPTICITY
310	0.	276	.5752	242	.1673
309	0.	275	.6571	241	.2149
308	0.	274	.7450	240	.2768
307	0.	273	.8392	239	.3463
306	0.	272	.9393	238	.4170
305	0.	271	1.0404	237	.4847
304	.0038	270	1.1447	236	.5473
303	.0035	269	1.2561	235	.6025
302	-.0003	268	1.3835	234	.6495
301	-.0062	267	1.5316	233	.6843
300	-.0125	266	1.7020	232	.7025
299	-.0192	265	1.8910	231	.7027
298	-.0273	264	2.0961	230	.6851
297	-.0368	263	2.3176	229	.6497
296	-.0493	262	2.5477	228	.5955
295	-.0656	261	2.7754	227	.5237
294	-.0833	260	2.9886	226	.4365
293	-.0986	259	3.1648	225	.3365
292	-.1111	258	3.2833	224	.2273
291	-.1221	257	3.3328	223	.1109
290	-.1306	256	3.3001	222	-.0106
289	-.1325	255	3.1743	221	-.1336
288	-.1247	254	2.9558	220	-.2522
287	-.1066	253	2.6519	219	-.3608
286	-.0769	252	2.2854	218	-.4604
285	-.0345	251	1.8883	217	-.5320
284	.0173	250	1.4883	216	-.5780
283	.0748	249	1.1143	215	-.6000
282	.1377	248	.7911	214	-.5980
281	.2060	247	.5297	213	-.6300
280	.2774	246	.3369	212	-.6800
279	.3495	245	.2158	211	-.7700
278	.4221	244	.1549	I	I
277	.4971	243	.1426	I	I

POLY GC POLY GC   EXPERIMENTAL SPECTRUM AT 25 DEG

WAVELENGTH	ELLIPTICITY	WAVELENGTH	ELLIPTICITY	WAVELENGTH	ELLIPTICITY
310	-.1000	276	-.1946	242	-.2388
309	-.1080	275	.0735	241	-.3115
308	-.1320	274	.3674	240	-.3935
307	-.1736	273	.6746	239	-.4818
306	-.2352	272	.9823	238	-.5731
305	-.3000	271	1.2752	237	-.6647
304	-.3507	270	1.5408	236	-.7538
303	-.4217	269	1.7702	235	-.8381
302	-.4966	268	1.9558	234	-.9135
301	-.5741	267	2.0965	233	-.9737
300	-.6533	266	2.1936	232	-1.0138
299	-.7333	265	2.2464	231	-1.0423
298	-.8107	264	2.2571	230	-1.0323
297	-.8811	263	2.2284	229	-1.0165
296	-.9408	262	2.1649	228	-.9845
295	-.9887	261	2.0707	227	-.9384
294	-1.0241	260	1.9490	226	-.8811
293	-1.0463	259	1.8025	225	-.8190
292	-1.0560	258	1.6335	224	-.7605
291	-1.0554	257	1.4469	223	-.7123
290	-1.0464	256	1.2483	222	-.6840
289	-1.0321	255	1.0441	221	-.6894
288	-1.0143	254	.8426	220	-.7468
287	-.9934	253	.6539	219	-.8676
286	-.9735	252	.4852	218	-1.0588
285	-.9582	251	.3419	217	-1.3740
284	-.9463	250	.2272	216	-1.8060
283	-.9348	249	.1387	215	-2.3500
282	-.9174	248	.0725	214	-3.0060
281	-.8844	247	.0220	213	-3.9000
280	-.8277	246	-.0220	212	-3.9000
279	-.7379	245	-.0662	211	-5.6000
278	-.6042	244	-.1160	I	I
277	-.4229	243	-.1739	I	I

POLY UG POLY CA   EXPERIMENTAL SPECTRUM AT 25 DEG

WAVELENGTH	ELLIPTICITY	WAVELENGTH	ELLIPTICITY	WAVELENGTH	ELLIPTICITY
310	-.0500	276	.5718	242	-.0042
309	-.0640	275	.6414	241	-.1790
308	-.0860	274	.7252	240	-.3344
307	-.1176	273	.8284	239	-.4565
306	-.1612	272	.9535	238	-.5373
305	-.2000	271	1.0985	237	-.5778
304	-.2170	270	1.2578	236	-.5836
303	-.2452	269	1.4241	235	-.5618
302	-.2688	268	1.5897	234	-.5186
301	-.2858	267	1.7456	233	-.4565
300	-.2948	266	1.8835	232	-.3800
299	-.2981	265	2.0001	231	-.2989
298	-.2980	264	2.0960	230	-.2190
297	-.2942	263	2.1713	229	-.1409
296	-.2823	262	2.2283	228	-.0664
295	-.2595	261	2.2719	227	.0018
294	-.2282	260	2.3033	226	.0611
293	-.1929	259	2.3196	225	.1064
292	-.1562	258	2.3149	224	.1343
291	-.1195	257	2.2869	223	.1455
290	-.0835	256	2.2397	222	.1444
289	-.0469	255	2.1793	221	.1345
288	-.0077	254	2.1021	220	.1137
287	.0332	253	1.9977	219	.0708
286	.0731	252	1.8629	218	.0304
285	.1123	251	1.7045	217	-.0380
284	.1552	250	1.5324	216	-.1320
283	.2043	249	1.3522	215	-.2500
282	.2569	248	1.1656	214	-.3920
281	.3094	247	.9720	213	-.4500
280	.3618	246	.7701	212	-.5600
279	.4136	245	.5649	211	-.6100
278	.4634	244	.3662	I	I
277	.5138	243	.1786	I	I

POLY GA POLY CU   EXPERIMENTAL SPECTRUM AT 25 DEG

WAVELENGTH	ELLIPTICITY	WAVELENGTH	ELLIPTICITY	WAVELENGTH	ELLIPTICITY
310	0.	276	2.3069	242	-.5834
309	-.0100	275	2.3366	241	-.7199
308	-.0200	274	2.3569	240	-.8369
307	-.0308	273	2.3777	239	-.9056
306	-.0436	272	2.4079	238	-.9399
305	-.0500	271	2.4506	237	-.9370
304	-.0448	270	2.5020	236	-.9040
303	-.0417	269	2.5526	235	-.8483
302	-.0317	268	2.5910	234	-.7756
301	-.0135	267	2.6075	233	-.6866
300	.0143	266	2.5959	232	-.5848
299	.0506	265	2.5570	231	-.4768
298	.0944	264	2.4931	230	-.3678
297	.1461	263	2.4066	229	-.2558
296	.2121	262	2.3054	228	-.1403
295	.2971	261	2.1976	227	-.0243
294	.3969	260	2.0855	226	.0886
293	.5044	259	1.9713	225	.1919
292	.6165	258	1.8572	224	.2815
291	.7322	257	1.7426	223	.3556
290	.8496	256	1.6300	222	.4172
289	.9681	255	1.5265	221	.4682
288	1.0878	254	1.4284	220	.5063
287	1.2072	253	1.3208	219	.5214
286	1.3226	252	1.1961	218	.5292
285	1.4339	251	1.0485	217	.5150
284	1.5482	250	.8882	216	.4800
283	1.6708	249	.7133	215	.4250
282	1.7967	248	.5239	214	.3500
281	1.9171	247	.3247	213	.5350
280	2.0281	246	.1211	212	-.0100
279	2.1257	245	-.0798	211	.2800
278	2.2044	244	-.2663	I	I
277	2.2635	243	-.4322	I	I

Appendix 3

Computer Programs

The following programs, written in Fortran IV.
for use on a CDC 6600 computer, perform simple
arithmetic operations on CD spectra. The subroutines
PRNPLT and PLSCAL which are repeatedly used by these
programs were written by Dr. Marty Itzkowitz, and are
listed at the end of this Appendix. NNPOLY, which
was written by Phil Borer, served as the basis for
MTADMS and SHASTA.

All the programs to be listed are quite similar
in their input and output. To begin, it is useful to
define the sorts of cards that repeatedly occur in
the Input and Output of these programs, and the usual
order in which they occur.

(1) IDEXP or IDCAL card contains a 72 character
identification of the spectrum.

(2) Control card contains an 8 character ID and 6
controls. In order, the controls are starting
wavelength (mμ), ending wavelength (mμ), wavelength
increment between data points ($\overset{\circ}{A}$), wavelength
interval during which pen is to be averaged for
each point ($\overset{\circ}{A}$), OD$_{258}$, and extinction coefficient.

(3) Data cards contain 10 data points per card in a
10F8.4 format.

(4) * card contains * in all 80 columns. This type
of card is useful in separating sets of data cards.

(5) IPUNPR card may precede all the sets of spectra.

It specifies whether punched data and a plot of the spectrum are desired YES is columns 1 to 3 indicated that data is to be punched. YES in columns 4 to 6 indicates that a plot of the spectrum is desired.

Paper tapes from the PDP 8/S are converted to cards by BAKER. The output deck consists of a series of spectra each of which begins with an * card, followed by a Control card, the data cards, and ends with another * card. The * card preceding each set of data is replaced by an IDEXP card. The spectra are then run through GLACER which corrects for baseline shifts, TAHOMA which smooths the spectra, RANIER which averages several spectra, and STHLNS which obtains difference spectra.

The Input and Output for all these programs is quite similar: IDEXP card, Control card, data cards, * card. All the data cards in the Input of GLACER and TAHOMA are preceded by an IPUNPR card. The end of the deck of input spectra for each of these programs is signalled by two blank cards. The punched output has a similar format except there is no IPUNPR card. The printed output in all cases consists of a listing and plot of the spectra. The Input for RANIER begins with a card telling how many spectra are to be averaged in an I4 format. Data for STHLNS, which calculates difference spectra, is arranged in sets of two spectra and the second spectrum is subtracted from the first.

The difference spectrum is then punched, listed, and
plotted. Parameters specified when calling PRNPLT
in all these cases determine the scale of the abscissa
of the plotted spectrum.

```
      PROGRAM GLACER(INPUT,OUTPUT,PUNCH)
      DIMENSION CONTRL(6), CD(200), IPUNPR(3), XWAVE(200), IDEXP(12)
C     CONTROLS ARE(1) LAMBDA MAX, (2) LAMBDA MIN, (3) A PER POINT, (5)OD
C     (6) IS EXTINCTION COEFFIECIENT
C     IPUNPR INDICATES WHETHER  PUNCHED DATA AND A PLOT OF THE SPECTRUM
C     ARE DESIRED        (3) INDICATES WHETHER CD IS TO BE CALCULATED
C     BLANK CARD AT END OF DATA SIGNALS STOP
C     AVERAGE IS TAKEN BETWEEN 345 AND 325 MU FOR BASELINE CORRECTION
  500 FORMAT(10F8.4)
  501 FORMAT(3A3)
  902 FORMAT(A8,2X,4(F8.3,2X),2(E13.6,2X))
  903 FORMAT(5(E13.6,2X))
  904 FORMAT(*1SPECTRUM ID= *,A8,20X,*BASELINE CORRECTION=*,E13.4,10X,
     $*USING*, I3, * POINTS*)
  905 FORMAT(1X)
  906 FORMAT(1H1)
  907 FORMAT(80(1H*))
  908 FORMAT(3(13X,F6.0,3X,F13.4))
  909 FORMAT(12A6)
  109 FORMAT(7F8.4)
  910 FORMAT(// ,3(15X,*LAMBDA*,3X,*ELLIPTICITY*),//)
  912 FORMAT (*1*)
  913 FORMAT(F8.4)
      READ 501, (IPUNPR(I), I= 1,3)
      PRINT 912
  302 CONTINUE
      READ 909, IDEXP
      READ  902,ID,CONTRL
      IF(ID.EQ.8H          )STOP
      XMAX=CONTRL(1)
      XINC=CONTRL(3)/10.
      NPTS=(CONTRL(1)-CONTRL(2))*10./CONTRL(3)
      READ 500,(CD(I),I=1,NPTS)
      READ 905
      NPTAV=0
      SUM=0
C     AVERAGE IS TAKEN BETWEEN LIMITS OF DO LOOP BELOW
      DO 3 I= 11,30
      NPTAV = NPTAV+1
    3 SUM = SUM+CD(I)
      CRCN = SUM/NPTAV
      PRINT 904, ID, CRCN, NPTAV
      PRINT 909, (IDEXP(I), I=1,12)
      DO 5 I=1,NPTS
      XWAVE(I)=CONTRL(1)-FLOAT(I-1)*CONTRL(3)/10.
      IF(IPUNPR(3).EQ.3HYES)2,4
    2 CD(I) =CD(I)*10.
      GO TO 5
    4 CD(I)=CD(I)-CRCN
    5 CONTINUE
      IF (IPUNPR(1).EQ.3HYES)8,9
    8 PUNCH 909,(IDEXP(I), I=1,12)
      PUNCH 902,ID,CONTRL
      PUNCH 500,(CD(I), I=1,NPTS)
      PUNCH 907
    9 CONTINUE
      PRINT 910
      II=NPTS/3.+1.
      DO 20 I= 1,II
      J=I+II
      K=J+II
   20 PRINT 908, XWAVE(I), CD(I), XWAVE(J), CD(J), XWAVE(K), CD(K)
      PRINT 904,ID,CRCN,NPTAV
      NUM = NPTS-40.
      XMAX=XMAX-40.
      IF(IPUNPR(2).EQ.3HYES) 7,302
    7 CALL PRNPLT(XWAVE(41),CD(41),XMAX,XINC,2.5,-1.0,0,NUM)
      GO TO 302
      END
```

```
      PROGRAM TAHOMA(INPUT,OUTPUT,PUNCH)
      DIMENSION CONTRL(6), CD(2CO), IPUNPR(3), XWAVE(200), IDEXP(12),T(1
     13), R(200)
C     PROGRAM APPLIES A 13 POINT SMOOTH (CUBIC) TO INPUT DATA.
C     CONTROLS ARE(1) LAMBDA MAX, (2) LAMBDA MIN, (3) A PER POINT, (5)DD
C     (6) IS EXTINCTION COEFFIECIENT
C     IPUNPR INDICATES WHETHER  PUNCHED DATA AND A PLOT OF THE SPECTRUM
C     ARE DESIRED
C     BLANK CARD AT END OF DATA SIGNALS STOP
  900 FORMAT(*1*)
  903 FORMAT(X,A8,2X,4(F8.3,2X),2(E13.6,2X))
  501 FORMAT(2A3)
902   FORMAT(A8,2X,4(F8.3,2X),2(E13.6,2X))
  904 FORMAT(12A6)
905   FORMAT(1X)
906   FORMAT(1H1)
  907 FORMAT(80(1H*))
  908 FORMAT(3(13X,F6.0,3X,F13.4))
  909 FORMAT(*1*,12A6)
  109 FORMAT(7F8.4)
  500 FORMAT (10F8.4)
  910 FORMAT(// ,3(15X,*LAMBDA*,3X,*ELLIPTICITY*),//)
  913 FORMAT(F8.4)
      READ 501, (IPUNPR(I), I= 1,2)
      PRINT 900
302   CONTINUE
      READ   904, IDEXP
      READ   902,ID,CONTRL
      IF(ID.EQ.8H        )STOP
      PRINT 909, (IDEXP(I), I=1,12)
      XMAX=CONTRL(1)
      XINC=CONTRL(3)/10.
      NPTS=(CONTRL(1)-CONTRL(2))*10./CONTRL(3)
      READ 500,(R(I),I=1,NPTS)
      READ 905
C     R=UNSMOOTHED DATA,   CD= SMOOTHED DATA, T= TEMPORARY STORAGE
      N = NPTS - 12
      DO 10 I=2,13
      J= I-1
   10 T(I) = R(J)
      DO 200 I=1,N
      J = I+12
      DO 11 K= 1,12
      KK = K+1
   11 T(K) = T(KK)
      T(13) = R(J)
      SUM = 25.*T(7) + 24.*(T(6)+T(8)) + 21.*(T(5)+ T(9)) +16.*(T(4)+T(1
     10)) + 9.*(T(3)+T(11)) - 11*(T(1)+T(13))
      L = I+6
      CD(L)=SUM/143.
  200 CONTINUE
      PRINT 903, ID, CONTRL
      NSMTH=NPTS-6
      DO 21 I=1,6
   21 CD(I)=R(I)
      DO 22 I= NSMTH,NPTS
```

```
22 CD(I)=R(I)
   DO 5 I=1,NPTS
 5 XWAVE(I)=CONTRL(1)-FLOAT(I-1)*CONTRL(3)/10.
   IF (IPUNPR(1).EQ.3HYES)8,9
 8 PUNCH 909,(IDEXP(I), I=1,12)
   PUNCH 902,ID,CONTRL
   PUNCH 500, (CD(I),I=1,NPTS)
   PUNCH 907
 9 CONTINUE
   PRINT 910
   II=NPTS/3.+1.
   DO 20 I= 1,II
   J=I+II
   K=J+II
20 PRINT 908, XWAVE(I), CD(I), XWAVE(J), CD(J), XWAVE(K), CD(K)
   NUM = NPTS-40.
   XMAX=XMAX-40.
   PRINT 909,(IDEXP(I), I=1,12)
   IF(IPUNPR(2).EQ.3HYES) 7,302
 7 CALL PRNPLT(XWAVE(41),CD(41),XMAX,XINC,2.5,.1,0,0,NUM)
   GO TO 302
   END
```

```
      PROGRAM RANIER( INPUT,OUTPUT,PUNCH)
      DIMENSION CONTRL(6), CD(200, 10),XWAVE(200),IDEN(12),CDAV(200)
C     THIS PROGRAM AVERAGES SETS OF NAV SPECTRA
C     CONTROLS ARE(1) LAMBDA MAX, (2) LAMBDA MIN, (3) A PER POINT, (5)OD
C     (6) IS EXTINCTION COEFFIECIENT
C     NPTS IS THE NUMBER OF WAVELENGTHS
C     BLANK CARD AT END OF DATA SIGNALS STOP
  900 FORMAT (12A6)
  901 FORMAT(I4)
  902 FORMAT(X,A8,2X,4(F8.3,2X),2(E13.6,2X))
  903 FORMAT(10F8.4)
  904 FORMAT(*1*,12A6,I4,*  SPECTRA AVERAGED*)
  905 FORMAT(X,A8,2X,4(F8.3,2X),2(E13.6,2X ) )
  906 FORMAT(1H1)
  907 FORMAT(80(1H*))
  908 FORMAT(3(13X,F6.1,3X,F13.5))
  909 FORMAT(*1*, I4, *SPECTRA AVERAGED*)
  910 FORMAT( / ,3(15X,*LAMBDA*,3X,*ELLIPTICITY*),/)
  911 FORMAT(//,*    ID    LAMBDA MAX  LAMDA MIN     A        PTS AV
     S    OD       EXT COEFFICIENT*)
  912 FORMAT(X, 12A6)
  915 FORMAT(*1*)
      PRINT 915
      READ 901, NAV
  302 CONTINUE
      PRINT 909, NAV
      PRINT 911
      DO 1 J=1,NAV
      READ 900, IDEN
      IF(IDEN.EQ.6HSTOP   )STOP
      NPTS =100
      READ 903,(CD(I,J),I=1,NPTS)
      PRINT 912, IDEN
    1 CONTINUE
      XMAX=310.
      XINC=1.0
      DO 2 I=1,NPTS
      XWAVE(I)= 310. -FLOAT(I-1)
      SUM =0.
      DO 3 J=1,NAV
    3 SUM = SUM+CD(I,J)
    2 CDAV(I)=SUM/NAV
      II=NPTS/3.+1.
      PRINT 910
      DO 20 I= 1,II
      J=I+II
      K=J+II
   20 PRINT 908, XWAVE(I),CDAV(I), XWAVE(J), CDAV(J), XWAVE(K), CDAV(K)
      PRINT  906
      PRINT 904, IDEN,NAV
      NUM=NPTS
      PUNCH 912,IDEN
      PUNCH 905, ID, CONTRL
      PUNCH 903, (CDAV(I), I=1,NPTS)
      PUNCH 907
    7 CALL PRNPLT(XWAVE( 1),CDAV( 1),XMAX,XINC,2.5,.1,0,0,NUM)

      GO TO 302
      END
```

```
      PROGRAM STHLNS(INPUT,OUTPUT,PUNCH)
      DIMENSION  CONTRL(6), CD(200), XWAVE(200), A(200), B(200),IDIF(12)
     1,IDENA(12),IDENB(12)
C     THIS PROGRAM CALCULATES DIFFERENCE SPECTRA  A(I)-B(I)
C     NPTS IS THE NUMBER OF WAVELENGTHS
C     CONTROLS ARE(1) LAMBDA MAX, (2) LAMBDA MIN, (3) A PER POINT, (5)OD
C     (6) IS EXTINCTION COEFFIECIENT
C     BLANK CARD AT END OF DATA SIGNALS STOP
  900 FORMAT(12A4)
  902 FORMAT(X,A8,2X,4(F8.3,2X),2(E13.6,2X))
  903 FORMAT(10F8.4)
  906 FORMAT(1H1)
  907 FORMAT(80(1H*))
  908 FORMAT(3(13X,F6.1,3X,F13.5))
  910 FORMAT( / ,3(15X,*LAMBDA*,3X,*ELLIPTICITY*),/)
  911 FORMAT( /,*    ID    LAMBDA MAX  LAMDA MIN    A        PTS AV
     $    OD      EXT COEFFICIENT*)
  912 FORMAT(/,X,12A4,* MINUS*, 12A4)
  913 FORMAT(12A4, * MINUS*, 12A4)
  915 FORMAT(*1*)
      PRINT 915
302   CONTINUE
      READ 900, IDENA
      IF(IDENA.EQ.4H      ).STOP
      READ   902,ID,CONTRL
      PRINT 915
      PRINT 911
      PRINT 902, ID, CONTRL
      XMAX=CONTRL(1)
      XINC=CONTRL(3)/10.
      NPTS=(CONTRL(1)-CONTRL(2))*10./CONTRL(3)
      READ 903, (A(I),I=1,NPTS)
      READ 906
      READ 900, IDENB
      READ   902,ID,CONTRL
      PRINT 902,ID,CONTRL
      READ 903, (B(I),I=1,NPTS)
      READ 906
      DO 2 I=1,NPTS
      XWAVE(I)=CONTRL(1)-FLOAT(I-1)*CONTRL(3)/10.
    2 CD(I)= A(I)-B(I)
      PUNCH 913,IDENA,IDENB
      PUNCH 902, ID,CONTRL
      PUNCH 903, (CD(I)   , I=1,NPTS)
      PUNCH 907
      II=NPTS/3.+1.
      PRINT 912, IDENA,IDENB
      PRINT 910
      DO 20 I= 1,II
      J=I+II
      K=J+II
   20 PRINT 908, XWAVE(I), CD(I), XWAVE(J), CD(J), XWAVE(K), CD(K)
      NUM=NPTS-40.
      XMAX=XMAX-40.
      PRINT 915
      PRINT 912, IDENA, IDENB
      CALL PRNPLT(XWAVE(41),CD(41),XMAX,XINC,1.0,.04,0,0,NUM)
      PRINT 915
      GO TO 302
      END
```

MTHOOD compares a set of calculated spectra with an experimental spectrum to see how well they fit. The first data card tells at how many wavelengths the fit is to be computed in an I4 format. The input consists next of a set of calculated spectra. Each of these spectra consists of 12 cards: an IDCAL card, 10 data cards, and an * card. The end of the set of calculated spectra is signalled by STOP in the first four columns of an IDCAL card. The program then goes on to read the experimental spectra which will be compared with these calculated spectra. These experimental spectra are arranged in the same manner previously described: an IDEXP card, a control card, data cards, and an * card. The end of the set of experimental spectra is signalled by two blank cards. IDCAL, IDEXP, the fit between the two spectra being compared as defined in Equation 3-17, and the numerator and denominator of this equation are printed out for each set of spectra being compared.

```
      PROGRAM MTHOOD(INPUT,OUTPUT)
      DIMENSION CONTRL(6),  CDCAL(200,18), CDEXP( 200 ),   XWAVE(200),
     1DIFF(200),IDEXP(12),IDCAL(25,13)
C     THIS PROGRAM CALCULATES HOW WELL AN EXPERIMENTAL CD SPECTRUM IS FIT BY A
C     SERIES OF CALCULATED CD SPECTRA
C     M IS THE NUMBER OF WAVELENGTHS AT WHICH RMS DEV IS COMPUTED BEGINNING
C     WITH 310 AND CONTINUING EVERY 1 MU
C     NPTS IS THE NUMBER OF WAVELENGTHS
C     PUT A CARD SAYING STOP AT THE END OF THE CALCULATED SPECTRA
C     PUT A BLANK CARD AFTER EACH SET OF CALCULATED SPECTRA
C     PUT TWO BLANK CARDS AT THE END OF THE DATA
C      FITNESS =RMS DEVIATION BTN CALC AND EXP SPECTRUMDIVIDED BY RMS OF
C     EXP SPECTRUM CALC AT M WAVELENGHTS9
  900 FORMAT (12A6)
  901 FORMAT (I4)
  902 FORMAT(X,A8,2X,4(F8.3,2X),2(E13.6,2X))
  903 FORMAT(10F8.4)
  904 FORMAT(*1*, 12A6,*EXPERIMENTAL SPECTRUM TO BE FIT*)
  905 FORMAT(*1*)
  907 FORMAT(//,* FIT WITH*, 12A6, *CALCULATED SPECTRUM*)
  911 FORMAT(//,*       ID*)
  912 FORMAT(/,*FITNESS EQUALS*,F7.3(* DIVIDED BY*,F7.3,* EQUALS*,F7.3
     1,//)
  915 FORMAT(//, 12A6,* CALCULATED SPECTRUM*)
  920 FORMAT (1H1)
      READ 901, M
      K=1
    4 READ 900, (IDCAL(K,L), L=1,12)
      PRINT 900 , (IDCAL(K,L),L=1,12)
      IF(IDCAL(K,1).EQ.6HSTOP   )GO TO 1
      READ 903, (CDCAL(J,K), J=1,100         )
      READ 920
      K=K+1
      GO TO 4
    1 KISS=K-1
  300 CONTINUE
      READ 900, IDEXP
      IF(IDEXP.EQ.6H         )STOP
      PRINT 904, IDEXP
      READ 902, ID, CONTRL
      PRINT 911
      PRINT 902, ID, CONTRL
      XMAX=CONTRL(1)
      XINC=CONTRL(3)/10.
      NPTS=(CONTRL(1)-CONTRL(2))*10./CONTRL(3)
      READ 903,(CDEXP(I),I=1,NPTS)
      READ 905
      DO 2 I=1,NPTS
    2 XWAVE(I)=CONTRL(1)-FLOAT(I-1)*CONTRL(3)/10.
      DO 6 JO=1,KISS
      PRINT 915, (IDCAL(JO,L), L=1,12)
      SUMDIF=0.
      SUMEXP=0.
      DO 5 K=1,M
      J=K
      I=40+K

      DIFF(K)=(CDCAL(J,JO )-CDEXP(I))**2
      SUMDIF=SUMDIF+DIFF(K)
    5 SUMEXP=SUMEXP+(CDEXP(I)**2)
      EXP=SQRT(SUMEXP)
      DIFSQ=SQRT(SUMDIF)
      FIT=DIFSQ/EXP
      PRINT 912, DIFSQ,EXP,FIT
    6 CONTINUE
      GO TO 300
      END
```

SHASTA, which is used to calculate sums of monomer, dimer, and polymer spectra, and MTADMS, which calculates double strand pairing interaction sums, are quite similar. The Input deck for SHASTA begins with a card specifying the number of output spectra, the number of input spectra, and the number of wavelengths at which the CD is to be calculated per spectrum in a 3I4 format. This is followed by 20 single strand basis spectra, 6 double strand basis spectra, 4 monomer basis spectra, a possible TψCG basis spectrum, and a zero basis spectrum. Each basis spectrum consisted of 12 cards: an ID card, 10 data cards, and an * card or blank card.

Following the basis spectra are groups of four cards, each corresponding to a spectrum to be calculated. The first of these cards specifies FNAME, an 80 character identification for the calculated spectrum. The second card lists the number of times each of the 20 nearest neighbor interactions occurs in the single strand regions of the RNA in a 20F2.0 format. The third card lists how many times each of the 6 double strand interactions occurs in hydrogen bonded regions of the molecule in a 6F3.0 format. The fourth card specifies the monomers at either end of the RNA in a 4F2.0 format. After these sets of four cards, there is a final card specifying the maximum wavelength and the interval between data points in mμ in a 2F10.3 format.

```
      PROGRAM SHASTA( INPUT,OUTPUT,PUNCH )
C     NN= NUMBER OF OUTPUT SPECTRA
C     N= NUMBER OF INPUT SPECTRA
C     M= NUMBER OF WAVELENGTHS PER SPECTRUM
C     NSM = NUMBER OF NUCLEOTIDES IN NUCLEIC ACID
C     C(I,K) IS THE FREQUENCY OF THE KTH COMPONENT FOR THE ITH POLYMER
      DIMENSION ENN(35,100),C(35,35),EPOLY(35,100),ENATIVE(100),NSM(35
     1), FNAME(25,25)    ,ID(8)
      COMMON N,JD1,M,JD2,ENN,EPOLY,D3(25,25),D4(25,25),D5(25,25),C, NSM
     1 ,FNAME
  100 FORMAT(6F3.0)
  102 FORMAT(20F2.0)
  202 FORMAT(6F2.0)
  103 FORMAT(10F8.4)
  104 FORMAT(3I4)
  108 FORMAT(2X, 20F6.3)
  109 FORMAT(8A10)
  901 FORMAT(*            *,8A10)
  110 FORMAT(X,I2)
  501 FORMAT(/)
  502 FORMAT(*1*)
   99 FORMAT(1H1)
      READ 104,NN,N,M
      PRINT 502
      DO 98 I=1,32
      READ 109,(ID(I),I=1,8 )
      READ 103,  (ENN(I,J),J=1,M)
      PRINT 901,(ID(I),I=1,8     )
      PRINT 501
      READ 99
   98 CONTINUE
      PRINT 502
      DO 8 I=1,NN
      READ 109,((FNAME(I ,J), J=1,8))
C     READ COEFFICIENTS OF SINGLE STRAND NN INTERACTIONS
      READ 102, (C(I,K), K=1,20)
C     READ COEFFICIENTS OF DOUBLE STRAND POLYMER INTERACTIONS
      READ 100, (C(I,K), K=21,26)
C     READ COEFFICIENTS OF MONOMER SPECTRA, TSCG, AND 2 FOR EADCH -C(I,K)
      READ 202, (C(I,K), K=27,32)
      DO 7 K=1,26
      C(I,K)=(C(I,K)*2.)
    7 CONTINUE
      DO 9 K=31,32
      C(I,K)=(C(I,K)*2.)
    9 CONTINUE
    8 CONTINUE
      DO 107 I=1,NN
      NSM(I) =0.
      DO 107 K=1,N
      NSM(I) = C(I,K) + NSM(I)
  107 CONTINUE
      DO 6 I=1,NN
      NSM(I)=NSM(I)/2
    6 CONTINUE
      DO 105 I=1,NN
      DO 105 K=1,N
      C(I,K) =C(I,K)/2.
  105 C(I,K) = C(I,K)/NSM(I).
      DO 20 I=1,NN
      DO 20 J=1,M
      EPOLY(I,J)=0.
      DO 20 K=1,N
   20 EPOLY(I,J) = ENN(K,J) * C(I,K) + EPOLY(I,J)
      CALL SETPLT(0,1,NN)
      STOP
      END
```

```
      SUBROUTINE  SETPLT(IFLAG,KFLAG,NN)
      DIMENSION A(35,100),CD(35,100),C(35,35),WAVE(100),FNAME(25,25),Y(1
     100), NSM(35)
      COMMON N,JD1,M,L,A,CD,D3(25,25),D4(25,25),D5(25,25),C,NSM
     1,FNAME
C     SUBROUTINE SETPLT, PHILIP BORER, JULY 6, 1969
C     PROGRAM SETS UP USE OF PROGRAMS PRNPLT AND PLSCAL WRITTEN BY
C     M.S. ITZKOWITZ.  IFLAG = 0 CAUSES INPUT NEAREST NEIGHBOR
C     FREQUENCIES TO BE DISPLAYED.  THE X AXIS FOR THE PLOT IS GENERATED
C     FROM WAVMAX AND DELT.
C     FNAME IS A NAME (70 CHARACTERS OF LESS) FOR THE OUTPUT POLYMER
C     WAVMAX = MAXIMUM WAVELENGTH IN MMU
C     DELT = WAVELENGTH INTERVAL IN MMU
  100 FORMAT(//*   INTERACTION FREQUENCIES ARE*//)
  102 FORMAT(14F8.4)
  103 FORMAT(10F8.4)
  105 FORMAT(*1*,8A10)
  502 FORMAT(*  *, 7A10)
  106 FORMAT(*1*)
  107 FORMAT(16,*  BASES*)
  110 FORMAT (2F10.3)
  908 FORMAT(3(13X,F6.0,3X,F13.4))
  910 FORMAT(// ,3(15X,*LAMBDA*,3X,*ELLIPTICITY*),//)
  113 FORMAT(10F8.4)
  711 FORMAT (*  *)
      DO 6 I=1,NN
      PUNCH 502, (FNAME(I,J), J=1,7)
      PUNCH 711
      PUNCH 711
      PUNCH 711
      PUNCH 711
      PUNCH 113, (CD(I,J), J=1,100)
      PUNCH 711
      PUNCH 711
    6    CONTINUE
      READ 110, WAVMAX,DELT
      WAVE(M)=WAVMAX
      MM=M-1
      DO 10 I=1,MM
   10 WAVE(M-I)=WAVE(M-I+1)-DELT
C     REVERSE Y VECTOR SO SMALL WAVELENGHTS HAVE SMALL Y SUBSCRIPTS.
C     PRINT AND PLOT.
      DO 60 I=1,NN
      PRINT 105, (FNAME(I,J), J=1,7)
C     DOES USER WANT DISPLAY OF INPUT NEAREST NEIGHBOR FREQUENCIES
      IF (IFLAG .NE.0) GO TO 20
      PRINT 107, NSM(I)
      PRINT 100
      PRINT 102, (C(I,K),K=1,N )
   20 K=M
      IF(KFLAG .NE. 0) GO TO 35
      DO 30 J=1,M
      Y(K) = A(I,J)
   30 K=K-1
      GO TO 50
   35 DO 40 J=1,M

      Y(K)=CD(I,J)
   40 K=K-1
   50 CONTINUE
      PRINT 910
      NPTS=M
      II=NPTS/3.+1.
      DO 21 L= 1,II
      J=L+II
      K=J+II
   21 PRINT 908,  WAVE(L),  Y(L),  WAVE(J),  Y(J),  WAVE(K),  Y(K)
      PRINT 105, (FNAME(I,J), J=1,7)
      CALL PRNPLT(WAVE,Y,WAVMAX,1.,3.0,-12,0,0,M)
   60 CONTINUE
      RETURN
      END
```

The input data for MTADMS is similar except
that the card specifying FNAME follows the three
cards specifying the number of various sorts of
interactions, and there are only 6 double strand pairing
spectra in basis spectra deck.

The punched output for these programs consists of
a series of calculated CD spectra consisting of an
IDCAL card, and 10 data cards. Also, the calculated
spectra are listed and plotted by PRNPLT.

```
      PROGRAM MTADMS(INPUT,OUTPUT,PUNCH)
      DIMENSION ENN(25,100),C(30,30), EPOLY(30,100),ENATIVE(100),NSM(25)
C     I SURE HOPE THIS DAMN THING WORKS THIS TIME.
C     NN= NUMBER OF OUTPUT SPECTRA
C     N= NUMBER OF INPUT SPECTRA
C     M= NUMBER OF WAVELENGTHS PER SPECTRUM
C     NSM = NUMBER OF NUCLEOTIDES IN NUCLEIC ACID
C     C(I,K) IS THE FREQUENCY OF THE KTH COMPONENT FOR THE ITH POLYMER
     1 ,FNAME(25,25), D(25,25)
      COMMON N,JD1,M,JD2,ENN,EPOLY,D3(25,25),D4(25,25),D5(25,25),C, NSM
     1, FNAME
  100 FORMAT(6F2.0)
   99 FORMAT(1H1)
  101 FORMAT(/16F8.4)
  102 FORMAT(20F2.0)
  103 FORMAT(10F8.4)
  104 FORMAT(3I4)
  108 FORMAT(2X, 20F6.3)
  109 FORMAT(8A10)
  110 FORMAT(1H1)
  501 FORMAT(/)
      READ 104,NN,N,M
      DO 98 I=1,N
      READ 99
      READ 103, (ENN(I,J),J=1,M)
      PRINT108, ((ENN(I,J),J=1,M))
      PRINT 501
   98 CONTINUE
      DO 5 I=1,NN
      READ 102,(D(I,K), K=1,20)
      READ 100,(C(I,K), K=1,N)
      READ 110
      READ 109,((FNAME(I ,J), J=1,8))
      PRINT 109,((FNAME(I ,J), J=1,8))
    5 CONTINUE
      DO  6  J=1,NN
      NSM(J) =0.
      DO 107 I=1,N
      NSM(J)=NSM(J)+C(J,I)
  107 CONTINUE
      DO 6 K=1,17
      NSM(J)=NSM(J)+D(J,K)
    6 CONTINUE
      DO 105 I=1,NN
      DO 105 K=1,N
  105 C(I,K) = C(I,K)/NSM(I)
      DO 20 I=1,NN
      DO 20 J=1,M
      EPOLY(I,J)=0.
      DO 20 K=1,N
   20 EPOLY(I,J) = ENN(K,J) * C(I,K) + EPOLY(I,J)
      CALL SETPLT(0,1,NN)
      STOP
      END
```

```
      SUBROUTINE  SETPLT(IFLAG,KFLAG,NN)
      DIMENSION A(35,100),CD(35,100),C(35,35),WAVE(100),FNAME(25,25),Y(1
     100), N M(35)
      COMMON  ,JD1,M,L,A,CD,D3(25,25),D4(25,25),D5(25,25),C,NSM
     1,FNAME
C     SUBROUTINE SETPLT, PHILIP BORER, JULY 6, 1969
C     PROGRAM SETS UP USE OF PROGRAMS PRNPLT AND PLSCAL WRITTEN BY
C     M.S. ITZKOWITZ.   IFLAG = 0 CAUSES INPUT NEAREST NEIGHBOR
C     FREQUENCIES TO BE DISPLAYED.  THE X AXIS FOR THE PLOT IS GENERATED
C     FROM WAVMAX AND DELT.
C     FNAME IS A NAME (70 CHARACTERS OF LESS) FOR THE OUTPUT POLYMER
C     WAVMAX = MAXIMUM WAVELENGTH IN MMU
C     DELT = WAVELENGTH INTERVAL IN MMU
  100 FORMAT (//* NEAREST NEIGHBOR FREQUENCIES ARE */*    AA        AU
     1  AC        AG       UA       UU      UC       UG  ,  CA        CU
     2CC        CG       GA       GU       GC       GG*)
  104 FORMAT(F6.4, * OF THE INTERACTIONS INVOLVE UH2 AND ARE SET = 0* /)
  401 FORMAT(* APD=*,F6.4,*DPA=*,F6.4,*GPD=*,F6.4)
  101 FORMAT ( /* INTERACTION FREQUENCIES ARE*/*     A/U        G/C
     1 AU/AU    GC/GC    AC/GU    AG/CU *)
  102 FORMAT(16F8.4)
  103 FORMAT(10F8.4)
  301 FORMAT(* A=*,F6.4,*  U=*, F6.4,* C=*,F6.4,* G=*,F6.4,)
  105 FORMAT(*1*,8A10)
  502 FORMAT(*  *, 7A10)
  106 FORMAT(*1*)
  107 FORMAT(I6,*  BASES*)
  110 FORMAT (2F10.3)
  908 FORMAT(3(13X,F6.0,3X,F13.4))
  910 FORMAT(// ,3(15X,*LAMBDA*,3X,*ELLIPTICITY*),//)
  113 FORMAT(10F8.4)
      DO 6 I=1,NN
      PUNCH 502, (FNAME(I,J), J=1,7)
      PUNCH 113, (CD(I,J), J=1,100)
    6    CONTINUE
      READ 110, WAVMAX,DELT
      WAVE(M)=WAVMAX
      MM=M-1
      DO 10 I=1,MM
   10 WAVE(M-I)=WAVE(M-I+1)-DELT
C     REVERSE Y VECTOR SO SMALL WAVELENGHTS HAVE SMALL Y SUBSCRIPTS.
C     PRINT AND PLOT.
      DO 60 I=1,NN
      PRINT 105, (FNAME(I,J), J=1,7)
C     DOES USER WANT DISPLAY OF INPUT NEAREST NEIGHBOR FREQUENCIES
      IF (IFLAG .NE.0) GO TO 20
      PRINT 107, NSM(I)
      PRINT 100
      PRINT 102, (C(I,K),K=1,16)
      PRINT 104, C(I,17)
      PRINT 401,(C(I,K),K=18,20)
      PRINT 101
      PRINT 103, (C(I,K),K=21,26)
      PRINT 301, (C(I,K),K=27,30)
   20 K=M
      IF(KFLAG .NE. 0) GO TO 35
      DO 30 J=1,M
      Y(K) = A(I,J)
   30 K=K-1
      GO TO 50
   35 DO 40 J=1,M
      Y(K)=CD(I,J)
   40 K=K-1
   50 CONTINUE
      PRINT 910
      NPTS=M
      II=NPTS/3.+1.
      DO 21 L= 1,II
      J=L+II
      K=J+II
   21 PRINT 908,  WAVE(L),  Y(L),  WAVE(J),  Y(J),  WAVE(K),  Y(K)
      PRINT 105, (FNAME(I,J), J=1,7)
      CALL PRNPLT(WAVE,Y,WAVMAX,1.,3.0,.12,0,0,M)
   60 CONTINUE
      RETURN
      END
```

```
      PROGRAM LASSEN(INPUT,OUTPUT,PUNCH)
      DIMENSION CONTRL(6), CD(200), IPUNPR(3), XWAVE(200), IDEXP(12)
     1 ,ZM(150,5), BASVEC(150), M(5), ZMON(150)
C     REPLACE IST * CARD IN EACH DIMER WITH  BASE COMPOSITION CARD
C     CONTRCLS ARE(1) LAMBDA MAX, (2) LAMBDA MIN, (3) A PER POINT, (5)OO
C     (6) IS EXTINCTION COEFFIECIENT
C     BLANK CARD AT END OF DATA SIGNALS STOP
  500 FORMAT(10F8.4)
902   FORMAT(A8,2X,4(F8.3,2X),2(E13.6,2X))
903   FORMAT(5(E13.6,2X))
  904 FORMAT(*1BASIS SPECTRUM CALCULATED FROM DIMER    *, A8)
905   FORMAT(1X)
906   FORMAT(1H1)
  907 FORMAT(80(1H*))
  908 FORMAT(3(13X,F6.0,3X,F13.4))
  909 FORMAT(12A6)
  109 FORMAT(7F8.4)
  910 FORMAT(// ,3(15X,*LAMBDA*,3X,*ELLIPTICITY*),//)
  912 FORMAT (*1*)
  913 FORMAT(10F8.4)
  914 FORMAT(5I1)
  915 FORMAT(X,A8)
      PRINT 912
      DO 11 J=1,5
      READ 913,(ZM(I,J), I=1,150)
      PRINT 913, (ZM(I,J), I=1,150)
   11 CONTINUE
      PRINT 912
302   CONTINUE
      READ 914,(M(J), J=1,5)
      READ  902,ID,CONTRL
      IF(ID.EQ.8H         )STOP
      XMAX=CONTRL(1)
      XINC=CONTRL(3)/10.
      NPTS=(CONTRL(1)-CONTRL(2))*10./CONTRL(3)
      READ 500,(CD(I),I=1,NPTS)
      READ 905
      DO 5 I=1,NPTS
      XWAVE(I)=CONTRL(1)-FLOAT(I-1)*CONTRL(3)/10.
    5 CONTINUE
      DO 10 I=1,NPTS
      ZMON(I)=0.
      DO 20 J=1,5
      ZMON(I) = M(J)*ZM(I,J) +ZMON(I)
   20 CONTINUE
      BASVEC(I) =2.*CD(I)-ZMON(I)/2.
   10 CONTINUE
      PUNCH 915, ID
      PUNCH 500,(BASVEC(I), I=41,140)
      PUNCH 907
    9 CONTINUE
      PRINT 904, ID
      PRINT 910
      DO 30 I=1,NPTS
      CD(I)=BASVEC(I)
   30 CONTINUE
      II=NPTS/3.+1.
      DO 25 I= 1,II
      J=I+II
      K=J+II
   25 PRINT 908, XWAVE(I), CD(I), XWAVE(J), CD(J), XWAVE(K), CD(K)
      NUM = NPTS-40.
      XMAX=XMAX-40.
      PRINT 904, ID
    7 CALL PRNPLT(XWAVE(41),CD(41),XMAX,XINC,3.,.12,0,0,NUM)
      GO TO 302
      END
```

The following two subroutines PRNPLT and PLSCAL,
are used by most of the preceding programs and
were written by Marty Itzkowitz.

```
      SUBROUTINE PRNPLT(X,Y,XMAX,XINCR,YMAX,YINCR,ISX,ISY,NPTS)
      DIMENSION X(NPTS),Y(NPTS),IGRID(105),XAXIS(11)
C  PRINTER PLOT ROUTINE         M.S.ITZKOWITZ    MAY,1967
C
C    PLOTS THE 'NPTS' POINTS GIVEN BY 'X(I),Y(I)' ON A 51 X 101 GRID
C    USING A TOTAL OF 56 LINES ON THE PRINTER
C      IF 'ISX' OR 'ISY' ARE NON-ZERO, THE CORRESPONDING MAXIMUM AND
C       INCREMENTAL STEP SIZE ARE COMPUTED
C      IF EITHER INCREMENTAL STEP SIZE IS ZERO, THE PROGRAM EXITS
C      NEITHER OF THE INPUT ARRAYS ARE DESTROYED.  IF SCALING IS DONE
C      THE CORRESPONDING NEW VALUES OF MAXIMUM AND STEP SIZE ARE RETURNED
      INTEGER BLANK,DOT,STAR,IGRID,PLUS
      DATA BLANK,DOT,STAR,PLUS / 1H ,1H.,1H*,1H+ /
C
901   FORMAT(14X,105A1)
902   FORMAT(1XF10.1,2X,1H+,105A1,1H+)
903   FORMAT(15X,103(1H.))
904   FORMAT(7X,11(F10.0),2H (,I4,5H PTS)  )
905   FORMAT(16X,11(1H+,9X))
9800  FORMAT(46H1SCALING ERROR IN PRNPLT, EXECUTION TERMINATED )
C
      IF(ISX.NE.0) CALL PLSCAL(X,XMAX,XINCR,NPTS,100)
      IF(ISY.NE.0) CALL PLSCAL(Y,YMAX,YINCR,NPTS,50)
      IF(XINCR.EQ.0..OR.YINCR.EQ.0.) GO TO 800
      YAXMIN=0.01*YINCR
      XAXMIN=0.01*XINCR
      IZERO=YMAX/YINCR+1.5
      JZERO=103.5-XMAX/XINCR
      IF(JZERO.GT.103.OR.JZERO.LT.4) JZERO=2
      PRINT 905
      PRINT 903
      DO 10 I=1,51
      IF ( I.NE.IZERO) GO TO 16
      DO 14 J=1,105
14    IGRID(J)=PLUS
      GO TO 15
16    DO 11 J=1,105
11    IGRID(J)=BLANK
15    IGRID(JZERO)=PLUS
      IGRID(104)=DOT
      IGRID(2)=DOT
      DO 12 K=1,NPTS
      ITEST =(YMAX-Y(K))/YINCR+1.5
      IF(ITEST .NE.I) GO TO 12
      J=103.5-(XMAX-X(K))/XINCR
      IF(J.GT.103)J=105
      IF(J.LT.3) J=1
      IGRID(J)=STAR
12    CONTINUE
      IF(MOD(I,10).EQ.1) GO TO 13
      PRINT 901,IGRID
      GO TO 10
13    YAXIS=YMAX-(I-1)*YINCR
      IF(ABS(YAXIS).LT.YAXMIN) YAXIS=0.
      PRINT 902,YAXIS,(IGRID(J),J=1,105)
10    CONTINUE
      PRINT 903
      PRINT 905
      DO 20 M=1,11
      XAXIS(M)=XMAX-XINCR*(FLOAT(11-M))*10.0
      IF(ABS(XAXIS(M)).LT.XAXMIN)XAXIS(M)=0.
20    CONTINUE
      PRINT 904,XAXIS,NPTS
      RETURN
800   PRINT 9800
      CALL EXIT
      END
```

```fortran
      SUBROUTINE PLSCAL(V,VMAX,VINCR,NPTS,NDIVIS)
C
C     SCALING PROGRAM FOR USE WITH PRNPLT   M.S.ITZKOWITZ  MAY,1967
C  THIS VERSION ADJUSTS THE FULL SCALE TO 2.5,5.0, OR 10. TIMES 10**N
C  AND ADJUSTS THE MAXIMUM POINT TO AN INTEGER MULTIPLE OF 5*VINCR
C
      DIMENSION V(NPTS)
C
      VMIN=V(1)
      VMAX=V(1)
      DO 10 I=1,NPTS
      IF(V(I).LT.VMIN) VMIN=V(I)
      IF(V(I).GT.VMAX) VMAX=V(I)
      QRANGE=VMAX-VMIN
10    CONTINUE
      IF(QRANGE.EQ.0.) GO TO 8000
      QRANGE=C.4342944*ALOG(QRANGE)
      IF(QRANGE)20,20,30
30    IRANGE=QRANGE
      GO TO 40
20    IRANGE=-QRANGE
      IRANGE=-IRANGE-1
40    QRANGE=QRANGE-FLOAT(IRANGE)
      RANGE=10.**QRANGE
C
C  RANGE IS BETWEEN 1.0 AND 10.0
C
43    IF(RANGE.GT.2.5) GO TO 41
      RANGE=2.5
      GO TO 50
41    IF(RANGE.GT.5.0) GO TO 42
      RANGE=5.0
      GO TO 50
42    RANGE=10.0
50    TRANGE=RANGE*(10.**IRANGE)
C
C  TRANGE IS NOW 2.5,5.0, OR 10.0 TIMES A POWER OF TEN
C
      VINCR=TRANGE/FLOAT(NDIVIS)
      IF(VMAX)51,51,52
52    IMAX=VMAX/(5.0*VINCR)
      XMAX=5.0*VINCR*FLOAT(IMAX+1)
      GO TO 53
51    IMAX=-VMAX/(5.0*VINCR)
      XMAX=5.0*VINCR*FLOAT(-IMAX+1)
53    IF(VMIN.GT.XMAX-TRANGE) GO TO 100
      RANGE=RANGE*2.0
      IF(RANGE-10.) 43,43,54
54    RANGE=RANGE/10.
      IRANGE=IRANGE+1
      GO TO 43
100   VMAX=XMAX
      VMIN=XMAX-TRANGE
      RETURN
8000  PRINT 9800
9800  FORMAT(45H1PLSCAL CALLED TO SCALE ARRAY WITH ZERO RANGE)
      CALL EXIT
      END
```